FEDERAL UNIVERSITY OF CEARÁ
TECHNOLOGY CENTER
DEPARTMENT OF ELECTRICAL ENGINEERING
GRADUATE PROGRAM IN ELECTRICAL ENGINEERING

FELIPE JOSÉ DE SOUSA VASCONCELOS

CONTROL OF INDUSTRIAL PROCESSES USING PREDICTORS-BASED CONTROL STRUCTURES

FORTALEZA

2024

FELIPE JOSÉ DE SOUSA VASCONCELOS

CONTROL OF INDUSTRIAL PROCESSES USING PREDICTORS-BASED CONTROL STRUCTURES

Thesis presented to the Graduate Program in Electrical Engineering of Federal University of Ceara as a partial requirement to obtain the title of Doctor in Electrical Engineering. Concentration field: Electric Power Systems.

Supervisor: Prof. Dr. Bismark Claure Torrico
Co-supervisor: Prof. Dr. Fabrício Gonzalez Nogueira

FORTALEZA

2024

Dados Internacionais de Catalogação na Publicação
Universidade Federal do Ceará
Sistema de Bibliotecas
Gerada automaticamente pelo módulo Catalog, mediante os dados fornecidos pelo(a) autor(a)

V45c Vasconcelos, Felipe José de Sousa.
Control of industrial processes using predictors-based control structures / Felipe José de Sousa Vasconcelos. – 2024.
154 f. : il. color.

Tese (doutorado) – Universidade Federal do Ceará, Centro de Tecnologia, Programa de Pós-Graduação em Engenharia Elétrica, Fortaleza, 2024.
Orientação: Prof. Dr. Bismark Claure Torrico.
Coorientação: Prof. Dr. Fabrício Gonzalez Nogueira.

1. Cascade control. 2. Dead-time systems. 3. Disturbance attenuation. 4. Robust control systems. 5. Smith predictor. I. Título.

CDD 621.3

FELIPE JOSÉ DE SOUSA VASCONCELOS

CONTROL OF INDUSTRIAL PROCESSES USING PREDICTORS-BASED CONTROL STRUCTURES

Thesis presented to the Graduate Program in Electrical Engineering of Federal University of Ceara as a partial requirement to obtain the title of Doctor in Electrical Engineering. Concentration field: Electric Power Systems.

Approved at Fortaleza, July 26, 2024.

EXAMINATION BOARD

Prof. Dr. Bismark Claure Torrico (Supervisor)
Federal University of Ceará

Prof. Dr. Fabrício Gonzalez Nogueira (Co-supervisor)
Federal University of Ceará

Prof. Dr. Marcus Vinícius Americano da Costa Filho
Federal University of Bahia

Prof. Dr. Cláudio Marques de Sá Medeiros
Federal Institute of Education, Science and Technology of Ceará

Profa. Michela Mulas, Ph.D.
Federal University of Ceará

This work is dedicated to my parents, Francisco and Maria.

ACKNOWLEDGEMENTS

To my Supervisor, Prof. Dr. Bismark Claure Torrico, and my Co-supervisor, Prof. Dr. Fabrício Gonzalez Nogueira, for sharing their expertise in process control theory and practice, for guiding me to this research topic, and for their invaluable teachings and advice, which were fundamental for the development of this work.

To all members of the examination board, for their time, attention, and valuable contributions to improving this work.

To my colleagues at the Research Group in Automation, Control, and Robotics (GPAR), for the knowledge shared, the teamwork spirit, and the mutual support in our research endeavors. I am also grateful to my colleagues from IFCE for their valuable insights.

To the Coordenação de Aperfeiçoamento de Pessoal de Nível Superior (CAPES), for the financial support provided through a scholarship.

A special thanks to my family and my wife, Cassandra, for their understanding, unwavering encouragement, and motivation, which were crucial for the completion of this work.

All we have to decide is what to do with the time that is given us.

J.R.R. Tolkien

ABSTRACT

This work discusses the analysis and design of predictors-based controllers applied to single-input single-output (SISO) and multiple-input multiple-output (MIMO) stable, unstable and integrative dead-time processes. Dead-time is a characteristic behavior of several industrial processes, capable of leading the system to undesired behaviors and even instability. The greater the delay, the more difficult it becomes to design efficient controllers, and an effective way to address the challenges presented is by using dead-time compensator (DTC) structures. Thus, this thesis proposes new structures for controllers based to the Simplified filtered Smith predictor (SFSP) in order to extend its advantages to multivariable processes and to linear parameter-varying (LPV) dead-time processes. First, it is proposed a delay compensator series cascade control structure for two first-order processes plus dead-time (FOPDT). The industrial environment has some systems with these characteristics, so designing a controller that improves the performance and robustness of these types of systems is quite relevant. The controller incorporates a predictor for each process to manage unstable processes in the discrete-time domain, with the detail that each robustness filter is adjusted related to the perturbation applied to its respective loop. Simulation results show that, when compared with another controller present in the literature, the proposed controller presented better performance results, robustness, better attenuation to disturbances (mainly in the internal loop, due to the cascade structure) and noise, both in the nominal case and in the presence of uncertainties. Second, it is proposed a DTC structure for parallel cascade control of systems with dead time. For the proposed structure there is no need for integrators in the primary controller. Also, a robustness filter is used to reject disturbances and guarantee zero error at a steady state. Simulation results show equivalent performance compared to other recently published work, and better rejection to noise. This thesis also presents a robust dead-time compensator for two-input two-output (TITO) processes with multiple dead time based on the generalized predictive control (GPC). The proposed strategy focus mainly in disturbance rejection by means of a predictor structure proposal. Simulation results show better disturbance rejection performance compared to other DTC in literature. Finally, it is proposed a method to design a LPV controller for dead-time systems based on the SFSP. The advantage of this structure is that there are fewer parameters to tune, as there is no explicit integrator in the primary controller, which only consists of an LPV gain. For this work, the dead time is considered fix and uncertain, so it is treated as uncertainty and an LPV robustness filter is designed in order to deal with disturbances. The main contribution of the proposed SFSP-LPV is the possibility of dealing with nonlinear systems with dead time in an LPV framework. Simulations performed for stable and unstable systems show that the SFSP-LPV provides better performance when compared to other LPV controllers based on the Smith predictor published recently.

Keywords: Cascade control, Dead-time systems, Disturbance attenuation, Robust control systems, Smith predictor.

RESUMO

Este trabalho discute a análise e o projeto de controladores baseados em preditores aplicados a processos de tempo morto estáveis, instáveis e integrativos de entrada única e saída única (SISO) e de entrada múltipla e saída múltipla (MIMO). O tempo morto é um comportamento característico de diversos processos industriais, capaz de levar o sistema a comportamentos indesejados e até mesmo à instabilidade. Quanto maior o atraso, mais difícil se torna projetar controladores eficientes, e uma maneira eficaz de enfrentar os desafios apresentados é utilizando estruturas de compensação de tempo morto (DTC). Assim, esta tese propõe novas estruturas para controladores baseados no preditor de Smith filtrado simplificado (SFSP) a fim de estender suas vantagens para processos multivariados e para processos de tempo morto linearmente variáveis (LPV). Primeiramente, propõe-se uma estrutura de controle em cascata de compensação de atraso para dois processos de primeira ordem mais tempo morto (FOPDT). O ambiente industrial possui alguns sistemas com essas características, então projetar um controlador que melhore o desempenho e a robustez desses tipos de sistemas é bastante relevante. O controlador incorpora um preditor para cada processo para gerenciar processos instáveis no domínio discreto, com o detalhe de que cada filtro de robustez é ajustado em relação à perturbação aplicada ao seu respectivo loop. Os resultados da simulação mostram que, quando comparado com outro controlador presente na literatura, o controlador proposto apresentou melhores resultados de desempenho, robustez, melhor atenuação a perturbações (principalmente no loop interno, devido à estrutura em cascata) e ruído, tanto no caso nominal quanto na presença de incertezas. Em segundo lugar, esta tese propõe uma estrutura de DTC para controle em cascata paralelo de sistemas com atraso de tempo. Para a estrutura proposta, não é necessário integradores no controlador primário. Em relação às perturbações ao sistema, um filtro de robustez é usado para rejeitar perturbações e garantir erro zero em estado estacionário. Os resultados da simulação mostram desempenho equivalente em comparação com outros trabalhos recentemente publicados e melhor rejeição a ruído. Esta tese também apresenta um compensador de tempo morto robusto para processos de duas entradas e duas saídas (TITO) com múltiplos atrasos de tempo baseado no controle preditivo generalizado (GPC). A estratégia proposta foca principalmente na rejeição de perturbações por meio de uma proposta de estrutura de preditor. Os resultados da simulação mostram melhor desempenho de rejeição de perturbações em comparação com outros compensadores de tempo morto propostos recentemente. Por fim, é proposto um método para projetar um controlador LPV para sistemas de tempo morto baseado no SFSP. A vantagem desta estrutura é que há menos parâmetros para ajustar, pois não há integrador explícito no controlador primário, que consiste apenas em um ganho LPV. Para este trabalho, o tempo de atraso é considerado fixo e incerto, portanto, é tratado como incerteza e um filtro de robustez LPV é projetado para lidar com perturbações. A principal contribuição do SFSP-LPV proposto é a possibilidade de lidar com sistemas atrasados não lineares em um framework LPV. Simulações são realizadas para sistemas estáveis e instáveis que mostram que o SFSP-LPV fornece uma resposta com melhor

desempenho quando comparado a outros controladores LPV baseados no preditor de Smith publicados recentemente.

Palavras-chave: Atenuação de perturbações, Controle em cascata, Preditor de Smith, Sistemas de controle robusto, Sistemas de tempo morto.

LIST OF FIGURES

LIST OF TABLES

LIST OF ABBREVIATIONS AND ACRONYMS

DTC *Dead-time compensator*

FIR *Finite impulse response*

FOPDT *First order plus dead time*

FSP *Filtered Smith predictor*

LPV *Linear parameter-varying*

MIMO *Multiple input multiple output*

NMP *Non-minimum phase*

SFSP *Simplified filtered Smith predictor*

SISO *Single-input single-output*

SOPDT *Second order plus dead time*

SP *Smith predictor*

CONTENTS

1 INTRODUCTION

Dead-time often appears in several systems and industrial applications such as aerospace, biomedical, networked plants, and chemicals. These phenomena usually involve delayed transportation of mass, information, energy, or even in processes with accumulation of sequential time-lag dynamics. It also decreases the phase of the system and can not be expressed as a rational transfer function, consequently increasing the complexity of controller design and analysis (NORMEY-RICO; CAMACHO, 2007).

Despite the difficulties the dead time can cause in a process, especially when it has a high order value, a predictor structure can improve the performance of the closed-loop system. These type of controller is known as *Dead-time compensator* (DTC) and have been applied in many fields (NORMEY-RICO; CAMACHO, 2008).

The first ideas related to dead-time compensation through a closed-loop controller were proposed by Smith (1957) and the technique was called *Smith predictor* (SP). Its operation basically consists of including a dynamic model of the delay-free process in order to predict the behavior of the system. For this to be accomplished, a model of the delay is also included into the feedback loop so that dead time is removed from the control-loop characteristic equation. The result was an improvement in the closed-loop performance for systems with dead time over classical PI or PID controllers. The main drawbacks of SP are that it is not able to handle integrative and unstable systems, the disturbance rejection performance is degraded, and the settling time is slower than in open loop (MORARI; ZAFIRIOU, 1989; MICHIELS; NICULESCU, 2003).

In the following years several approaches were proposed in order to overcome SP deficiencies, as surveyed by (NORMEY-RICO; CAMACHO, 2007; NORMEY-RICO; CAMACHO, 2008). These controllers are mostly designed for processes, commonly found in industry (HANG; WANG; YANG, 2003; NOGUEIRA et al., 2011; MATAUŠEK; RIBIĆ, 2012; ZHENG; GAO, 2014; NOWAK; CZECZOT, 2017), which are modeled as *First order plus dead time* (FOPDT) or *Second order plus dead time* (SOPDT) systems. The majority of these techniques are based on extensions and adaptations of the SP, where some of them extends it for unstable processes (WATANABE; ITO, 1981; ARTSTEIN, 1982; LIU et al., 2005; NORMEY-RICO; CAMACHO, 2009; TORRICO et al., 2013a) while others deals with multiple delays (TORRICO; CORREIA; NOGUEIRA, 2016), *Multiple input multiple output* (MIMO) processes (GARCÍA; ALBERTOS, 2010). Some of them improve the robustness (NORMEY-RICO; CAMACHO, 2009; TORRICO et al., 2013a) or enhance the tracking performance of the SP (RODRÍGUEZ et al., 2016).

Considering *Single-input single-output* (SISO) systems, the classical SP and most design adaptations are tuning by first predict the process output explicitly for then design a controller considering the delay-free model. However, these approaches were not concerned with distur-

bance rejection performance or robustness. Therefore, in Normey-Rico, Bordons and Camacho (1997), in addition to the primary controller that deals with the delay-free model, it was proposed to include a robustness filter in the feedback path SP to deal with predictor stabilization, hence the new controller called *Filtered Smith predictor* (FSP). This DTC is well established, with many variations and applications (SANTOS; BOTURA; NORMEY-RICO, 2010; ROCA et al., 2011; ROMERO-GARCÍA et al., 2012; LIMA; SANTOS; NORMEY-RICO, 2015; RODRÍGUEZ et al., 2016; GIRALDO; FLESCH; NORMEY-RICO, 2016; GIRALDO et al., 2018).

In the study of Torrico et al. (2013a) it was noticed that if the integral action of the FSP was removed, it would still be possible to tune the gain of the primary controller for tracking and use the robustness filter to deal with the disturbance rejection. This meant a simplified design for the primary controller and the new structure is the well-known *Simplified filtered Smith predictor* (SFSP). However, this strategy has the disadvantage that it is only suitable for FOPDT processes. So in Torrico, Correia and Nogueira (2016) came the idea of adding *Finite impulse response* (FIR) filters to SFSP to deal with higher-order plants. Later, in Torrico et al. (2018), an elegant tuning procedure was developed to design the robustness filter of the SFSP focusing on industrial applications. Finally, recently the SFSP was extended to a state space representation in order to deal with high-order *Non-minimum phase* (NMP) processes (TORRICO et al., 2021).

Dead-time compensators continue to be a widely explored field of study today due to their ability to improve the performance and robustness of systems with dead time, combined with simplified implementation. Also, its characteristics of ease tuning of parameters and a good trade-off between disturbance rejection, robustness, and noise attenuation are desirable to be achieved in control systems, and any proposals for the improvements of these characteristics are very important for the control of dead-time systems. Furthermore, its characteristics of ease tuning of parameters and a good trade-off between disturbance rejection, robustness and noise attenuation are desirable to be achieved in any control system, so any proposals to improve these characteristics are important for the control of dead-time systems.

1.1 Motivation

In the field of dead-time processes control, the problem of designing and tuning controllers is directly attached to the complexity of the processes models, which means that the search for more simpler structures, designs and tunings for high-order process with dead-time is a constantly necessity.

Additionally, there is also a need to improve the disturbance rejection responses of control systems. Consequently, multivariable control and *Linear parameter-varying* (LPV) control of dead-time process presents itself as one of the more suitable alternatives for achieving improvements in disturbance rejection.

1.2 Objectives

The main objectives of this work is to propose SFSP-based controllers that can deal with high-order dead-time processes and that can obtain faster disturbance rejection responses by using series cascade control, parallel cascade control, two-input two-output (TITO) control and LPV control. To achieve this purpose, this text aims at:

- to presents a new series cascade control system for stable, integrating, and unstable processes with dead-time;
- to presents a new parallel cascade control system based on the extension of the discrete version of the SFSP (TORRICO et al., 2021) suitable for stable, integrating, and unstable processes with dead-time;
- to presents a new TITO control system based on the generalized predictive control (GPC) suitable for stable, integrating, and unstable processes with dead-time;
- to show that the proposed TITO control can improve the disturbance rejection by the addition of an FIR filter;
- to explore the modeling of nonlinear time-delay systems into a LPV framework;
- to extend the SFSP controller for LPV I/O systems keeping its main features and advantages;
- to show that all proposed controllers has the same tuning degrees of freedom as the original SFSP.

1.3 Organization of the work

The remaining of this manuscript is organized as follows. In Chapter 2 an overview of dead time compensators is provided and in Chapter 3 a summary of LPV control systems is presented, including DTC controllers for dead-time LPV systems. The proposed SFSP structure for series cascade discrete dead-time process is presented in Chapter 4, the extension of the SISO SFSP for parallel cascade dead-time discrete process is proposed in Chapter 5, a dead-time compensator for TITO process based on GPC is proposed and discussed in Chapter 6, and a method for design an LPV-SFSP is provided in Chapter 7. Finally, the conclusions and further steps are presented in Chapter 8.

2 DEAD-TIME COMPENSATORS

Several problems may arise when dealing with dead-time systems and the use of a traditional controller, such as PID, must require conservative adjustments in order to guarantee the stability of the closed loop system. Before to address this issue, first consider the closed-loop system represented by the block diagram in Figure 1.

Figure 1 – Representation of a traditional control system with delay.

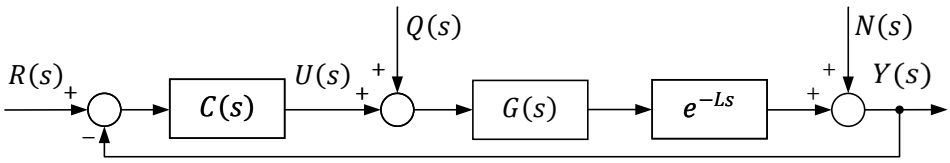

Source: The author.

The nominal process is denoted by $P = G(s)e^{-Ls}$, where $G(s)$ is called *fast process* and $L \in \mathbb{R}$ is the dead-time. The primary controller $C(s)$ is designed by traditional methods and can be structured as PI or PID. The signals $R(s)$, $U(s)$, $Q(s)$ and $N(s)$ represent the setpoint, control effort, disturbance and noise respectively. The closed-loop relations are given by:

$$H_{yr}(s) = \frac{Y(s)}{R(s)} = \frac{C(s)P(s)}{1+C(s)P(s)}, \tag{2.1}$$

$$H_{yq}(s) = \frac{Y(s)}{Q(s)} = \frac{P(s)}{1+C(s)P(s)}. \tag{2.2}$$

It is important to note that the delay L directly influences the dynamics of the system, participating in the calculation of the poles of the system, as it is part of both characteristic equations. This may reduces the phase margin of the closed-loop system and even leads to instability, since $\angle H_{yq}(j\omega_c)$ changes for every frequency ω_c. As an example, consider the process of a heated tank proposed in Normey-Rico and Camacho (2007) with

$$P(s) = \frac{1}{(1.5s+1)(0.4s+1)}e^{-Ls}, \tag{2.3}$$

and a PI controller such as

$$C(s) = K_p\frac{sT_i+1}{sT_i}. \tag{2.4}$$

The performance specification for the controlled response is a overshoot less than 5 %. First, it is considered the case without delay, that is $L = 0$, where the PI controller is tuned with

$K_p = 1$ and $T_i = 1.2$. The system response is shown in Figure 2a and the control effort is shown in Figure 2b (solid lines) which show a performance that meets the stipulated specifications. However, if the delay is increased to $L = 1.5$ s, then it can be seen that the system response becomes oscillatory, which is also shown in Figure 2 (dashed line). To improve this behavior, one can increase T_i or decrease K_p, as this makes the controller less aggressive and consequently reduces oscillations. However, this change in the gains also slows down the response, as can be seen in Figure 2 (dash-dotted line).

Figure 2 – Step response and control effort for variations of L, K_p, and T_i.

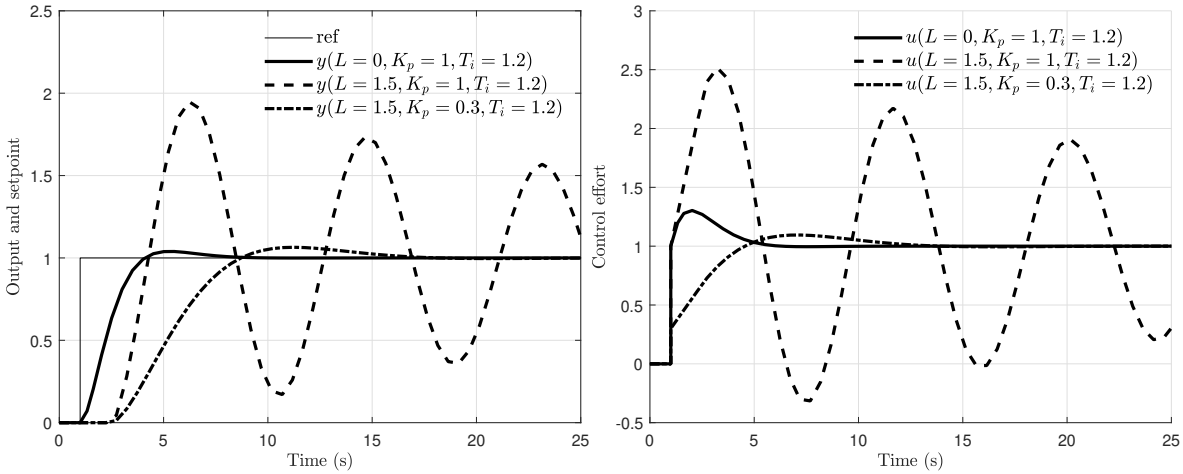

(a) (b)

Source: The author.

These changes in system response behavior can also be observed in frequency domain. In Figure 3 it is possible to see the frequency response for all previously situations considered in Figure 2. Initially take the system without delay ($L = 0$), where the phase margin is $PM = 67.5761^\circ$ at crossover frequency $\omega_{c1} = 0.7192$ rad/s. Note that after the delay is considered, the phase margin suffers a great decreasing to $PM = 5.7690^\circ$ at $\omega_{c2} = 0.7192$ rad/s, which results to a poor damping. Finally, after the controller redesign $(K_p = 0.3)$, to obtain a non oscillatory response, the PM is improved to $PM = 59.7343^\circ$ at frequency $\omega_{c3} = 0.2435$ rad/s, which causes a slower transient after the dead time, explaining the slow behavior in time domain.

Figure 3 – Step response and control effort for variations of L, K_p, and T_i.

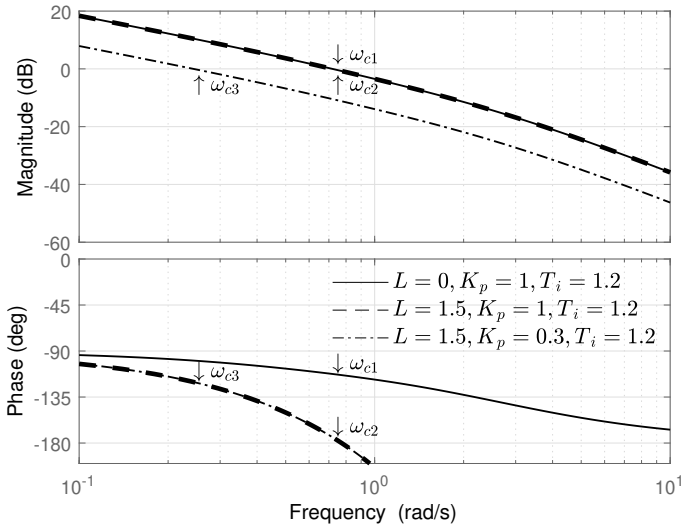

Source: The author.

This example is intended to demonstrate how delay can affect the closed-loop response of a control system. The solution to the decreasing PM is to change the gains of the controller, but if a faster response is required the solution may be increase the order of the controller, which can bring difficulties because is an endless process (NORMEY-RICO; CAMACHO, 2007).

2.1 The Smith predictor

As discussed in the previous section, in order to guarantee stability in dead-time systems using traditional controllers, conservative tuning is required. Thus, to deal with this problem, a different approach was proposed by Smith (1957) which became the first DTC. This technique is based on the idea of the ideal solution for a dead-time process, that is, to remove the delay from the output feedback (NORMEY-RICO; CAMACHO, 2007). A block diagram of such ideal controller is shown in Figure 4.

Figure 4 – Representation of the ideal predictor based control structure.

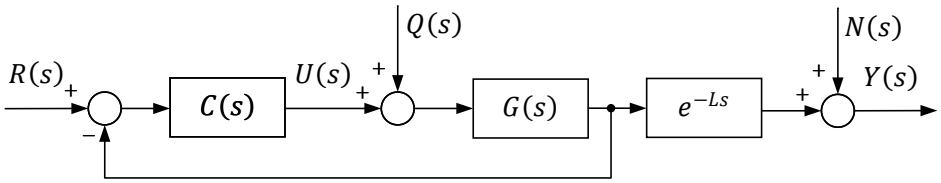

Source: The author.

As discussed in Normey-Rico and Camacho (2007), the implementation of the ideal controller is not possible due the impossibility of place a sensor in the right position for the cases where the dead time is part of the process, then a solution is to feed the output of process model to the controller as can be seen in Figure 5.

Figure 5 – Representation of the open-loop predictor based control structure.

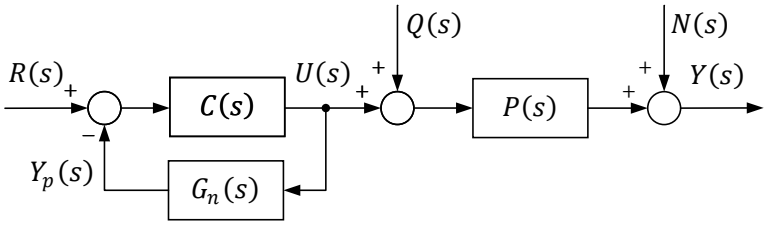

Source: The author.

where $G_n(s) = G(s)$ is a delay-free model of the plant and the tracking closed-loop relation is calculated as:

$$H_{yr}(s) = \frac{Y(s)}{R(s)} = \frac{C(s)P(s)}{1+C(s)G(s)}, \tag{2.5}$$

However, these types of controllers have the disadvantage of not being able to be used in practical situations due to model errors and they do not present guarantees of robustness and disturbance rejection since there is no feedback of the disturbed signal or the noisy output. Therefore, to overcome this issue, Smith (1957) proposed a modification in the controller which is now known as SP and it is shown in Figure 6

Figure 6 – Representation of a the Smith predictor controller structure.

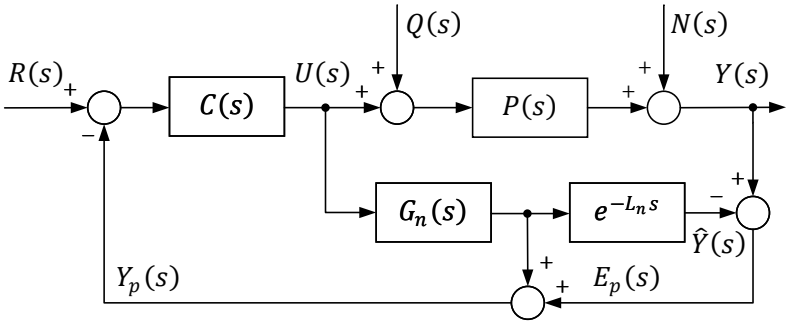

Source: The author.

The structure contains a primary controller $C(s)$ and a predictor, which is composed by the fast model $G_n(s)$ and a model of the dead time e^{-Ls}. The signal $E_p(s) = Y(s) - \hat{Y}(s)$ is the

prediction error and is add to the control loop in order to deal with model uncertainties or input disturbances. For this structure, the primary controller $C(s)$ can be design to $G(s)$, that is the plant with no delay (NORMEY-RICO; CAMACHO, 2008).

From Figure 6, the input-output transfer functions for the SP in the nominal case are given by:

$$H_{yr}(s) = \frac{Y(s)}{R(s)} = \frac{C(s)G_n(s)e^{-L_n s}}{1+C(s)G_n(s)}, \tag{2.6}$$

$$H_{yq}(s) = \frac{Y(s)}{Q(s)} = G_n(s)e^{-L_n s}\left[1 - \frac{C(s)G_n(s)e^{-L_n s}}{1+C(s)G_n(s)}\right]. \tag{2.7}$$

From these relations, it can be seen that since $C(s)$ is a controller with only one degree of freedom, then it is not possible to define the setpoint response and the perturbation rejection response separately. Considering the equation (2.7) it can be noted that the poles of $G_n(s)$ directly influence the disturbance rejection response, which means that: (i) if the open-loop system $P(s)$ has a dynamic slower than the closed-loop system then it will dominate the disturbance rejection response and no controller $C(s)$ can interfere with the speed of this transient; (ii) the structure of the control system in Figure 6 is not internally stable when is considered open-loop unstable or integrative processes; and (iii) the SP controller is not able to reject step-like disturbances for integrative processes.

Another aspect to consider in order to properly design the SP is that, since it is a based model controller, modeling errors can appear and should be included in the analyzes of stability and robustness. Thus, a set of transfer functions is considered to describe unstructured additive or multiplicative uncertainties in the model. For the nominal process $P_n(s)$ the set of models may be given by:

$$P_i(s) = P_n(s) + \Delta P_i(s) \tag{2.8}$$

or

$$P_i(s) = P_n(s)(1 + \delta P_i(s)) \tag{2.9}$$

where $\Delta P_i(s)$ and $\delta P_i(s)$ are the additive and multiplicative errors, respectively. These modeling errors are bounded by their maximum values $|\overline{\Delta P(s)}|$ and $|\overline{\delta P(s)}|$, respectively, which are given by:

$$|\overline{\Delta P(s)}| \geq |\Delta P_i(s)|, \quad s = j\omega, \quad \omega > 0, \tag{2.10}$$

and

$$|\overline{\delta P(s)}| \geq |\delta P_i(s)|, \quad s = j\omega, \quad \omega > 0. \tag{2.11}$$

The SP structure in Figure 6, can be reduced to an analogous form by manipulating the diagram blocks in order to obtain an equivalent form to the controller such as in Figure 7.

Figure 7 – Equivalent form for the closed-loop system with SP.

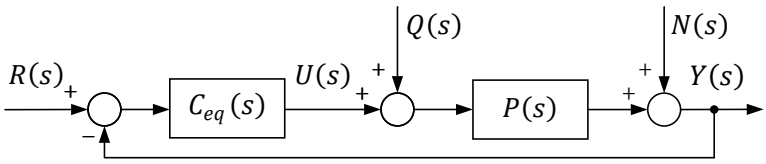

Source: The author.

where the equivalent controller in is given by

$$C_{eq} = \frac{C(s)}{1 + C(s)(G_n(s) - P_n(s))}. \tag{2.12}$$

Considering the condition for robust stability for additive uncertainty proposed by (MORARI; ZAFIRIOU, 1989):

$$|\Delta P(j\omega)| < \frac{|1 + C_{eq}(j\omega)G_n(j\omega)|}{|C_{eq}(j\omega)|}, \quad \forall\ \omega > 0 \tag{2.13}$$

or for multiplicative uncertainty:

$$|\delta P(j\omega)| < \frac{|1 + C_{eq}(j\omega)G_n(j\omega)|}{|C_{eq}(j\omega)G_n(j\omega)|}, \quad \forall\ \omega > 0 \tag{2.14}$$

and by using Equation (2.12) it is possible to define a robustness index for the SP such as:

$$I_R(\omega) = \frac{|1 + C(j\omega)G_n(j\omega)|}{|C(j\omega)|} > |\Delta P(j\omega)|, \quad \forall\ \omega > 0 \tag{2.15}$$

and

$$i_R(\omega) = \frac{|1 + C(j\omega)G_n(j\omega)|}{|C(j\omega)G_n(j\omega)|} > |\delta P(j\omega)|, \quad \forall\ \omega > 0, \tag{2.16}$$

which defines a graphical criterion to analyze controller tuning considering robust stability. Thus, an aggressive adjustment of the controller is indicated by a robustness index graph next to the considered uncertainty graph. It is worth mentioning that the case in which the robustness index graph crosses the uncertainty graph does not necessarily indicate that instability will exist, but it is a strong indication that the controller adjustment does not provide adequate robustness. Therefore, from these equations it can be inferred that if the primary controller $C(s)$ is designed for a fast tracking then the robustness index can violate conditions 2.15 or 2.16 which may brings poor robustness and even causes instability for small errors in the modeling, which means that the SP should be taking into account a trade off between tracking and robustness.

Considering the overall discussion, some properties can be inferred from SP when is considered the nominal case, that is $G_n(s) = G(s)$ and $L_n = L$, which provides an improvement in the performance of dead-time process comparing with traditional controllers:

1. *Dead-time compensation*: The delay L does not appear in the characteristic equation, for the nominal case, which means a certain compensation in the decreasing of the phase margin.

2. *Prediction*: The signal $Y_p(s)$ acts in the anticipation of the system output for changes in the setpoint, but not for disturbances. If $E_p(s) = 0$, which means the case with no disturbances $Q(s) = 0$, the feedback signal $Y_p(s) = \hat{Y}(s)e^{L_n s}$ and the controller can anticipate the output $Y(s)$ for changes in the setpoint. However, when both $R(s)$ and $Q(s)$ exists, $Y_p(s) = \hat{Y}(s)e^{L_n s} + P_n(s)[Q(s) - Q(s)e^{L_n s}]$. As discussed in Normey-Rico and Camacho (2007), this prediction can still be valid if there is a disturbance with slow variations, that is $Q(s) \simeq Q(s)e^{L_n s}$. However, if this variation is considered fast enough, then the disturbance signal cannot be taken from the feedback and the prediction is no longer valid.

3. *Ideal dynamic compensation*: The SP structure consists in the separation of process model and dead time model. By considering the idea of an ideal controller, that is, one with infinity gain, calculated as:

$$\frac{C(s)}{1 + C(s)G_n(s)} = (G_n(s))^{-1}, \tag{2.17}$$

then the ideal process output is given by

$$Y(s) = R(s)e^{-L_n s} + [G_n(s)e^{-L_n s} - G_n(s)e^{-2L_n s}]Q(s), \tag{2.18}$$

which means that the SP ideal transfer function for tracking is a simple delay and for disturbance rejection is determined, from $t = 0$ to $t = 2L_n$, by the open-loop behavior and then the control action on the output can take place. This ideal performance is unattainable, as it is achieved through a very aggressive tuning, which can lead to high control signals even for small model uncertainties.

2.2 The filtered Smith predictor

In order to deal with some of the drawbacks of the SP, in Normey-Rico, Bordons and Camacho (1997) it was proposed the FSP, which is represented in Figure 8.

Figure 8 – The filtered Smith predictor control structure.

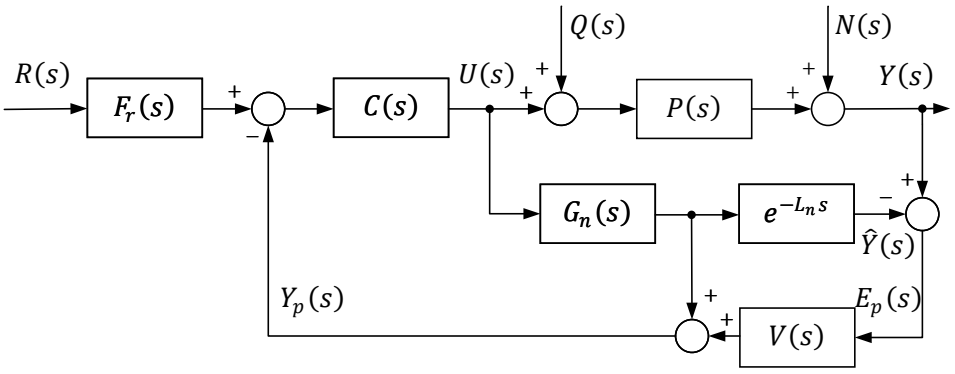

Source: The author.

The main difference from SP is the insertion of a robustness filter $V(s)$. The transfer functions for the FSP are given by:

$$H_{yr}(s) = \frac{Y(s)}{R(s)} = \frac{F_r(s)C(s)G_n(s)e^{-L_n s}}{1 + C(s)G_n(s)}, \tag{2.19}$$

and

$$H_{yq}(s) = \frac{Y(s)}{Q(s)} = G_n(s)e^{-L_n s}\left[1 - \frac{V(s)C(s)G_n(s)e^{-L_n s}}{1 + C(s)G_n(s)}\right], \tag{2.20}$$

and the robustness index is calculated as:

$$i_R(\omega) = \left|\frac{1 + C(s)G_n(s)}{V(s)C(s)G_n(s)}\right|_{s=j\omega}, \quad \forall\ \omega > 0. \tag{2.21}$$

From these equations, some properties can be inferred for the FSP:

1. The tracking is defined by the controller $C(s)$ and the reference filter $F_r(s)$;
2. The robustness filter $V(s)$ can be tuned to eliminate the undesired poles of unstable or integrative process model $G_n(s)$ from the disturbance rejection response;
3. As $V(s)$ appears in both $H_{yq}(s)$ and $i_R(\omega)$, this means that this filter must be designed according to a compromise between disturbance rejection and robustness.

Although the FSP has been presented in continuous time, the dead time in (2.19) and (2.20) turns them into non-rational transfer functions, which means that it can be difficult the cancellation of the model process by $V(s)$. Therefore, practical implementations of the FSP only take place in discrete time, with sampling time T_s chosen considering the lower time constant

of the process model. Thus, for the discrete nominal model $P_n(z) = G_n(z)z^{-d_n}$, one may get closed-loop relations such as:

$$H_{yr}(z) = \frac{Y(z)}{R(z)} = \frac{F_r(z)C(z)G_n(z)z^{-d_n}}{1+C(z)G_n(z)}, \tag{2.22}$$

and

$$H_{yq}(z) = \frac{Y(z)}{Q(z)} = G_n(z)z^{-d_n}\left[1 - \frac{V(z)C(z)G_n(z)z^{-d_n}}{1+C(z)G_n(z)}\right], \tag{2.23}$$

and

$$i_R(\omega) = \left|\frac{1+C(z)G_n(z)}{V(z)C(z)G_n(z)}\right|_{z=e^{j\omega T_s}}, \quad 0 < \omega < \pi/T_s, \tag{2.24}$$

where $F_r(z)$, $C(z)$ and $V(z)$ are the discrete time reference filter, primary controller and robustness filter respectively. It is also possible to rearrange the FSP block diagram, Figure 8, in an equivalent structure according to Figure9.

Figure 9 – Equivalent form for the closed-loop system with FSP.

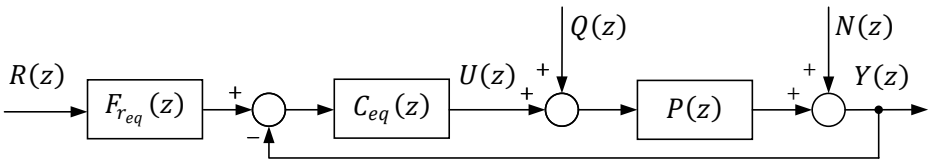

Source: The author.

with

$$F_{r_{eq}}(z) = \frac{F_r(z)}{V(z)}, \tag{2.25}$$

and

$$C_{eq}(z) = \frac{V(z)C(z)}{1+C(z)G_n(z)[1-V(z)z^{-d_n}]}. \tag{2.26}$$

For the nominal process, the closed-loop performance is tied to the behavior of both the steady-state error and the disturbance rejection. Considering a step response and a step-like disturbance, in order to guarantee the null steady state error, some conditions must be met: (i) $C_{eq}(z)$ must have at least one pole in $z = 1$, which can be achieved by imposing this pole in $C(z)$; (ii) and the reference equivalent filter must have unitary gain, that is, $F_{r_{eq}}(z)|_{z=1} = 1$, which is accomplished with a condition tuning for the reference filter $F_r(z)$ and for robustness filter $V(z)$ that provides an unitary static gain, which means that $F_r(z)|_{z=1} = 1$ and $V(z)|_{z=1} = 1$.

The filter $V(z)$ can also be tuned to deal with some drawbacks of the SP, namely: (i) define a trade-off between robustness and disturbance rejection; (ii) eliminate slow or unstable poles of the process model considering the disturbance rejection response; (iii) ensure disturbance rejection for integrative processes.

Although with the insertion of the filter $V(z)$ the FSP is mathematically capable of handling disturbance rejection for unstable or integrative open-loop processes, the structure of the control system represented in Figure 8 is not internally stable due to the process model $G_n(z)$ appearing explicitly in the disturbance rejection transfer function H_{yq} in (2.23). Therefore, an equivalent structure for implementation should be used, as proposed in Normey-Rico and Camacho (2009), which is represented in Figure 10,

Figure 10 – Discrete-time equivalent implementation structure for the filtered Smith predictor.

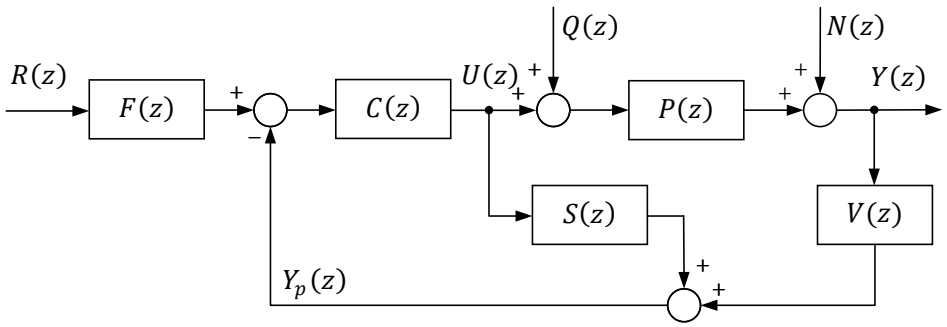

Source: The author.

where

$$S(z) = G_n(z)[1 - V(z)z^{-d_n}]. \tag{2.27}$$

Supposing a stable $S(z)$, then the controller structure in Figure 10 becomes internally stable for all kind of process (stable, unstable and integrative), since the primary controller $C(z)$ acts in the stabilization of the process $G_n(z)$, in other words, a stable $S(z)$ means that $H_{yq}(z)$ is also stable. Note that the task of making $S(z)$ stable is up to the robustness filter $V(z)$, so it is necessary that the filter tuning meets certain conditions so that slow or unstable poles are eliminated from the delay free model $G_n(z)$ in the disturbance rejection response. For open-loop stable or unstable processes, this can be achieved with the following condition of the process model pole cancellation:

$$\left[1 - V(z)z^{-d_n}\right]\Big|_{z=p_i} = 0, \tag{2.28}$$

where p_i are the undesired poles of $G_n(z)$, and for integrative process the condition is

$$\frac{d}{dz}\left[1 - V(z)z^{-d_n}\right]\Big|_{z=1} = 0. \tag{2.29}$$

Since these conditions are used to eliminate some unwanted poles of $G_n(z)$ then they are used to obtain only the zeros of $V(z)$. The poles of the robustness filter are design parameters, being a free choice of the designer. However, despite being free, this choice can cause several problems from a performance point of view. As an example, consider that the controller $C(s)$ is designed for a fast closed-loop response, so this certainly affects the robustness of the system. Thus, if the filter $V(s)$ is designed as a low-pass filter then the choice of small values can increase the robustness of the system in high frequencies, but at the same time it makes the response to disturbances slower. Thus, it can be concluded that the choice of poles of the filter $V(z)$ must meet a compromise between robustness and perturbation rejection.

2.3 The simplified filtered Smith predictor

2.3.1 Review of the discrete SFSP

The structure of the SFSP, proposed by Torrico et al. (2013b) and discussed in Torrico et al. (2021), is illustrated in Figure 11, where $P(z)$ represents the discrete process, $G(z)$ is the free-delay model of the process, d denotes the dead time, k and k_r are static gains that compose the primary controller, and $V(z)$ is a filter that ensures predictor stability and disturbance attenuation. The signals $R(z)$, $Q(z)$, $N(z)$, and $Y(z)$ are the reference, input disturbance, output disturbance, and process output, respectively. In this review, the model $G(z)$ is given by:

$$G(z) = \frac{b}{z-a}. \tag{2.30}$$

Figure 11 – Conceptual structure of the SFSP.

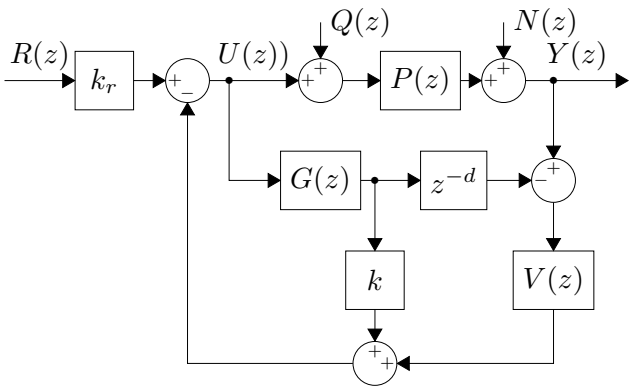

Source: The author.

The control design follows two steps: i) for setpoint tracking and ii) for attenuating disturbances. In both cases, it is assumed that there is no model mismatch, which means, $P(z) = G(z)z^{-d}$.

2.3.1.1 Setpoint tracking

For the nominal case, the desired closed-loop transfer function from the setpoint to the output is defined as:

$$\frac{Y(z)}{R(z)} = \frac{k_r b}{z-p} z^{-d}, \tag{2.31}$$

where p is the desired closed loop pole. While the closed-loop transfer function from the setpoint to the output of the SFSP is:

$$H_{yr}(z) = \frac{k_r b\, z^{-d}}{z+kb-a}, \tag{2.32}$$

thus, to Equation (2.32) be equivalent to Equation (2.31), then:

$$k = \frac{a-p}{b}. \tag{2.33}$$

Since the SFSP has no explicit integral controller, then the static gain k_r has the task of guarantee zero error in tracking steady state. Thus, k_r is calculated such as $H_{yr}(1) = 1$, which brings to:

$$k_r = \frac{1-p}{b}. \tag{2.34}$$

2.3.1.2 Disturbance attenuation

To proper analyze the disturbance attenuation properties, the transfer function between the input disturbance and the output is calculated for the nominal case ($P(s) = G(s)e^{-Ls}$) as in the following:

$$\frac{Y(z)}{Q(z)} = \frac{b}{z-a} z^{-d} \left[1 - \frac{k_r b}{z-p} z^{-d} V(z) \right]. \tag{2.35}$$

Assuming that

$$V(z) = \frac{b_1 z + b_2}{(z-\alpha)^{n_v}}, \tag{2.36}$$

where $0 < \alpha < 1$ is a free tuning parameter to set the settling time of the disturbance attenuation response and n_v is the filter order, and from Equation (2.35), it is possible to see that the disturbance attenuation is mainly affected by the filter $V(z)$, which plays two roles i) defines the dynamics of the disturbance attenuation response and the steady-state error; and ii) cancels the undesired model pole from the predictor structure. Thus, from Figure 11, it is possible to calculate the equivalent controller for the SFSP such as:

$$C_{eq} = \frac{V(z)}{1 + G(z)(k - V(z)z^{-d}}, \tag{2.37}$$

which can lead to the following conditions for tuning $V(z)$ (TORRICO et al., 2013b; TORRICO et al., 2019):

$$\frac{d^n}{dz^n}\left[1+G(z)\left(k-V(z)z^{-d}\right)\right]\Big|_{z=1}=0, \tag{2.38}$$

$$k-V(z)z^{-d}\Big|_{z=a}=0. \tag{2.39}$$

where $n=0$ for stable and unstable processes ($a\neq 1$) and $n=1$ for integrative processes ($a=1$). Note that (2.38) is intended to include integral action to the equivalent controller so that constant disturbances can be rejected at a steady state while (2.39) to avoid a be a pole of the predictor.

2.3.2 SFSP for high order process

In Torrico, Correia and Nogueira (2016) and Torrico et al. (2018) was proposed a new structure for the SFSP which can deal with dead-time processes of any order, which is represented in Figure 12,

Figure 12 – Discrete-time structure for the simplified filtered Smith predictor for systems of any order.

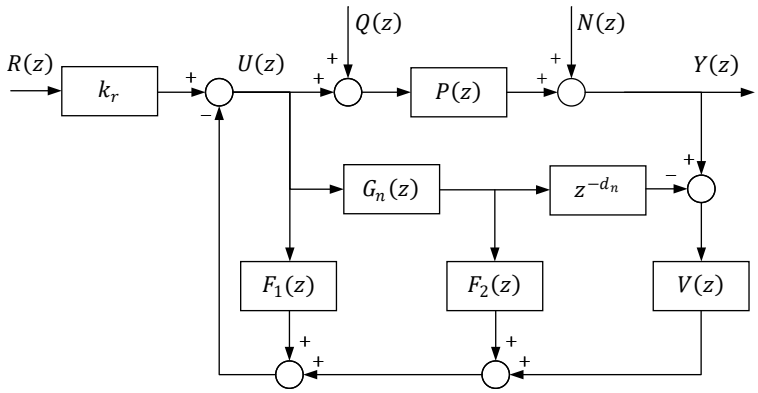

Source: The author.

where $P(z)$ is the real process and $P_n(z)=G_n(z)z^{-d_n}$ is the the nominal process model, with $G_n(z)$ being the fast process model and d_n the model of the dead time. The controller is composed by the constant k_r, the finite impulse response (FIR) filters $F_1(z)$ and $F_2(z)$, and the robustness filter $V(z)$. From the diagram in Figure 12, and for the nominal case $P(z)=P_n(z)$, it is possible to infer the following transfer functions:

$$H_{yr}(z)=\frac{Y(z)}{R(z)}=\frac{k_rP_n(z)}{1+F_1(z)+G_n(z)F_2(z)}, \tag{2.40}$$

$$H_{yq}(z)=\frac{Y(z)}{Q(z)}=P_n(z)\left[1-\frac{P_n(z)V(z)}{1+F_1(z)+G_n(z)F_2(z)}\right], \tag{2.41}$$

$$H_{un}(z) = \frac{U(z)}{N(z)} = \frac{-V(z)}{1 + F_1(z) + G_n(z)F_2(z)}, \tag{2.42}$$

$$I_r(\omega) = \left| \frac{1 + F_1(z) + G_n(z)F_2(z)}{G_n(z)V(z)} \right|_{z=e^{j\omega T_s}} > \overline{\delta P}(e^{j\omega T_s}), \tag{2.43}$$

where $Y(z)$, $R(z)$, $Q(z)$, $U(z)$, and $N(z)$ are the Z-transform of the process output, reference signals, input load disturbance, control action and measurement noise, respectively. The robustness index $I_r(\omega)$ is defined in terms of the upper bound of the multiplicative uncertainty norm $\overline{\delta P}(e^{j\omega T_s})$. T_s is the simple time and the frequency must be in $0 < \omega < \pi/T_s$.

The design of the controller is also made by two steps: (i) Calculate k_r and the coefficients of the FIR filters $F_1(z)$ and $F_2(z)$ in order to obtain the desired tracking and (ii) Tuning of the robustness filter $V(z)$ in order to deal with disturbance rejection and to attenuate the effect of measurement noise, always considering a trade-off between robustness and disturbance rejection provided by the analysis of the robustness index $I_r(\omega)$.

For the desired tracking, first considering that the FIR filters $F_1(z)$ and $F_2(z)$ are given by:

$$F_1(z) = f_{1_1} z^{-1} + f_{1_2} z^{-2} + \cdots + f_{1_n} z^{-n+1}, \tag{2.44}$$

$$F_2(z) = f_{2_0} + f_{2_1} z^{-1} + \cdots + f_{2_n} z^{-n+1}, \tag{2.45}$$

where n is the order of $G_n(z)$. It is possible to note that if $F_1(z) = 0$ and $F_2(z) = f_{2_0}$ the result controller is equivalent to the one proposed in Torrico et al. (2013a). In order to compute the filters coefficients one may use a pole placement approach, so the following matrix equation was proposed in Torrico, Correia and Nogueira (2016) and Torrico et al. (2018):

$$x = \Phi^{-1} y \tag{2.46}$$

where

$$\Phi = \begin{bmatrix} 1 & 0 & \cdots & 0 & b_1 & \cdots & 0 \\ a_1 & 1 & \cdots & \vdots & b_2 & \cdots & \vdots \\ \vdots & a_1 & \cdots & 0 & \vdots & \cdots & 0 \\ a_n & \vdots & \cdots & 1 & b_n & \cdots & b_1 \\ 0 & a_n & \cdots & a_1 & 0 & \cdots & \vdots \\ 0 & 0 & \cdots & a_n & 0 & \cdots & b_n \end{bmatrix}, \quad x = \begin{bmatrix} f_{1_1} \\ \vdots \\ f_{1_{n-1}} \\ f_{2_0} \\ \vdots \\ f_{2_{n-1}} \end{bmatrix}, \quad \text{and} \quad y = \begin{bmatrix} c_1 - a_1 \\ \vdots \\ c_n - a_n \\ c_{n+1} \\ \vdots \\ c_{2n-1} \end{bmatrix}. \tag{2.47}$$

$\underbrace{}_{n-1}$ $\underbrace{}_{n}$

The matrix Φ must be non-singular, square with dimension $2n-1$, and composed by the elements of

$$G_n(z) = \frac{b_1 z^{-1} + b_2 z^{-2} + \cdots + b_n z^{-n}}{1 + a_1 z^{-1} + a_2 z^{-2} + \cdots + a_n z^{-n}}, \tag{2.48}$$

and the coefficients $c_1 \cdots c_{2n-1}$ in y, are given by a desired characteristic equation such as:

$$1 + c_1 z^{-1} + c_2 z^{-2} + \cdots + c_{2n-1} z^{-2n+1} = (1 - r_1 z^{-1})(1 - r_2 z^{-1}) \cdots (1 - r_{2n-1} z^{-1}). \tag{2.49}$$

It should be noted that the desired closed-loop poles $r_1 \cdots r_{2n-1}$ must be in $0 \leq r_i \leq 1$ and are responsible for the tracking dynamics, which means that for a aggressive/robust tracking, one may chose smaller/higher values of r_i. Finally, For a zero steady error in the tracking, the gain k_r is calculate as:

$$k_r = \frac{1 + F_1(1) + G_n(1)F_2(1)}{P_n(1)}. \tag{2.50}$$

The robustness filter was proposed such as Torrico et al. (2018):

$$V(z) = \frac{v_0 + v_1 z^{-1} + \cdots + v_n z^{-n}}{(1 - \beta z^{-1})...(1 - \beta_{n+1} z^{-1})} \tag{2.51}$$

where the numerator is designed to attend some conditions:

1. Ensure a proper step-like disturbances rejection to guarantee the tracking. Thus, at $z = 1$, it must be equal to zero, which means:

   $$V(1) = k_r = \frac{1 + F_1(1) + F_2(1)}{P_n(1)}. \tag{2.52}$$

2. Eliminate slow or unstable poles from the $P_n(z)$ model so that they do not appear in the disturbance rejection response.

   $$\left[1 - \frac{P_n(z)V(z)}{1 + F_1(z) + G_n(z)F_2(z)}\right]_{z=p_i \neq 1} = 0, \tag{2.53}$$

   and

   $$\frac{d}{dz}\left[1 - \frac{P_n(z)V(z)}{1 + F_1(z) + G_n(z)F_2(z)}\right]_{z=p_i=1} = 0, \quad i = 1, \cdots, n, \tag{2.54}$$

   where p_i are the n undesired poles of $P_n(z)$ to be canceled, which leads to a set of $n+1$ equations (considering Equations (2.52), (2.53) and (2.54)) to calculate the coefficients $v_0 \cdots v_n$. For the cases where one must consider to track higher order references and/or to reject higher order disturbances such as ramps, parabolas, etc., the FIR filters also must be designed with higher order. Finally, the free tuning parameter *beta* must be choose consider the trade-off between robustness and disturbance rejection.

2.3.3 Reformulation of the SFSP

The SFSP (TORRICO et al., 2013b) was reformulated as a state space predictor (TORRICO et al., 2019), which allows working with higher order SISO systems. The structure of the controller for the process

$$P_r(z) = G_r(z) z^{-d}, \tag{2.55}$$

where $G(z)$ represents the dynamic without the delay d is shown in Figure 13

Figure 13 – SFSP structure control.

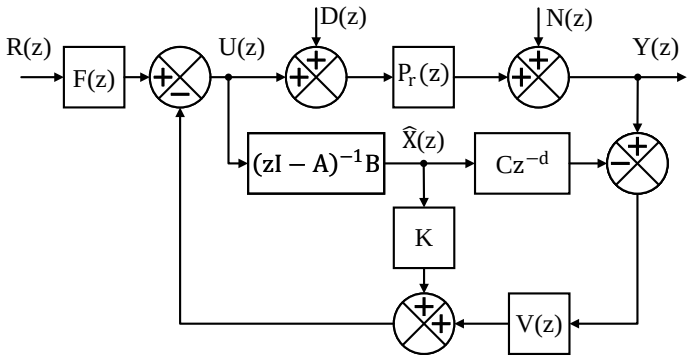

Source: The author.

The nominal process model $(P(z) = P_r(z))$ is given by

$$P(z) = \frac{b_n z^{n-1} + b_{n-1} z^{n-2} + \cdots + b_2 z + b_1}{z^n + a_n z^{n-1} + \cdots + a_2 z + a_1} z^{-d} = C(zI - A)^{-1} B z^{-d}, \tag{2.56}$$

where the pairs (A,B) and (C,A) must to be controllable and observable, respectively. In this work, the matrices A, B and C are in the canonical observable form.

The primary controller of the SFSP is composed by a feedback gain K, used to control the free-delay model, and reference filter $F(z)$, which adds a freedom degree to improve setpoint tracking. A robustness filter $V(z)$ is designed for both disturbance attenuation and to achieve a desired trade-off between robustness and performance, at steady state.

2.3.3.1 Primary controller tuning

Considering the nominal process P, the reference tracking response is computed as

$$H_{yr}(z) = F(z)C(zI - A + BK)^{-1} B z^{-d}. \tag{2.57}$$

The primary controller K can be tuned based on pole allocation techniques to obtain the desired characteristic polynomial

$$C_p = \prod_{i=1}^{n} (z - p_i) = \det(zI - A + BK), \tag{2.58}$$

where p_i represents the desired closed-loop poles. To obtain the gain K, one can use any method for pole allocation such as the Ackermann formula (ACKERMANN, 1977):

$$K = [0\ 0\ \ldots\ 1] \left[B\ AB\ \ldots\ A^{n-1}B\right]^{-1} C_p(A). \tag{2.59}$$

2.3.3.2 *Reference filter*

The reference filter can improve the tracking performance without affecting disturbance rejection. As this work does not focus on setpoint tracking, then $F(z)$ is chosen constant to guarantee $H_{yr}(1) = 1$, that is

$$F(z) = f_r = \left[C(I - A + BK)^{-1}B\right]^{-1}. \tag{2.60}$$

2.3.3.3 *Robustness filter*

As discussed in Torrico et al. (2021), for a properly design of the filter $V(z)$, the block diagram from Figure 13 was reduced to a 2DOF structure which has an equivalent controller calculated as

$$C_{eq}(z) = \frac{V(z)}{1 + S(z)}, \tag{2.61}$$

where

$$S = (K - z^{-d}V(z)C)(zI - A)^{-1}B. \tag{2.62}$$

This equivalent structure provided the definition of two design conditions for $V(Z)$: (1) the undesired zeros of $S(z)$, which came from the poles of $P(z)$, must be canceled and (2) the filter must reject any disturbance at steady state. Thus, to accomplish this goals, the following equations can be derived (TORRICO et al., 2013b; TORRICO et al., 2021)

$$\begin{cases} 1 + S(z)|_{z=p_i \neq 1} = 0, \\ 1 + S(z)|_{z=e^{\pm j\omega_k}} = 0, \\ \dfrac{d^k}{dz^k}(1 + S(z))|_{z=1} = 0, k = 0, \ldots, m-1, \end{cases} \tag{2.63}$$

where p_i represent the poles of the process and ω_k are the frequencies regarding sinusoidal disturbances. The parameter $m = m_1 + m_2$ express the sum of the number of model poles m_1 at $z = 1$ and the disturbance order m_2.

The robustness filter, is designed as the following transfer function form

$$V(z) = \frac{v_0 + v_1 z^{-1} + \ldots + v_{n_u} z^{-n_u}}{(1 - \alpha_1 z^{-1})(1 - \alpha_2 z^{-1})\ldots(1 - \alpha_{n_v} z^{-1})} \tag{2.64}$$

where number of poles is given by the inequality $n_v \leq n_u + 1$, in which $n_u + 1$ is the number of equations in (2.63). The coefficients of the filter $V(z)$ are calculated by a linear system derived from (2.63) and (2.64) and the poles α_i are free for tuning.

2.3.3.4 Stable implementation structure

The SFSP structure from Figure 13 is meant only for open loop stable process. As discussed in Torrico et al. (2021), to avoid internal instability for unstable and integrating process, it is used the structure represented in Figure 14,

Figure 14 – Implementation structure of SFSP for unstable and integrative process.

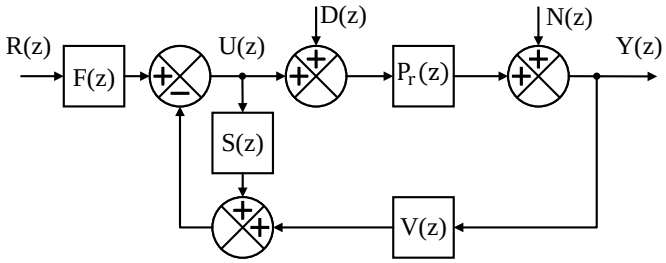

Source: The author.

where S can no longer be given by (2.62). Therefore, the implementation of $S(z)$ is extended for higher-order models with the following expression:

$$S(z) = \sum_{i=1}^{d} KA^{i-1}Bz^{-i} + V^*(z)z^{-d} \tag{2.65}$$

where

$$V^*(z) = \frac{N_v^*(z)}{D_v(z)} \tag{2.66}$$

The numerator of (2.66), $N_v^*(z)$, can be obtained from the following partial decomposition:

$$G(z)V(z) = \frac{N_g(z)N_v(z)}{D_g(z)D_v(z)} = \frac{N_g^*(z)}{D_v(z)} + \frac{N_v^*(z)}{D_g(z)},\ D_g(z) \neq D_v(z) \tag{2.67}$$

Thus, from (2.65), it is possible to see that the poles of $G(z)$ are no longer part of $S(z)$, which means that this structure guarantees internal stability.

2.3.3.5 Robustness analysis

For robust stability, the well known norm-bound multiplicative uncertainty condition is used, which can be defined as

$$\overline{\delta P}(e^{j\Omega}) < I_r(\omega) = \frac{\left|1 + C_{e_q}(e^{j\Omega})P(e^{j\Omega})\right|}{\left|C_{e_q}(e^{j\Omega})P(e^{j\Omega})\right|}, \tag{2.68}$$

where $I_r(\omega)$ is the robustness index and the parameter $\Omega = T_s\omega$ within a range defined as $[0, \pi]$. Substituting (2.61) and (2.62) into (2.68), then, it can be written as

$$\overline{\delta P}(e^{j\Omega}) < I_r(\omega) = \frac{\left|1 + K(e^{j\Omega}I - A)^{-1}B\right|}{\left|V(e^{j\Omega})G(e^{j\Omega})\right|} \tag{2.69}$$

from which it is possible to see that the robustness filter $V(z)$ is essential to achieve the desired robust stability condition.

2.4 Dead-time compensators for series cascade dead-time processes

A widely applied control strategy in various industrial processes for controlling pressure, temperature, and flow is cascade control (NANDONG; ZANG, 2014; KAYA; NALBANTOĞLU, 2016; SHOGA et al., 2019; CAMPOS-RODRÍGUEZ et al., 2019; MA; LI; ZHAO, 2020; ELAHI; ALFI, 2020). Franks and Worley (1956) were the first to present the cascade control structure (CCS) to improve the performance of systems when subjected to input disturbances. Series or parallel are the formats offered by this type of controller. The choice of format to use depends on how the processes are connected. In the series structure, a manipulated variable ($U(s)$) influences a controlled variable ($Y_2(s)$), which, in turn, affects a second controlled variable ($Y_1(s)$), as can be seen in Figure 15. Conversely, a manipulated variable ($U(s)$) in the parallel structure simultaneously influences both controlled variables ($Y_2(s)$ and $Y_1(s)$). This way, the control action to attenuate disturbances occurs faster than in conventional control with just a single feedback. Hence, the researchers developed papers focusing on these two strategies to control different types of processes.

Figure 15 – Block diagram of classical cascade series control system.

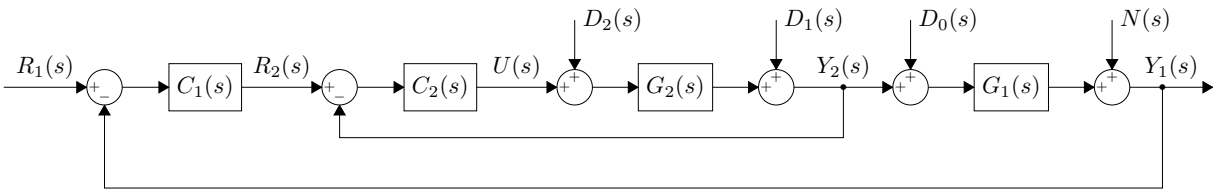

Source: The author.

Years later, Kaya (2001) was the first to propose a Smith predictor strategy in the outer loop, as can be seen in Figure 16, to improve a cascade control structure since it considered process models where delay had a value significant only in the outer loop. The results showed a considerable improvement compared to other methods used at the time; from there, this type of control strategy aroused the interest of many researchers.

Figure 16 – Improved cascade control system proposed in Kaya (2001).

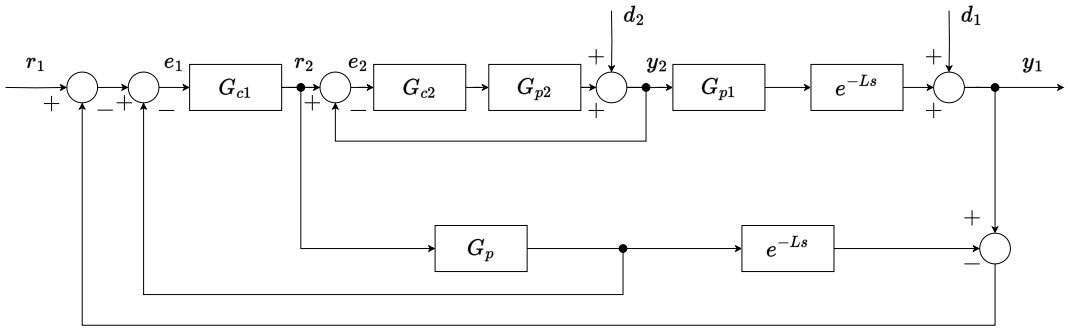

Source: Kaya (2001).

Next are some examples of integrative processes (UMA et al., 2010; PADHAN; MAJHI, 2013; RAJA; ALI, 2021). Uma et al. (2010) suggested a cascade control using a modified SP, which is shown in Figure 17. This structure has three controllers: G_{c2}, an internal model control (IMC) controller in the secondary loop, a primary setpoint controller G_{cs} designed as a proportional-integral-derivative (PID) with a lead-lag filter G_{cd}, and a disturbance rejection controller G_f designed as a proportional-derivative (PD) with a lead-lag filter.

Figure 17 – Modified Smith predictor structure proposed in Uma et al. (2010)

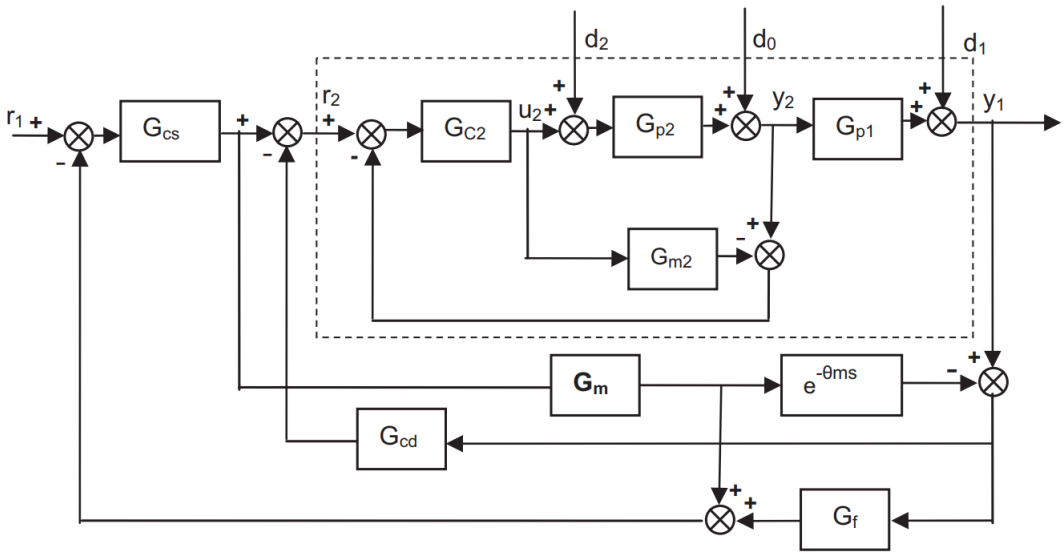

Source: Uma et al. (2010).

Padhan and Majhi (2013) presented a CCS with two controllers and a setpoint filter G_{c1}, showed in Figure 18. The inner loop controller G_{c2} uses the IMC approach, and for the primary load disturbance rejection controller, a PID controller in series with a lead/lag compensator G_{c3}.

Figure 18 – Series cascade control structure proposed in Padhan and Majhi (2013)

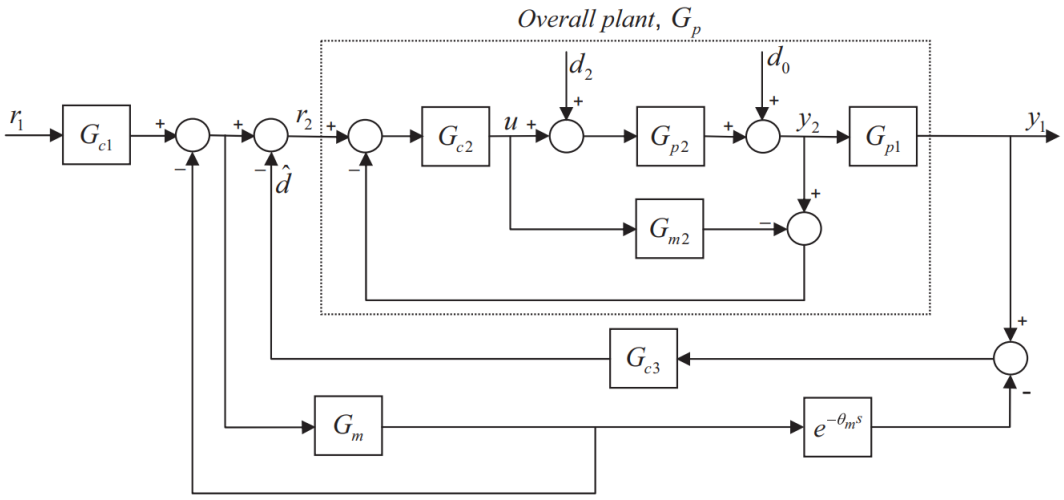

Source: Padhan and Majhi (2013).

Recently, Raja and Ali (2021) designed a CCS using strategies of Smith predictor, moment matching, and outer loop decomposition. A proportional-integral (PI) controller is employed in the loop having a first-order lag, whereas proportional (P) control is used if the loop contains an integrator. The controller structure is shown in Figure 19(a) for second-order integral with dead time (SOIWDT) and double integral with dead time (DIWDT) G_{p1} and 19(b) for first-order integral with dead time (FOIWDT) G_{p1}. The design tuning involves three to six controller parameters depending on the external loop plant model.

Figure 19 – Block diagram of the SCCS used in Raja and Ali (2021) for (a) second-order integral with dead time (SOIWDT) and double integral with dead time (DIWDT) G_{p1}; (b) first-order integral with dead time (FOIWDT) G_{p1}.

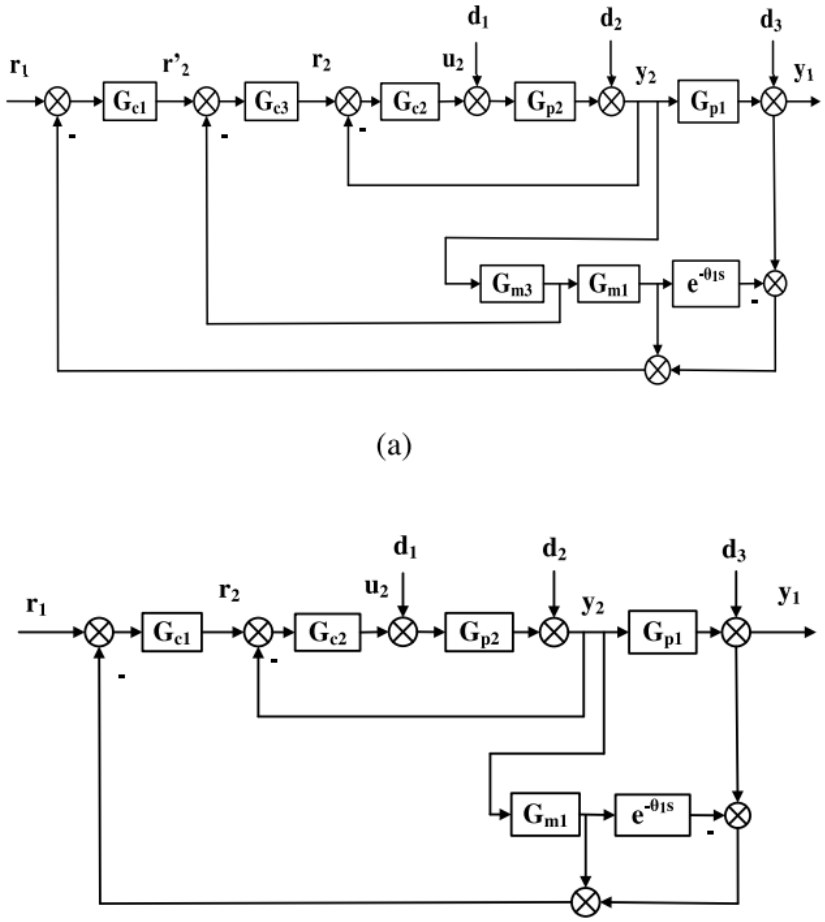

Source: Raja and Ali (2021).

Unstable processes are considered more challenging to control. Some examples of controllers for these types of systems are presented by Garcia et al. (2010), Padhan and Majhi (2012a), Yin et al. (2019). Garcia et al. (2010) introduced two cascaded controllers based on two SP dead time compensator strategies. The secondary loop uses an IMC framework, while the primary controller is set by two proposals: a filtered Smith predictor (FSP), shown in Figure 20(a), and a generalized predictor (GP), shown in Figure 20(b). Both structures are capable of controlling stable or unstable open-loop cascade processes with dead time.

Figure 20 – Block diagram for CCS proposed in Garcia et al. (2010) using (a) FSP and (b) GP.

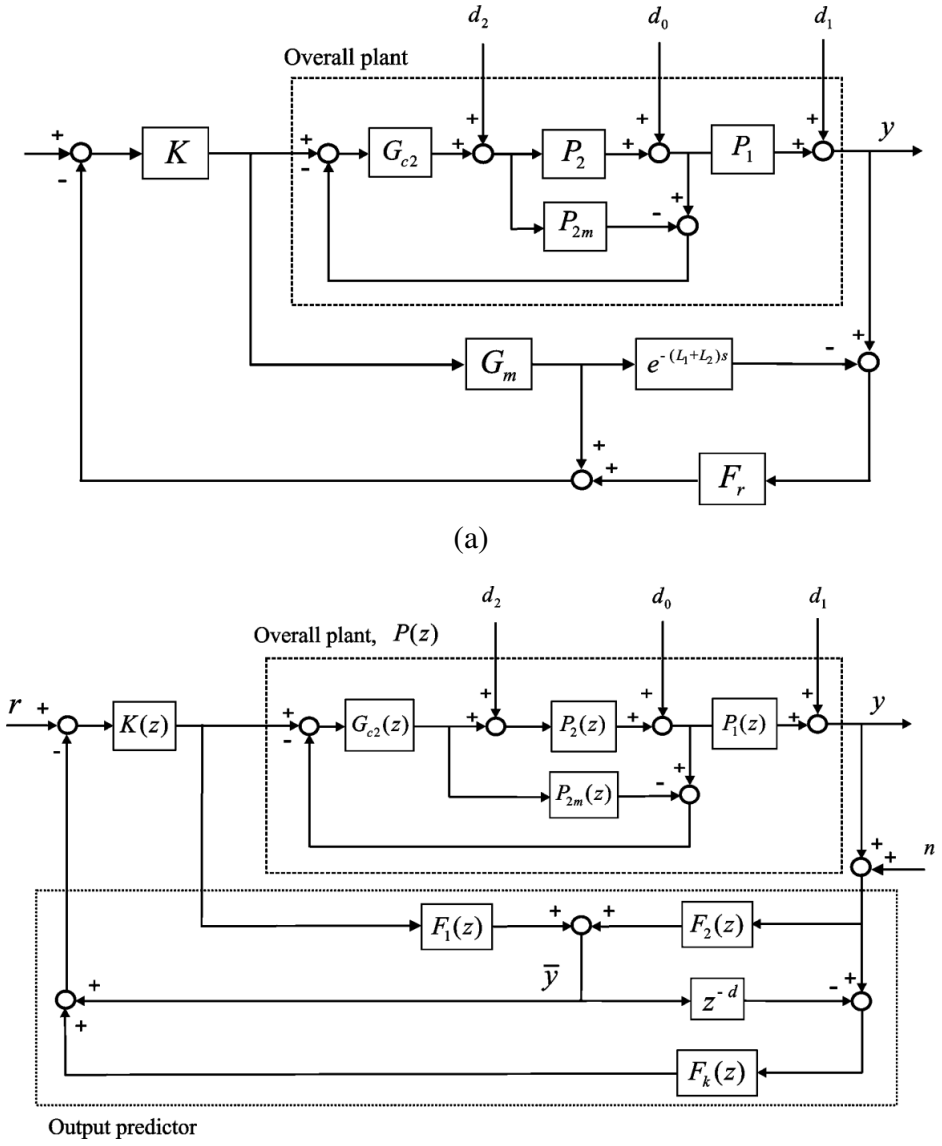

Source: Garcia et al. (2010).

In Padhan and Majhi (2012a), the CCS was designed with three controllers: one, G_{cs}, for servo response using the direct synthesis method and the other two for regulatory responses, in the form of PID controller cascaded, G_{cd2}, with a second-order lead/lag filter, G_{cd1}. The controller structure is shown in Figure 21.

Figure 21 – Cascade scheme with modified Smith predictor proposed in Padhan and Majhi (2012a).

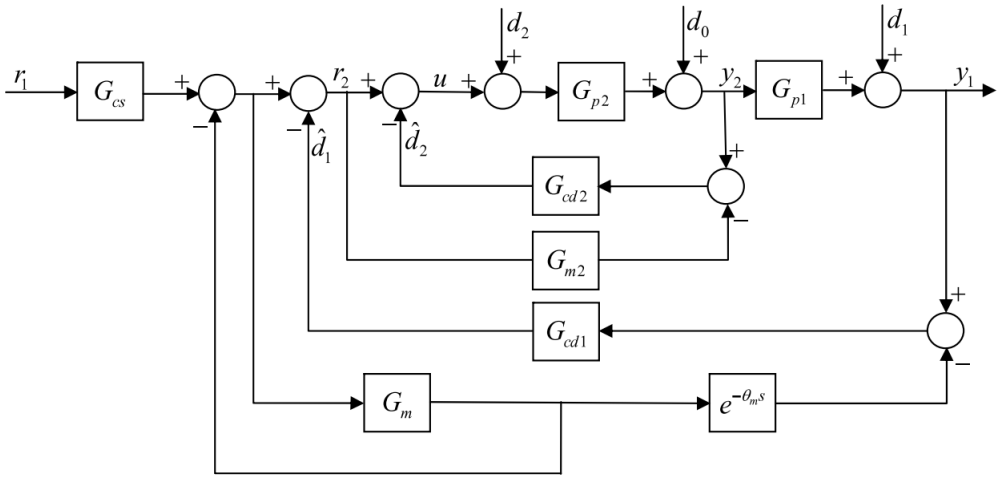

Source: Padhan and Majhi (2012a).

Similar to the previously mentioned controller, the CCS suggested by Yin et al. (2019) is composed of three controllers: the secondary loop controller uses IMC principles, G_{c2}, while in the primary loop, the setpoint tracking controller, G_{cs}, and the disturbance rejection controller,G_{cd}, uses a modified SP, as shown in Figure 22.

Figure 22 – Cascade control structure used in Yin et al. (2019).

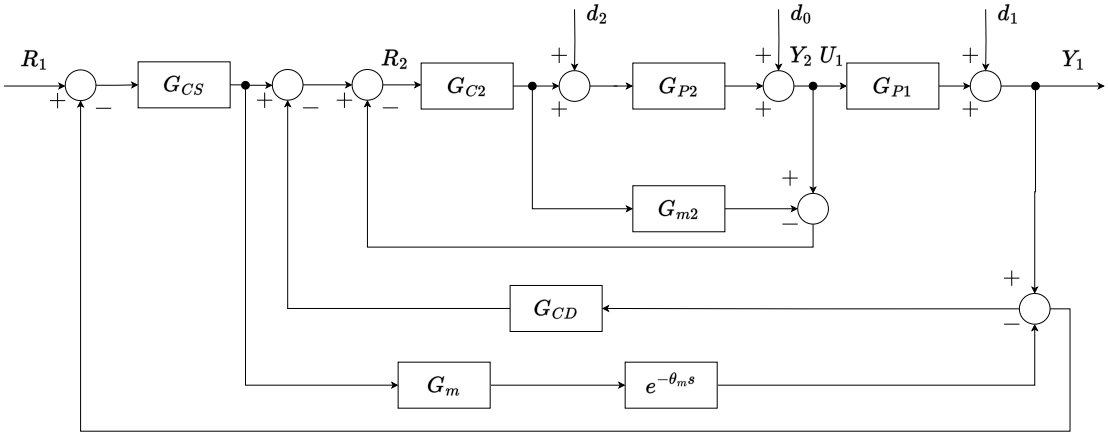

Source: Yin et al. (2019).

In the work of Bhaskaran and Rao (2020) it was proposed a generalized predictive control for unstable series cascade processes with dead time. The controller structure was composed by a secondary loop with a secondary controller based on simple IMC, $G_{c2}(z)$, whereas the primary loop, $G_{c1}(z)$, is designed using synthesis method. Also, the predictor uses two filters, $F_1(z)$ and $F_2(z)$, to deals with the dead time. The controller structure is presented in Figure 23.

Figure 23 – Generalized predictor based cascade loop for unstable processes with dead time used in Bhaskaran and Rao (2020).

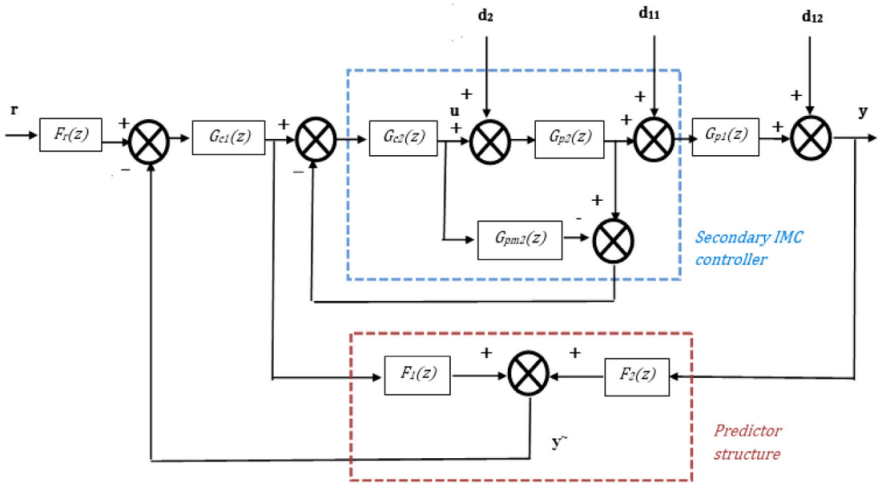

Source: Bhaskaran and Rao (2020).

2.5 Dead-time compensators for parallel cascade dead-time processes

Most of the latest contributions of DTCs are related to improving disturbance rejection (PADHAN; MAJHI, 2012b; RAJA; ALI, 2016; RAJA; ALI, 2017). In some particular processes, like cascade series or cascade parallel, cascade control structures can significantly improve the disturbance rejection. These type of controllers consists of two control loops, a primary (or outer) and a secondary (or inner) loop. The main idea is that the inner loop reduces the effects of disturbances before it affects the outer loop, thus providing better dynamic performance of the closed-loop system (SANTOSH; CHIDAMBARAM, 2016).

Luyben (1973) presented the parallel cascade control structure (PCCS) for the first time in 1973. The structure is shown in Figure 24, where it can be seen that the manipulated variable acts in both loops simultaneously. The novelty of this proposal was the use of a property of any cascade control structure, in which the secondary controller performs disturbance rejection internally before affecting the primary controller, which brings several performance advantages when compared to traditional controllers.

Figure 24 – Block diagram of classical parallel cascade control system.

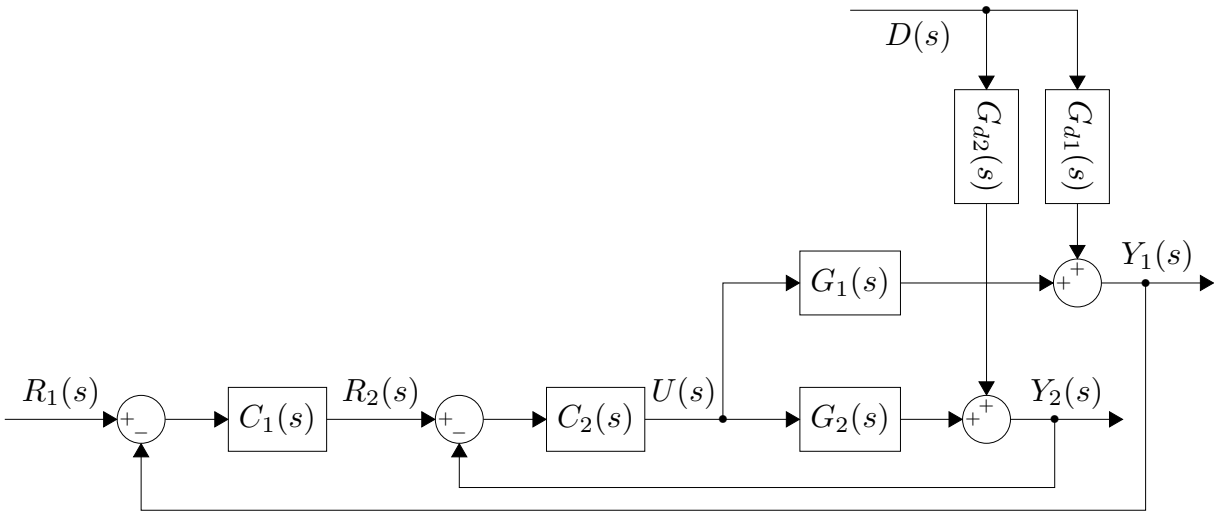

Source: The author.

In the work of Raja and Ali (2016) was proposed a PCCS in which the rejection disturbance controller, for the secondary loop, G_{cd2},uses the IMC approach, a proportional-integral (PI) controller G_{c1} for setpoint tracking, and a proportional-derivative (PD), G_{cd1}, to stabilizing the unstable/integrating primary process model. The used structure is shown in Figure 25.

Figure 25 – Parallel cascade control structure used in Raja and Ali (2016).

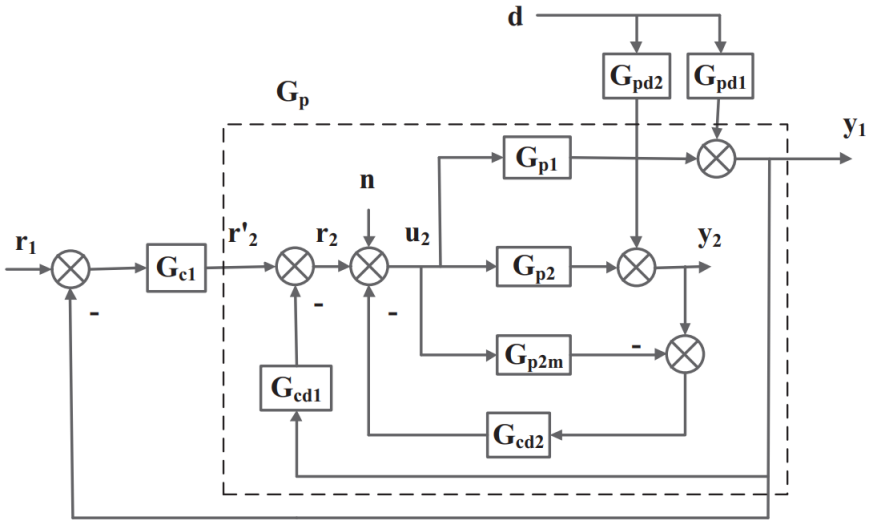

Source: Raja and Ali (2016).

In Santosh and Chidambaram (2016), the authors proposed a PCCS with P/PI control, for unstable FOPTD (first order plus time delay), tuned using the relay method. The block diagram used is presented in Figure 26.

Figure 26 – Parallel cascade control structure used in Santosh and Chidambaram (2016).

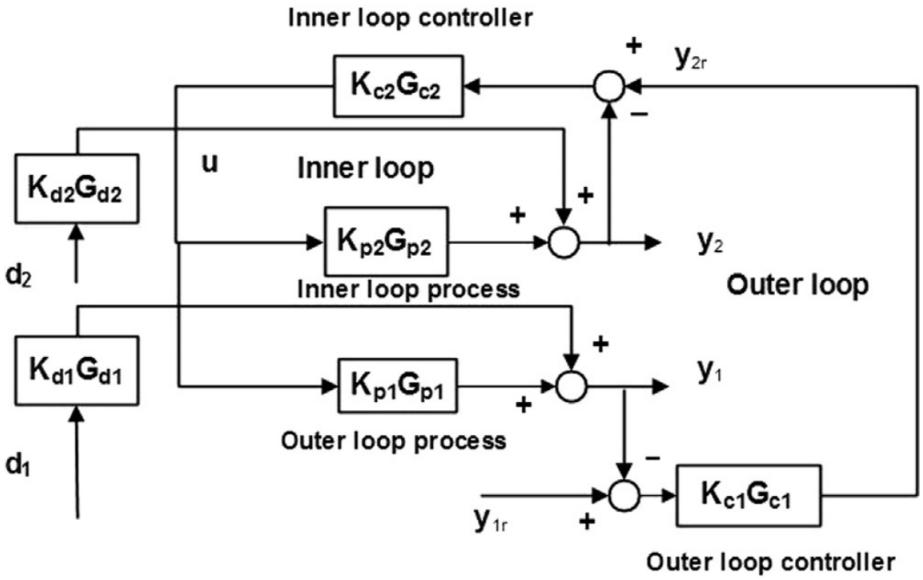

Source: Santosh and Chidambaram (2016).

One of the first works that combined the SP with PCCS appeared in Rao et al. (2009). The goal was to control processes with large dead time, but it was only valid for stable plants. The controller structures is shown in Figure 27. After that, many works used this idea to improve controllers for different cascade processes with SP-based controllers.

Figure 27 – Parallel cascade control structure used in Rao et al. (2009).

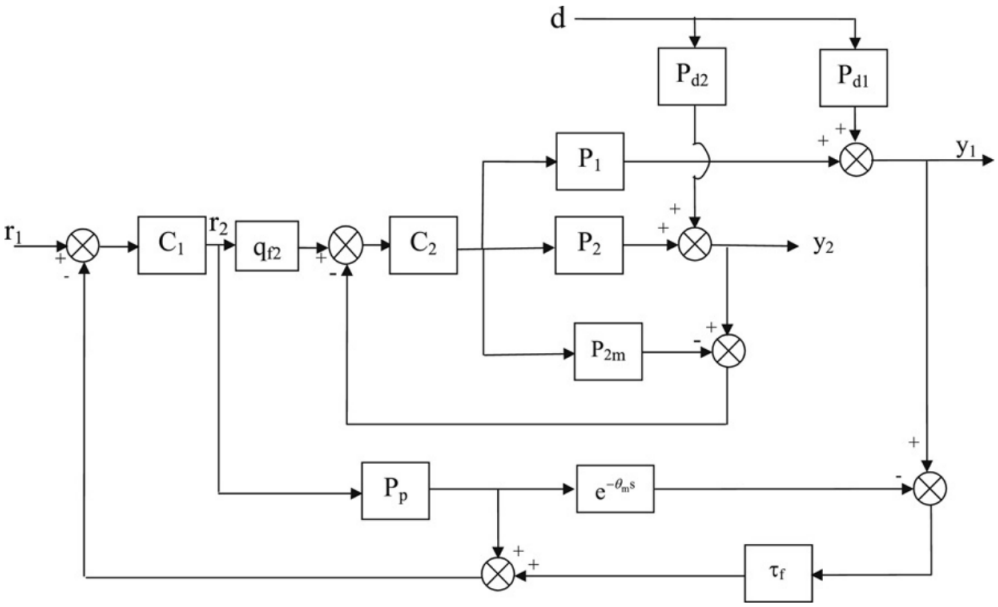

Source: Rao et al. (2009).

For example, in the study of Padhan and Majhi (2012b), the controller design was for controlling stable, unstable, or integrating processes with dead time using two controllers, G_{cd1}

and G_{cd2}, and one setpoint filter, G_{cs}, as can be seen in Figure 28,

Figure 28 – Cascade scheme with modified Smith predictor used in Padhan and Majhi (2012b).

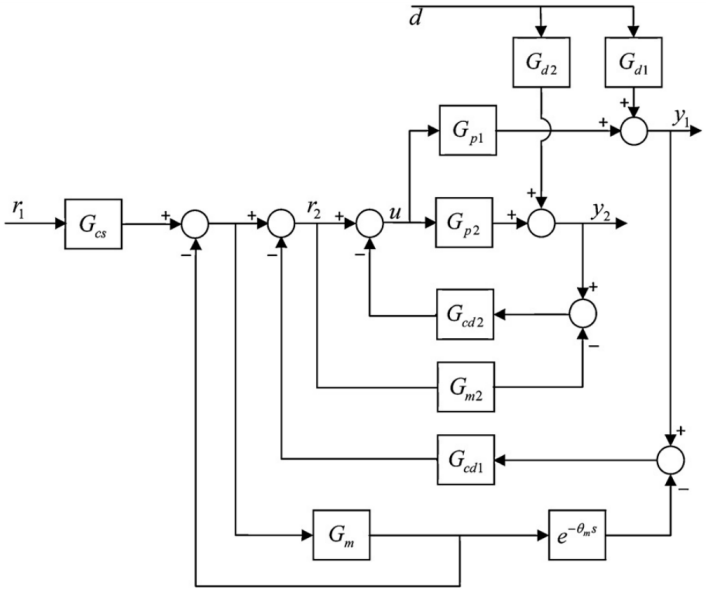

Source: Padhan and Majhi (2012b).

whereas in Raja and Ali (2017), the focus of the controller was on unstable and integrating processes with large dead time, which consists of a secondary disturbance rejection controller, G_{cd2}, a primary stabilizing controller, G_{cd1}, and a primary setpoint tracking controller, G_{c1}. The controller structure is shown in Figure 29.

Figure 29 – Smith predictor based parallel cascade control structure used in Raja and Ali (2017).

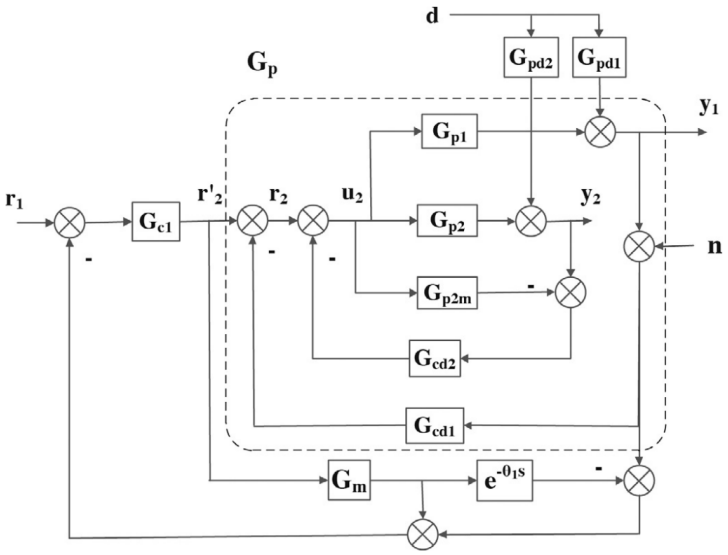

Source: Raja and Ali (2017).

Afterward, in Barros et al. (2017), based on the SFSP (TORRICO et al., 2013b), the

authors proposed the control design, shown in Figure 30, of a PCCS using two SFSP structures, one for each loop; nevertheless, it can be applied to stable processes with dead time only.

Figure 30 – Pparallel cascade control structure used in Barros et al. (2017).

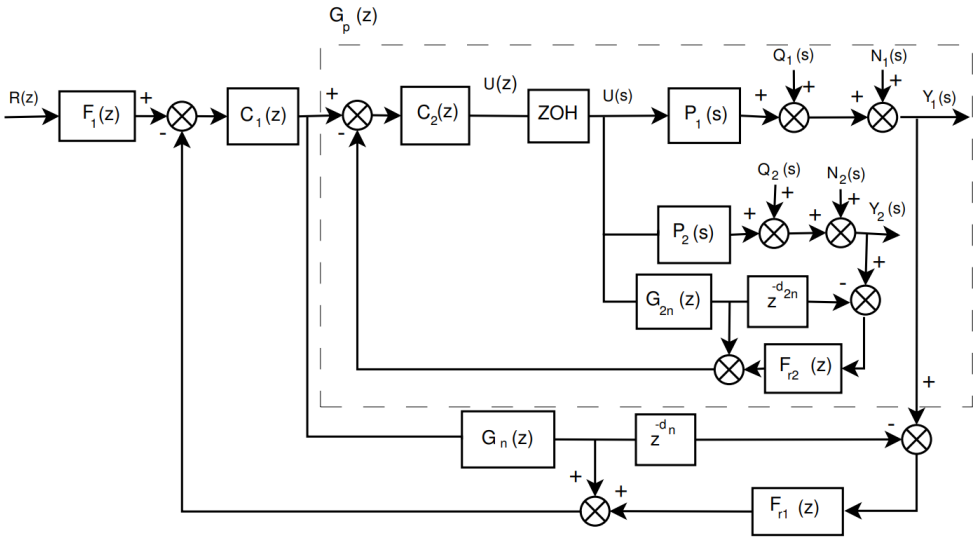

Source: Barros et al. (2017).

The work of Pashaei and Bagheri (2019) proposed a structure for PCCS based on Smith predictor, as can be seen in Figure 31, with setpoint tracking controller and disturbance rejection as fractional order controllers. Also, it was used the Routh–Hurwitz stability criteria to tuning a stabilizing controller.

Figure 31 – Modified PCCS used in Pashaei and Bagheri (2019).

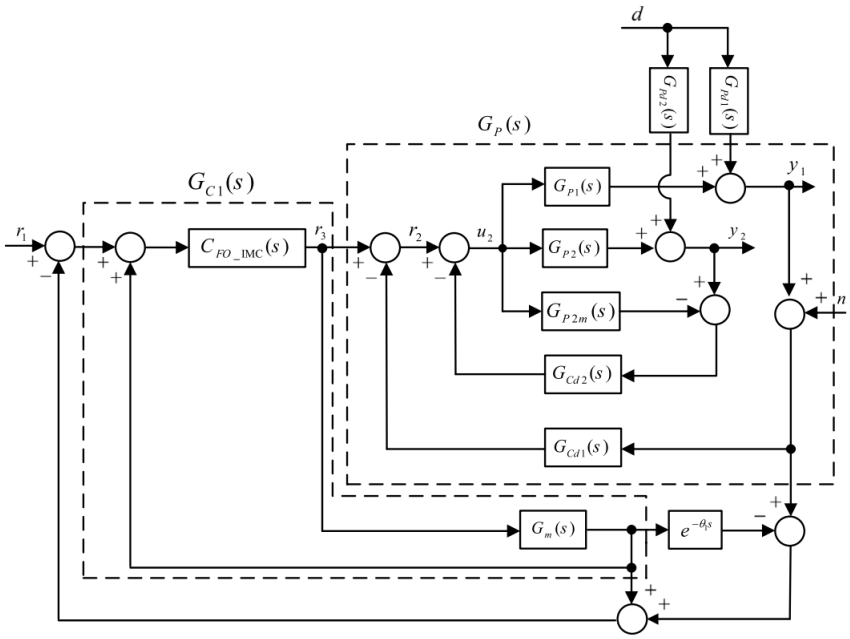

Source: Pashaei and Bagheri (2019).

2.6 Dead-time compensators for TITO dead-time processes

Among several strategies to deal with dead-time processes in industry, two of the most used are DTC and model-based predictive control (MPC) (GIRALDO et al., 2018). Considering the case of multi-input and multi-output (MIMO) processes with dead-time, the challenges of control increases and became more complex due the coupling effects between the processes in MIMO systems that are incremented to the problem of dead-time compensation. For this cases, usually an MPC is used since the control signal is calculated, each iteration, by an optimization problem (JEROME; RAY, 1986; CAMACHO; BORDONS, 2002; GIRALDO et al., 2018).

Another problem that occurs in MIMO systems is that different delays can occur in each of the signals between input and output (input actions, measurement paths, interconnection between internal variables, etc), which increase the difficult in the design of efficient controllers (GARCÍA; ALBERTOS, 2010). Since the MPC approach can presents robustness issues when uncertainty in the delays appears, which leads to control input calculations that require more time and that also not be able to completely decouple the closed-loop response (CAMACHO; BORDONS, 2002), then a DTC controller for MIMO processes with multiple delays can be a good strategy, since the design can be made to the process as if it were delay-free, leading to a good trade-off between performance and robustness (NORMEY-RICO; CAMACHO, 2008).

In the work of Alevisakis and Seborg (1973) was proposed an extension of the Smith predictor for a class of linear multivariable systems for both continuous-time and discrete-time systems with dead time in the control variables and/or in output variables. The structure for the case with both control and output variables with dead time is shown in Figure 32, where $G_c(s)$ is the matrix of transfer functions for feedback controller.

Figure 32 – Smith Predictor for a multivariable system with dead time in both control and output variables used in Alevisakis and Seborg (1973).

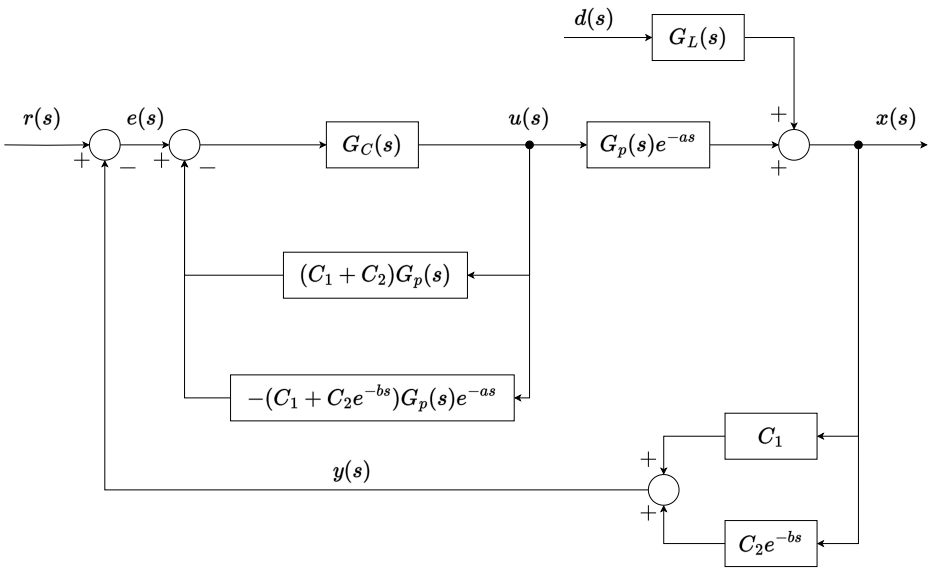

Source: Alevisakis and Seborg (1973).

Ogunnaike and Ray (1979) proposed a multivariable multidelay compensator for continuous and discrete dead time systems. The controller G_c^*, presented in Figure 33, is equivalent to the linear-quadratic optimal feedback controller for input delays and equivalent to Smith predictor for single dead time.

Figure 33 – Block diagram of dead time compensator for multivariable systems used in Ogunnaike and Ray (1979).

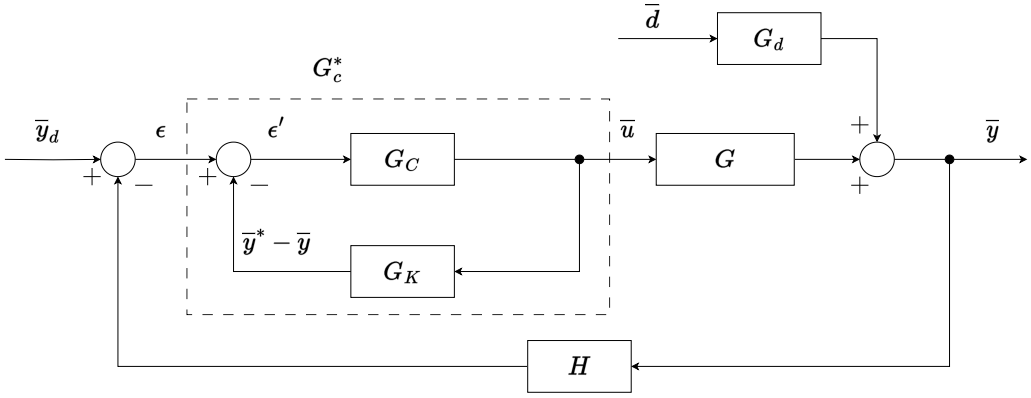

Source: Ogunnaike and Ray (1979).

In Chen, He and Qi (2011), an IMC was used to design a Smith delay compensation decoupling controller for multivariable non-square systems. The controller $G_{IMC}(s)$, shown in Figure 34, dynamically compensate for shortcoming caused by static decoupling and overcomes the impact of model error on system performance.

Figure 34 – Block diagram of IMC system used in Chen, He and Qi (2011).

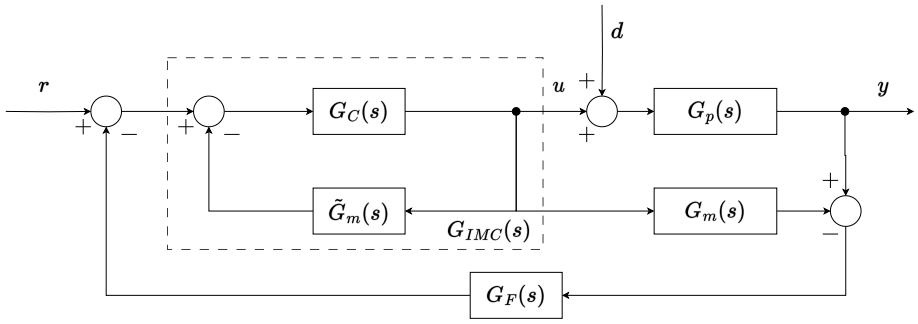

Source: Chen, He and Qi (2011).

Garrido et al. (2011) studied the advantages of inverted decoupling over simplified decoupling in TITO systems with dead time. The controllers c_1 and c_2, shown in Figure 35, presented improvements in the performance of the simulated examples. Later, in Garrido, Vázquez and Morilla (2014) it was proposed the controller , $Q(s)$ with a tuning method considering an IMC strategy for stable multivariable processes with multiple dead time based on the centralized inverted decoupling structure. Also, a filter $F(s)$ was included to improve disturbance. The structure is presented in Figure 36.

Figure 35 – Inverted decoupling control in Garrido et al. (2011).

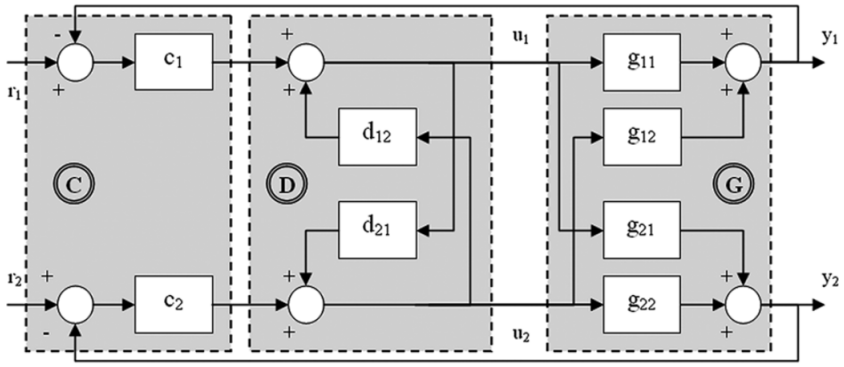

Source: Garrido et al. (2011).

Figure 36 – Inverted decoupling IMC scheme with filter used in Garrido, Vázquez and Morilla (2014).

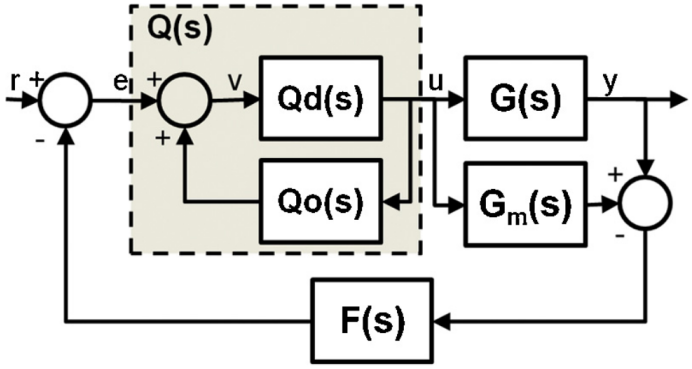

Source: Garrido, Vázquez and Morilla (2014).

In Albertos and García (2010) was proposed the use of disturbance observers, as can be seen in Figure 37, to extracting non-delayed information to generate the control and canceling the interactions in decoupling MIMO systems with multiple dead time.

Figure 37 – Control structure used in Albertos and García (2010).

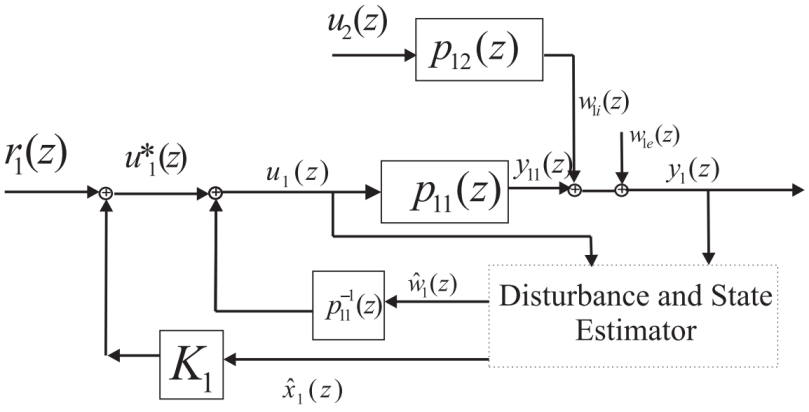

Source: Albertos and García (2010).

García and Albertos (2010) proposed a DTC to deal with dead-time unstable systems based on IMC. The method was divided in three steps, where a non-delayed output plant was predicted $\overline{H}(z)$, a stabilizer controller $Q(z)$ was designed and then for the stabilized plant, the control performance was improved to achieve desired requirements using $F(z)$. The controller is shown in Figure 38.

Figure 38 – Control structure used in García and Albertos (2010).

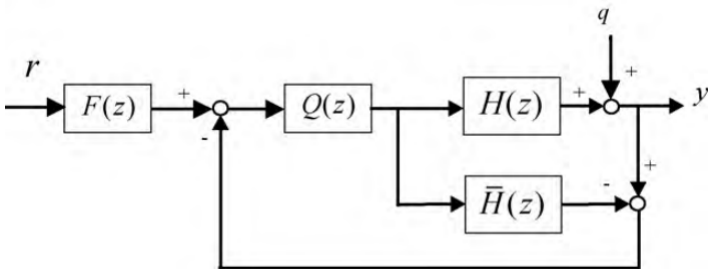

Source: García and Albertos (2010).

State space approaches for DTCs are also developed to deal with high order multivariable processes as an alternative to the use of primary PID controllers applied to MIMO processes. In the work of Pedro and Pedro (2016), the undelayed state of the process was obtained, an estimator was designed and then an LQR control was designed for the resulting non-delayed MIMO dead-time plant. The structure is shown in Figure 39.

Figure 39 – State feedback control used in Pedro and Pedro (2016).

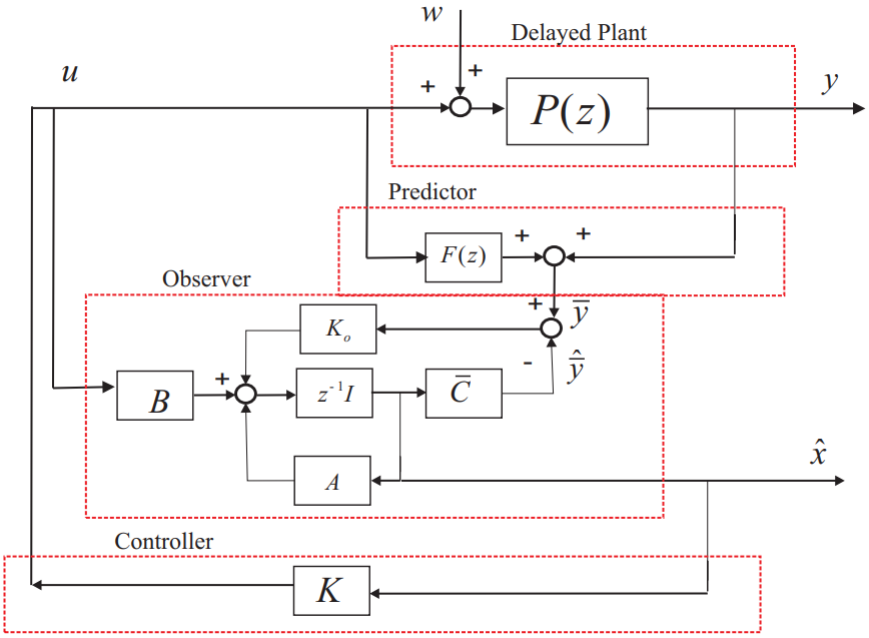

Source: Pedro and Pedro (2016).

Bezerra-Correia, Claure-Torrico and Olímpio-Pereira (2017) proposed a prediction structure combined with the best properties of both DTC and optimal control for MIMO linear

dead-time systems. The controller K_L is presented in Figure 40.

Figure 40 – Proposed control structure used in Bezerra-Correia, Claure-Torrico and Olímpio-Pereira (2017).

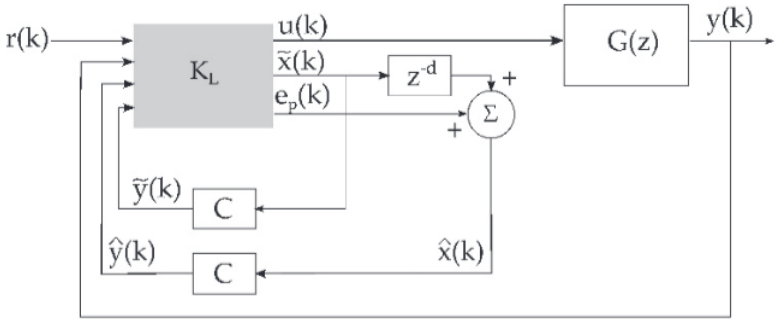

Source: Bezerra-Correia, Claure-Torrico and Olímpio-Pereira (2017).

The extension of controllers based on the Smith predictor to multivariable systems, among DTCs, represents a milestone in dealing with the challenges imposed on these types of systems. An FSP for MIMO stable, unstable, and integrating dead-time processes models with any order was first presented in Flesch et al. (2011), where it was proposed a unified dead-time compensator for MIMO $n \times n$ processes with multiple delays. In Flesch, Santos and Normey-Rico (2012), a MIMO DTC structure for non-square systems with multiple dead time was developed. Santos, Flesch and Normey-Rico (2014) studied a unified implementation structure of the FSP for square or non-square MIMO processes with multiple dead time, where it was analyzed Two kinds of dead-time free models to extend the original properties of the SISO SP to MIMO processes with multiple dead time.

In Giraldo et al. (2016) it was proposed a design to multivariable FSP for $n \times n$ for processes with multiple dead time based on the centralized direct decoupling structure. Pataro, Costa and Joseph (2019) compared an Infinite Horizon Predictive Controller (IHMPC) and a FSP applied to an ethanol distillation simulated process in order to ensure a desired quality range under feed variations as disturbances. Later, in Pataro, Costa and Joseph (2020) it was proposed a closed-loop dynamic real-time optimization (CL-DRTO) with advanced control strategies, such IHMPC, MIMO FSP and DTCGPC (Dead-Time Compensator Generalized Predictive Controller) applied in an ethanol distillation simulated process to improve production and minimize energy losses. Santos, Franklin and Torrico (2021) proposed an anti-windup implementation of the FSP for MIMO processes with dead time based on a modification of the primary controller that unifies continuous-time and discrete-time approaches. In Lima, Lima and Normey-Rico (2023), it was proposed a predictor for linear multivariable square systems, of any order or dynamics, with multiple dead-time (or delays) based on the Kalman Filter that has disturbance estimation. The advantage is that the Kalman predictor affects only the disturbance rejection, which helps in the improvement of closed-loop robustness in the uncertain case. An illustration of the structure of the FSP for all discussed controllers is shown in Figure 41.

Figure 41 – Proposed control structure used in Santos, Flesch and Normey-Rico (2014).

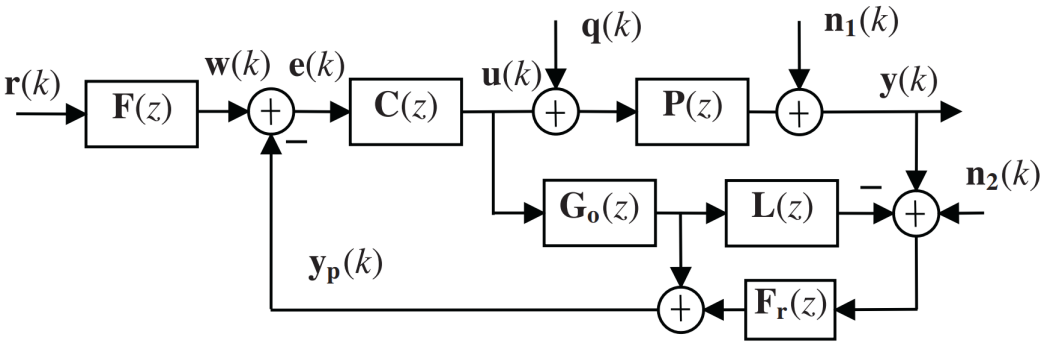

Source: Santos, Flesch and Normey-Rico (2014).

The extension of the SFSP for FOPDT MIMO process with dead time was formulated and proposed by Santos, Torrico and Normey-Rico (2016), where it was shown that it is possible to achieve offset-free control with step references and disturbances regardless of the poles of the primary controller. Also, the approach reduced the number of controller parameters and simplified the tuning procedure due the SFSP characteristic of not considers an explicit integrative controller in the design. The used structure is presented in Figure 42.

Figure 42 – Control structure used in Santos, Torrico and Normey-Rico (2016).

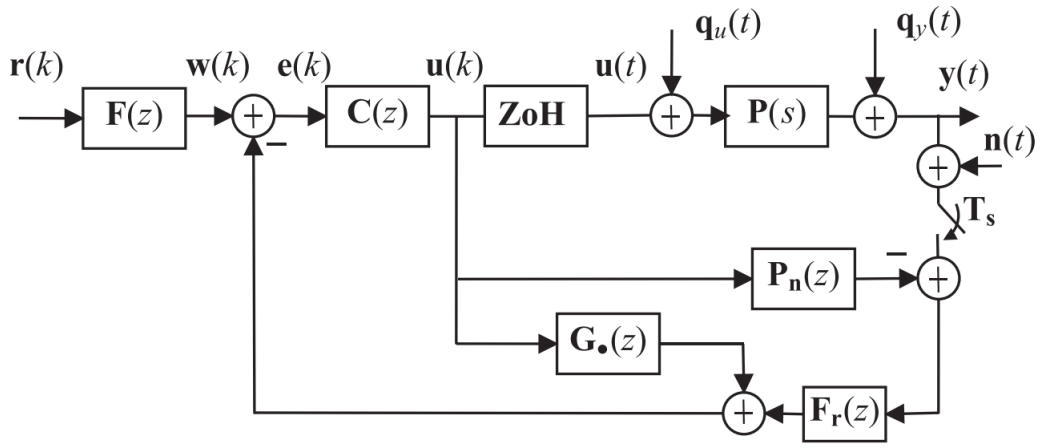

Source: Santos, Torrico and Normey-Rico (2016).

Finally, in Amaral et al. (2023), the SFSP from Torrico et al. (2021) was extended to MIMO processes and an unified tuning rule for both the SISO and the square MIMO high-order cases was proposed. The controller tuning was simplified by the proposed state feedback decoupling tuning for reference tracking and the inclusion of the disturbance model on the controller design it allows the trade-off between disturbance attenuation and stability. The controller structure is shown in Figure 43.

Figure 43 – Control structure used in Amaral et al. (2023).

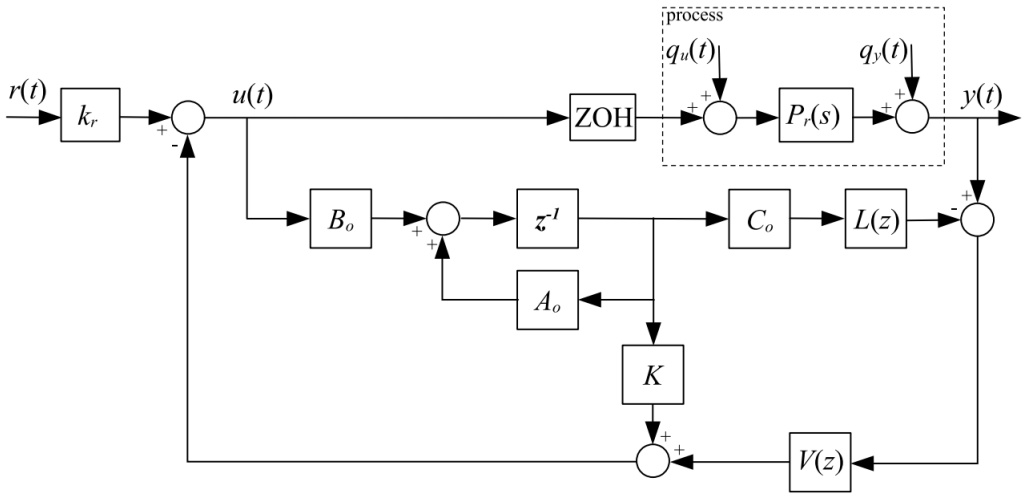

Source: Amaral et al. (2023).

2.7 Discussion

Dead-time compensators were discussed as a strategy to deal with dead-time systems, focusing on methods based on the Smith predictor, especially the SFSP (TORRICO et al., 2013a).

The main control strategies for multivariable systems with dead time in literature were also presented. As a contribution of this work, control strategies for series cascade systems with dead time, parallel cascade with dead time and TITO systems with dead time based on both the SFSP and predictive control will be proposed.

3 LINEAR PARAMETER-VARYING SYSTEMS

This chapter is dedicated to present some important concepts and definitions related to the study of Linear parameter-varying (LPV) systems.

3.1 System representation

An LPV system can be defined as a linear system with parameters that change over time or across operating points. These systems may be described by the following state equations representation:

$$\begin{aligned} \dot{x}(t) &= A(\theta(t))x(t) + B(\theta(t))u(t) \quad t \geq 0 \\ y(t) &= C(\theta(t))x(t) + D(\theta(t))u(t) \\ x(0) &= x_0, \end{aligned} \tag{3.1}$$

where $A \in \mathbb{R}^{n\times n}$, $B \in \mathbb{R}^{n\times m}$, $C \in \mathbb{R}^{p\times n}$ and $D \in \mathbb{R}^{p\times m}$. The variables $x(t)$, $u(t)$ and $y(t)$ represent the state, the input and the output of the system, respectively. The vector $\theta(t) = [\theta_1(t)\ \theta_2(t)\ \cdots\ \theta_{n_\theta}(t)] \in \Theta \subset \mathbb{R}^{n_\theta}$ is usually called scheduling parameter and represents the effect of the environment on the dynamics of the system by modifying its structure over time.

By considering that θ belongs to the set Θ, some typical assumptions are made in order to define the scheduling vector inside to this compact set. Thus, the scheduling parameters are bounded both in magnitude and in the rate of variation:

$$\theta_{min} \leq \theta \leq \theta_{max} \tag{3.2}$$

$$\dot{\theta}_{min} \leq \dot{\theta} \leq \dot{\theta}_{max}, \tag{3.3}$$

and depending on the type of assumption chosen, it is possible to use different strategies for both analysis and synthesis.

It can be said that LPV systems lie between nonlinear and linear systems, resulting in a linear and non stationary dynamics (MOHAMMADPOUR; SCHERER, 2012). Thus, the sets of LTI and LTV systems are contained in LPV systems, that is, they can be seen as particular cases of the LPV framework. The differences from LTI systems is due to non stationarity of LPV systems, so LTI systems can be seen simply as LPV systems with fixed scheduling parameters $\theta := \theta_0$. However, the distinctions from LTV systems are more subtle. This happens because an LTV system may be represented by an LPV system with a fixed scheduling trajectory $\theta := \theta_0(t)$, which means that for any trajectory of $\theta(\cdot)$, the dynamics of (3.1) compose a linear time varying system.

Although most representations of LPV systems in the literature are in state space, it is not uncommon the usage of LPV input-output (I/O) representations. Considering the structure of

an autoregressive with exogenous input (ARX) model, the extension for LPV systems may be given by:

$$A(\sigma,\theta)y(k) = B(\sigma,\theta)u(k) + e(k) \tag{3.4}$$

or written in a transfer function form:

$$G(\sigma,\theta) = \frac{B(\sigma,\theta)}{A(\sigma,\theta)} = \frac{b_m(\theta)\sigma^m + b_{m-1}(\theta)\sigma^{m-1} + \cdots + b_1(\theta)\sigma + b_0(\theta)}{a_n(\theta)\sigma^n + a_{n-1}(\theta)\sigma^{n-1} + \cdots + a_1(\theta)\sigma + a_0(\theta)} \tag{3.5}$$

where $\sigma \in \mathbb{C}$ may represent the Laplace or the Z transform operators.

It should be emphasized the differences of these representation to theirs LTI counterparts. An I/O LPV model represents parameter dependent polynomials, which means that their are not stationary and can represent a wider range of processes, including nonlinear models. However, LTI analysis tools can be used to evaluate such representations.

3.1.1 Modeling LPV systems

Basically there are three modes of obtain an LPV model:

(i) Interpolation: several linear models, from different operating points, are interpolated in order to obtain the LPV model;

(ii) Quasi-LPV: some convenient parameter of the nonlinear system is choose as scheduling parameter and then the expression is manipulated in order to obtain the LPV model;

(iii) Identification methods: first a model structure is choose (state space, ARX, ARMAX, etc) and then an identification algorithm is used to estimate the parameters of the model.

3.1.1.1 Interpolation of LPV models

Considering a class of parameter-dependent nonlinear systems in the form:

$$\begin{aligned} \dot{x}(t) &= f(x(t),u(t),\theta) \\ y(t) &= g(x(t),u(t),\theta), \end{aligned} \tag{3.6}$$

one may use linearization methods, such as Taylor series, or identification methods in order to obtain local linear models at different operating points of the system. Each of the computed local systems is defined by an equilibrium point model (x_0,u_0,y_0,θ_0) and described as follows

$$\begin{aligned} \dot{x}(t) &= A_l(\theta_0)\Delta x(t) + B_l(\theta_0)\Delta u(t) \\ \Delta y(t) &= C_l(\theta_0)\Delta x(t) + D_l(\theta_0)\Delta u(t) \end{aligned} \tag{3.7}$$

where $A_l = \dfrac{\partial f}{\partial x}$, $B_l = \dfrac{\partial f}{\partial u}$, $C_l = \dfrac{\partial g}{\partial x}$, $D_l = \dfrac{\partial f}{\partial u}$, $\Delta x(t) = x(t) - x_0$, $\Delta u(t) = u(t) - u_0$, and $\Delta y(t) = y(t) - y_0$.

Once the local models are obtained, some assumptions can be made in order to define the approach used to obtain the LPV model. The most classical method is to interpolate the coefficients of (3.7) for all operation points as a function of the scheduling parameter. However, with this approach there is no guarantee of stability between two consecutive points.

Some efforts were made in order to deal with this stability issue (LEITH; LEITHEAD, 1998). Usually the idea is to prove that the local systems are stables in their neighborhood under some restrictions: each one of them must to be uniformly stable and the variation rate of θ should be slow with respect to the dynamics of the system.

This technique is often used in gain scheduling works and is considered conservative (LEITH; LEITHEAD, 2000; RUGH; SHAMMA, 2000). When dealing with LPV systems, it is difficult to consider the constraint in the scheduling parameters in practical applications and is usually preferred others forms for modeling LPV systems.

3.1.1.2 Quasi-LPV models

The quasi-LPV or *qLPV* description is a very useful approximation of nonlinear systems by an LPV model. The strategy consists to replace the nonlinearities as functions of scheduling parameters (BRIAT, 2014). The best way to use this approach is when dealing with systems whose model is directly obtained.

The modeling of some nonlinear systems by a *qLPV* technique may be exact and characterize completely the stability of the original system, but it is important to emphasize that usually this approximation is not equivalent regarding properties such as stability, controllability, etc. Some approximation methods proposed in the literature can be seen in Shin (2002), Bruzelius, Pettersson and Breitholtz (2004).

Finding the most accurate *qLPV* approximation may be difficult. Consider the example given in Bruzelius, Pettersson and Breitholtz (2004), where a *Van del Pol* equation, in the following, is studying:

$$\begin{aligned} \dot{x}_1(t) &= -x_2(t) \\ \dot{x}_2(t) &= x_1(t) - 0.3(1 - x_1^2(t))x_2(t). \end{aligned} \tag{3.8}$$

The dynamics of this system has the characteristic that any trajectory initiated in a certain region of the phase plane remains in it, converging to zero and any others diverge, that is, it has a limit cycle (BRUZELIUS; PETTERSSON; BREITHOLTZ, 2004; KHALIL, 2002). This behavior is shown in Figure 44.

Figure 44 – Phase portrait of the Van der Pol Equation (3.8) with some trajectories.

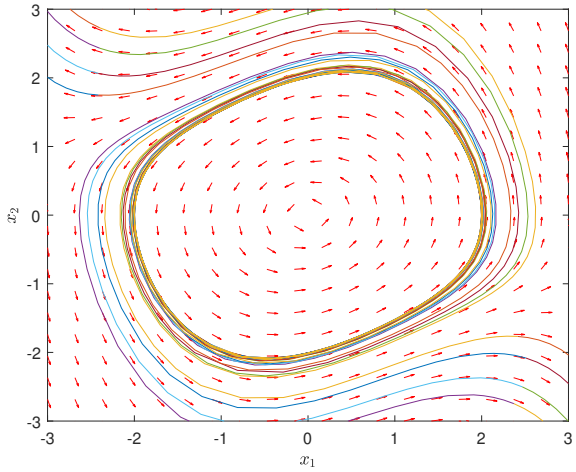

Source: The author.

First, the authors show that a simple LPV model can be given by:

$$\begin{bmatrix} \dot{x}_1(t) \\ \dot{x}_2(t) \end{bmatrix} = \begin{bmatrix} 0 & -1 \\ 1 & -0.3(1-\theta^2) \end{bmatrix} \begin{bmatrix} x_1(t) \\ x_2(t) \end{bmatrix} \tag{3.9}$$

where $\theta = x_1(t)$. If $|\theta| \leq 0.98$ it is possible to use the Lyapunov function $V(t) = x^T(t)Px(t)$ to show that the LPV system is quadratic and asymptotically stable with the attraction region as in Figure 45a. A less conservative and more accurate model is given by:

$$\begin{bmatrix} \dot{x}_1(t) \\ \dot{x}_2(t) \end{bmatrix} = \begin{bmatrix} 0 & -1 \\ 1+0.24\theta_1\theta_2 & -0.3+0.06\theta_1^2 \end{bmatrix} \begin{bmatrix} x_1(t) \\ x_2(t) \end{bmatrix} \tag{3.10}$$

where $\theta_1 = x_1(t)$ and $\theta_2 = x_2(t)$. If $|\theta_1| \leq 1.253$ and $|\theta_1\theta_2| \leq 0.85$. The system is asymptotically stable with attraction region represented in Figure 45b.

Figure 45 – Region of attraction based on the LPV systems (3.9) and (3.10)

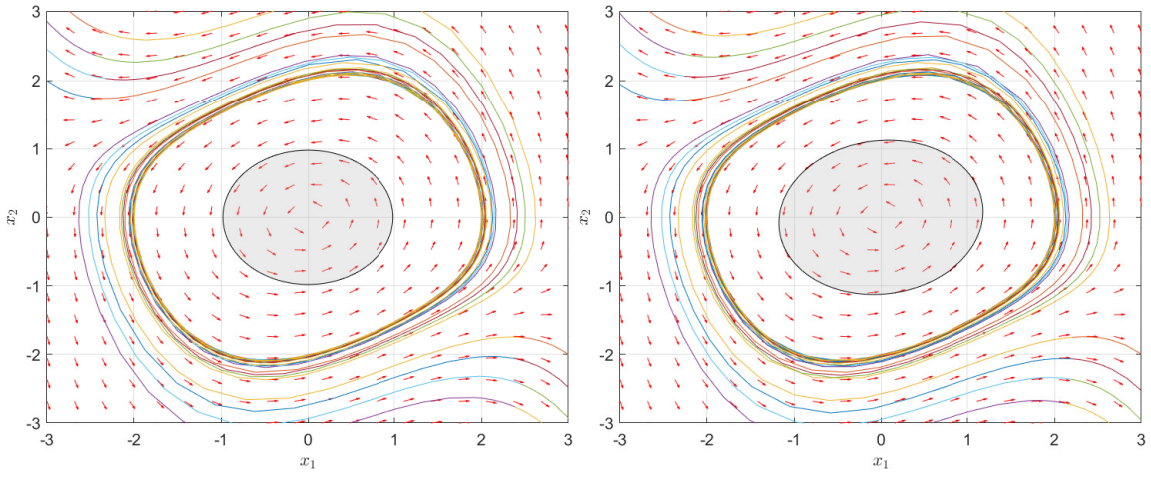

(a) (b)

Source: The author.

By the use of *qLPV* systems is possible to reach a wider range of nonlinear systems. In Figure 46 all class of systems are represented and is possible to see how far the LPV framework is from linear systems.

Figure 46 – Class of systems.

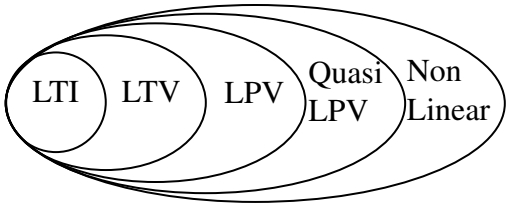

Source: The author.

3.1.1.3 Identification of LPV models

When there are no differential equations to model the system or even when they exist, but there is not enough information or data to estimate the parameters of the equation, it is possible to use system identification techniques to obtain an LPV model from data obtained by through experiments.

Even for LPV systems the basic identification cycle (LJUNG, 1998; TÓTH, 2010) is useful. The idea is to perform several steps in order to obtain a good model and it is named as a cycle due the fact that it may works as an recursive algorithm with several iterations until a desired model is reached. The steps are described in the following:

1. *Experiment, data collection and preprocessing*: this step consists of carrying out experiments in order to obtain adequate data sets for identification. Here, it is important the right choice of input signal (persistence and adequacy) to excite the system, so that the data sets can be used in the algorithms. The collected data sometimes have to be processed in order to attenuate disturbances, outliers or other similar issues.

2. *Choice of the model structure*: selection of a representation to the system, that is, I/O, state space. Also is usually choose the parametrization, the type of noise and the model order.

3. *Definition of the identification criterion*: choice of the performance measure of the model estimates. Generally, the mean square error of the output predicted from the model is used.

4. *Estimating a model*: in this step an algorithm is used following the structure choice and considering the defined criteria of performance. The result provides a model that represent the system.

5. *Validation of the result*: by comparing the output predicted of the model with the measured one for several input signals and by using performances criteria it is possible to determine

if the model is acceptable. If the response is considered inadequate for the established purpose, it is necessary to return to the previous steps in order to determine a better model.

A generic block diagram of an LPV system can be seen in Figure 47, representing the relationship between the input signals u and output y which is modified by the scheduling variable θ.

Figure 47 – LPV system block diagram.

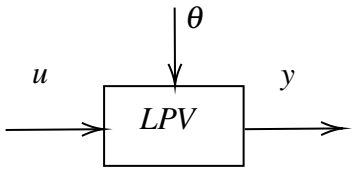

Source: The author.

Mathematically this relation can be represented as a convolution of u and θ:

$$y = \sum_{i=0}^{\infty} f(\theta) q^{-i} u \tag{3.11}$$

where q is the forward time shift operator and $f(\cdot)$ is a set of functions of the scheduling parameter. The goal is to choose a structure for $f(\cdot)$ and estimate its parameters, but since θ is a variant parameter, the identification algorithms are more complex. Usually, the estimation are made based on models structure such as state space or I/O models (TÓTH, 2010).

Considering I/O LPV systems, some basic developed methods are listed in the following:

- *Interpolation*: consists in identify the system for constants scheduling trajectories following by the interpolation of the parameters. Several methods of interpolating I/O LPV systems can be applied such as on the outputs or on the inputs of the local models, or on the polynomial coefficients (ZHU; XU, 2008; BOLEA et al., 2009; ZHU; JI, 2009).

- *Linear Regression*: these methods uses several special I/O structures such as LPV ARX from (3.4), output-error (OE) and Box-Jenkins (BJ) to extend classical LTI algorithms. The estimation of the LPV parameters can be made by linear regression, recursive least squares, extended least squares, instrumental variable, and so on (BAMIEH; GIARRE, 2002; WEI; RE, 2006; GIARRÉ et al., 2006; BUTCHER; KARIMI; LONGCHAMP, 2008; LAURAIN et al., 2010).

- *Set Membership*: consists in determine a set of feasible parameters that satisfy (3.11). The noise is considered as an uncertainty and the output error must be bounded by ε, that is, $||e|| \leq \varepsilon$. The final parameters values are obtained with the mean of the feasible set or by a polytopic approximation (BELFORTE; GAY, 2004; CERONE; REGRUTO, 2008).

- *Nonlinear Optimization*: the coefficients of the I/O LPV system are estimated by a nonlinear optimization algorithm in order to achieve a better result considering linear methods. Such approaches may use neural networks, mixed linear/nonlinear techniques or even non parametric methodologies (PREVIDI; LOVERA, 2003; PREVIDI*; LOVERA, 2004; HSU; VINCENT; POOLLA, 2008).

And for state space representations, it is possible to use several approaches such as:

- *Gradient Methods*: the state space matrices are estimated from the formulation of a nonlinear optimization problem, which is solved interactively based on gradient-search-based algorithms of a cost function. However, it must be noted that these solutions are locally optimal (LEE; POOLLA, 1996; VERDULT; LJUNG; VERHAEGEN, 2002; LACHHAB; ABBAS; WERNER, 2008).
- *Full-Measurement*: with the state space LPV system in the *linear fractional representation* (LFR) is possible to set some assumptions and restrictions in order to perform an estimation based on linear regression (NEMANI; RAVIKANTH; BAMIEH, 1995; LOVERA; VERHAEGEN; CHOU, 1998; MAZZARO; MOVSICHOFF; PENA, 1999).
- *Multiple-Model*: consists of a set of interpolation based methods in θ considering state space LPV representations (WASSINK et al., 2005; LOVERA; MERCERE, 2007; PAIJMANS et al., 2008).
- *Observer-Based Grey-Box*: on this method an adaptive observer is used to determine the parameters of a nonlinear model and then the gain-scheduling method is used to derive a state space LPV model with affine dependence (ANGELIS, 2003; GÁSPÁR; SZABÓ; BOKOR, 2005).

More of identification of LPV systems can be find in Tóth (2010), Cox (2018).

3.1.1.4 Hidden coupling terms

An important issue that may occur when dealing with connected LPV systems, regardless how it was modeling (interpolation, *qLPV* or identified), is the presence of hidden coupling terms, which can lead the closed-loop system to instability (RUGH; SHAMMA, 2000; BRIAT, 2014).

This problem may arise from the difference between the performance designed for an LPV controller and the one actually implemented, which occurs when variations in θ are not considered, as this introduces unforeseen dynamics, possible performance losses or even instability. More on hidden coupling terms can be seen in Nichols, Reichert and Rugh (1993), Lawrence and Rugh (1995), Wollnack et al. (2017).

3.1.2 Special representation approaches

Considering the following LPV system in the following:

$$\begin{aligned} \dot{x}(t) &= A(\theta)x(t) + B(\theta)u(t) \\ y(t) &= C(\theta)x(t) + D(\theta)u(t), \end{aligned} \tag{3.12}$$

it must be said that it is possible to represent, analyze and control this system with different methods, which are determined by the type of scheduling dependency. Some of the most common approaches are described in this section.

3.1.2.1 Generic LPV representation

As suggested by the name, this strategy presents a very generic choice of scheduling dependence such as polynomial, exponential, rational, etc. The idea is that no transformation is used in the system and the only conditions applied is that matrices A, B, C, D are all bounded by the vector of time-varying parameters $\Delta_\theta \implies \mathbb{R}^{n\times n}$ and that the scheduling parameters varies in such a way that the solutions of the differential equation are well-defined (BRIAT, 2014).

Considering a polynomial dependency, the system presented in Equation (3.12) may be represented as:

$$A(\theta) = A_0 + \sum_{i=1}^{N} A_i \theta^i \tag{3.13}$$

$$B(\theta) = B_0 + \sum_{i=1}^{N} B_i \theta^i \tag{3.14}$$

$$C(\theta) = C_0 + \sum_{i=1}^{N} C_i \theta^i \tag{3.15}$$

$$D(\theta) = D_0 + \sum_{i=1}^{N} D_i \theta^i. \tag{3.16}$$

where the index N represents the order of the scheduling dependency.

3.1.2.2 Polytopic LPV representation

Any LPV system can be described, with more or less accuracy, by a polytopic LPV system (BRIAT, 2014). The LPV system from Equation (3.12) may be represented by:

$$S(\lambda) = \begin{pmatrix} A(\lambda) & B(\lambda) \\ C(\lambda) & D(\lambda), \end{pmatrix} \tag{3.17}$$

where $S(\lambda)$ defines a polytope with vertices

$$\mathscr{C}o\{S_1, S_2, \cdots, S_N\} \triangleq \left\{ \sum_{i=1}^{N} \lambda_i S_i, \sum_{i=1}^{N} \lambda_i = 1 \right\} \tag{3.18}$$

with

$$\{S(\theta), \forall \theta \in \Theta\} \subset \mathscr{C}o\{S_1, S_2, \cdots, S_N\}. \tag{3.19}$$

Thus, the set of LPV systems is represented by a combination of the vertices of the polytope, which means that the matrices $S_1, \cdots, S_N$ covers all the dynamics of the LPV system. A representation of a polytope is shown in Figure 48.

Figure 48 – Polytope representation.

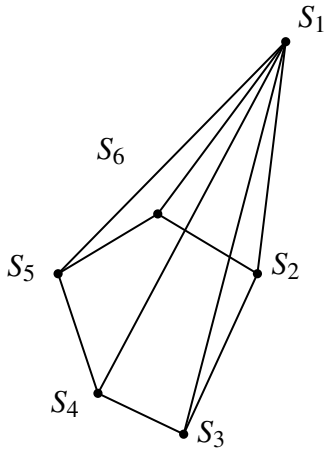

Source: The author.

Generally, this model is conservative, because there are infinity polytopes that contains $S(\theta)$. However, there are techniques to determine the smallest convex set which contains $S(\theta)$ (BRIAT, 2014). Polytopic systems are still attractive for its properties and due the efficiency of analysis and synthesis methods developed for them.

3.2 Analysis of LPV systems

In this section are described some of the most important methods of stability and performance analysis for LPV systems.

3.2.1 Stability in LPV systems

Since it is possible to consider LPV systems as uncertain systems with time-varying parameters, it is reasonable to assume that the analysis of these systems is based on robust stability analysis approaches. Let a generic LPV system be described by

$$\begin{aligned} &\dot{x}(t) = A(\theta)x(t), \quad t \leq 0, \\ &x(0) = x_0 \end{aligned} \tag{3.20}$$

where $x \in \mathbb{R}^n$ and $\theta \in \Theta$ are the state and the scheduling parameters trajectories, then one may consider $x(x_0, \theta, t)$ as the solution of the system and define the characteristics of the zero equilibrium point such as:

- *Stable* if there is a $\delta = \delta(\varepsilon)$ for each $\varepsilon > 0$ in such a way that

$$||x_0|| \leq \delta \implies ||x(x_0, \theta, t)|| \leq \varepsilon, \quad \forall t \geq 0 \quad \text{and} \quad \forall \theta \in \Theta. \tag{3.21}$$

- *Attractive* if there is δ such that

$$||x_0|| \leq \delta \implies \lim_{t \to \infty} ||x(x_0, \theta, t)|| = 0, \quad \forall \theta \in \Theta. \tag{3.22}$$

- *Asymptotically stable*, in the sense of Lyapunov, if it is stable and attractive at the same time.

- *Exponentially stable* if there are δ, $\alpha > 0$ and $\beta \geq 1$ such that

$$||x_0|| \leq \delta \implies ||x(x_0, \theta, t)|| \leq \beta e^{-\alpha t} ||x_0||, \quad \forall t \geq 0 \quad \text{and} \quad \forall \theta \in \Theta. \tag{3.23}$$

- *Unstable* if it is not stable in the sense of Lyapunov.

There are several ways to define stability concerning LPV systems, however the most usual approaches are *quadratic* and *robust* stability. The first one, that is quadratic stability, is a mere extension of its counterpart for LTI systems, which means that for the system presented in Equation (3.20) it is possible to define a *parameter-independent* Lyapunov function in the form

$$V(x) = x^T P x \tag{3.24}$$

in such way that if there is a feasible semidefinite positive matrix P in the linear matrix inequality (LMI)

$$A^T(\theta)P + PA(\theta) \prec 0, \quad \theta \in \Theta \tag{3.25}$$

then the system in Equation (3.20) is quadratically stable. This condition is only sufficient for asymptotic stability considering uncertain or LPV systems and it is important to emphasize that it is a conservative stability criteria since does not account for differences between time-invariant, slowly-varying and fast-varying arbitrarily parameters.

In order to avoid the conservative issues provided by parameter-independent Lyapunov functions, the robust stability approach proposes the use of *parameter-dependent* Lyapunov functions, which means that this strategy includes time-varying scheduling parameters and their rate of variation. Thus, considering a Lyapunov function in the form

$$V(x, \theta) = x^T P(\theta) x \tag{3.26}$$

it is possible to use the following LMI

$$A^T(\theta)P(\theta) + P(\theta)A(\theta) + \frac{\partial P(\theta)}{\partial t} \prec 0, \quad \theta \in \Theta \tag{3.27}$$

to calculate a feasible semidefinite positive matrix $P(\theta)$. It should be noted that the derivative of $P(\theta)$ indicates the rate of change of θ, which is difficult to measure. Thus, structures are usually chosen for $P(\theta)$, such as a polynomial function of θ, in order to solve the LMI problem (BRIAT, 2014).

LMIs, such as those presented in Equations (3.25) and (3.27), are a very useful numerical tool for dealing with optimization and control problems (BOYD et al., 1994). Since the set of matrices in $A(\theta$ are known, P or $P(\theta)$ are called *decision variables* and must be calculate numerically. Note that the LMIs in Equations (3.25) and (3.27) are parameterized as functions of the scheduling variable θ, which means that they represent an infinite set of LMIs that must be solved. In order to deal with this issue, several methods of relaxation have been developed, more or less conservative, to obtain a finite number of LMIs to solve (APKARIAN; TUAN, 2000). In the following, some of the more common approaches:

- *Gridding*: This approach consists of discretizing the parametric space, as in Figure , and then solve an LMI that contains all points of thegrid. There is no guarantee of stability between the intermediate points and the method is limited for a high number of scheduling parameters (APKARIAN; TUAN, 2000).

Figure 49 – Grid of the scheduling parameters set in a two dimension space.

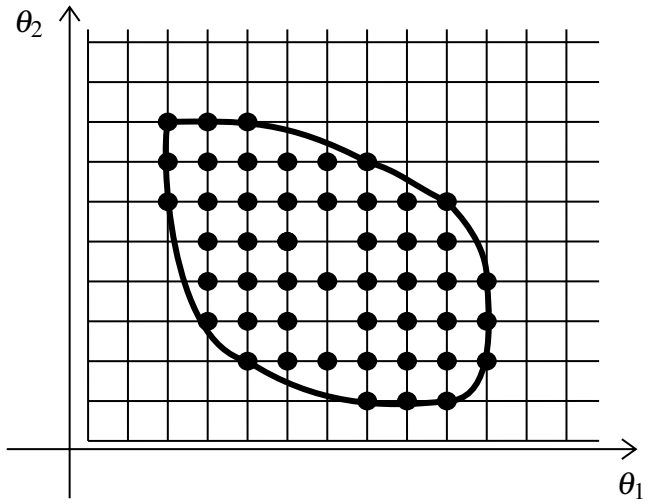

Source: The author.

- *Polytopic*: Note that Equations (3.25) and (3.27) represents an infinite set of LMIs, however if for these systems are considered an affine or polytopic dependence, with $\theta = \mathscr{C}o\{\theta_1 \cdots \theta_p\}$, then it is sufficient to determine a solution only for the vertices θ_i, $i = 1, \cdots, p$, which means that now one may use a finite set of LMIs. For the quadratic and robust stability approaches the LMIs are given by:

$$\exists P > 0 : \quad A^T(\theta_i)P + PA(\theta_i) < 0, \quad \forall i = 1, \cdots, p. \tag{3.28}$$

and

$$\exists P > 0: \quad A^T(\theta_i)P(\theta_i) + P(\theta_i)A(\theta_i + \frac{\partial P(\theta_i)}{\partial t}) < 0, \quad \forall i = 1, \cdots, p. \tag{3.29}$$

- *Sum of squares (SOS) decomposition*: When is considered a polynomial dependence in θ, it is possible to solve the problem with the theory of SOS (SCHERER, 2006). Since this technique is used in this thesis, more is explained in subsection 7.2.3.

3.2.2 *Performance analysis*

Generally the performance of an LPV system is measured by the extension of the notions of norm such as H_2 and H_∞. Considering a generic LPV given by:

$$\begin{aligned} \dot{x}(t) &= A(\theta)x(t) + B(\theta)w(t) \\ z(t) &= C(\theta)x(t) + D(\theta)w(t), \end{aligned} \tag{3.30}$$

then for admissible trajectories of $\theta \in \Theta$ the $\mathscr{L}_2$ gain is bounded by γ and:

$$\forall w \in \mathscr{L}_2, \quad \forall T \geq 0, \quad \int_0^T z^T(t)z(t)dt \leq \gamma^2 \int_0^T w^T(t)w(t)dt. \tag{3.31}$$

Denoting γ_∞ as the H_∞ norm of the system presented in Equation (3.30), which is equivalent to the smaller value of γ in Equation (3.31) that holds and computed by:

$$\gamma_\infty = \sup \sqrt{\frac{\int_0^T z^T(t)z(t)dt}{\int_0^T w^T(t)w(t)dt}} \tag{3.32}$$

By extending the real bounded lemma (BOYD et al., 1994), it is possible to determine a sufficient condition that combines the ideas of quadratic stability and performance measure H_∞.

3.3 Synthesis of LPV control systems

This section provides an introduction to the most common methods used to design LPV controllers.

3.3.1 *Gain scheduling*

One of the oldest and intuitive techniques for dealing with systems with varying parameters is gain scheduling (TAKAGI; SUGENO, 1985; LEITH; LEITHEAD, 2000).The method consists of first dividing a complex, or even nonlinear, system into several LTI subsystems for different operating points and then designing a controller for each of these subsystems with any synthesis methods, such as pole placement, H_∞, place of roots, etc. Finally, the controllers are interpolated in order to meet the entire determined operating range.

This approach can bring several problems to the analysis of the controlled system, for example, because it is not possible to guarantee stability between successive controllers. Another

problem that can arise is when the linearization process hides scheduling parameter behaviors and variations (SHAMMA; ATHANS, 1992).

A more efficient and rigorous manner of dealing with this type of problems may consists in use an LPV approach since the overall range of operation can be treat with a single model. The LPV controller is able to adapt to system variations with guaranteed stability.

3.3.2 Types of LPV controllers

Depending on the LPV model chosen to represent a system, it is possible to use different paradigms in the design of a controller. For this work, LPV systems of the I/O type are considered, so the polynomial synthesis method for the controller design is presented in the next chapter. Thus, in this section, the most common techniques for dealing with LPV systems in state space are presented. Consider an LPV system described in the following state-space format:

$$\begin{aligned} \dot{x}(t) &= A(\theta)x(t) + B(\theta)u(t) \\ y(t) &= C(\theta)x(t) \end{aligned} \tag{3.33}$$

where $u(t)$, $y(t)$ and $x(t)$ are the control input, the measured output and the state of the system, respectively. It is possible to formulate the control problem considering a bounded scheduling parameter or with an arbitrary variation rate (BRIAT, 2014).

There are basically three ways to design an LPV controller for a system in state space, the simplest being the gain scheduling state-feedback which can be formulated as

$$u(t) = K(\theta)x(t). \tag{3.34}$$

As can be seen, the idea is to extend the LTI state-feedback controller to the LPV framework. However it should be pointed that this approach requires knowledge of all system states to be implemented. When it is not possible to measure all states of a system, the control problem can be formulated as a gain scheduling static-output-feedback such as

$$u(t) = K(\theta)y(t), \tag{3.35}$$

which may have an easier implementation because it only needs the measured output. The main problem with this approach is that it can sometimes presents difficult conditions of tractability for controller design (FU, 2004; HENRION; LASSERRE, 2006; BRIAT, 2014). Finally, there is the class of LPV dynamic-output feedback controllers, which are computed in the form

$$\begin{aligned} \dot{x}_c(t) &= A_c(\theta)x_c(t) + B_c(\theta)y(t) \\ u(t) &= C_c(\theta)x_c(t) + D_c(\theta)y(t), \end{aligned} \tag{3.36}$$

where $x_c(t)$ is the state of the controller. If both controller and system orders are equal, then convex solutions can be found (PIERRE; PASCAL, 1995; SCHERER, 2001). For cases where this is not true, the problem becomes NP-hard and other types of solutions are needed (SCHERER; KOSE, 2012).

3.4 Smith predictor for LPV systems

Although its excellent disturbance and noise rejection, a great drawback of the SFSP is that it can only deal with fixed plants, using robustness to overcome uncertainties in the process parameters and delay. Variations on the plant parameters may appear in several ways in different processes. For such cases, control structures as FSP and SFSP need offline procedures or complex modifications (NORMEY-RICO; GARCIA; GONZALEZ, 2012).

Several studies over the years were concerned with extending control methods based on the Smith predictor to LPV systems with dead time. The main drawback of these studies, excepting the ones that propose methods for LPV-FSP, is that they use a classical SP structure, which means there is no concern about disturbance rejection performance and they are only suitable for stable open-loop plants. The general structure for the control system is represented in Figure 50.

Figure 50 – Representation of a the Smith predictor controller structure for LPV systems.

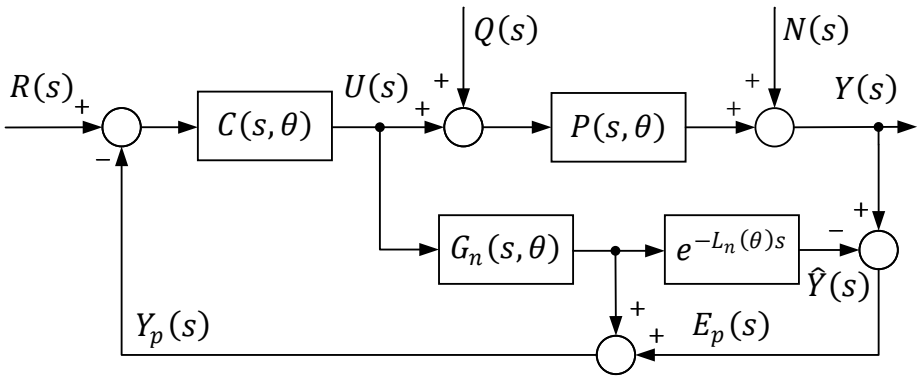

Source: The author.

In Bolea et al. (2009), Bolea, Puig and Blesa (2013) it was proposed a Smith Predictor PID-based LPV controller designed using H_∞ performance and linear matrix inequalities. The approach was validated on a single real reach canal. Later, the authors extended the controller to the multivariable LPV case applied to an irrigation canal system (BOLEA; PUIG, 2016).

The method considers LPV systems in the form:

$$P(s,\theta) = \frac{b_0(\theta)}{s^2 + a_1(\theta) + a_0(\theta)} e^{-\tau(\theta)s}, \tag{3.37}$$

and a LPV-PID given by:

$$C(s,\theta) = K_P(\theta) + \frac{K_I(\theta)}{s} + K_D(\theta)s. \tag{3.38}$$

Thus, the resultant negative feedback system can be conveniently rewrite as a state space system such as:

$$\begin{aligned}
\dot{x}(t) &= A(\theta)x(t) + B(\theta)u(t) + B_r r(t) \\
u(t) &= -K(\theta)x(t) + K_P(\theta)r(t) + K_D(\theta)\dot{r}(t) \\
y(t) &= Cx(t)
\end{aligned} \tag{3.39}$$

where $r(t)$ is the reference input, $y(t)$ is the system output, $x(t) = [y(t), \dot{y}(t), -\int e(t)dt]^T$ is the system state, with $e(t) = r(t) - y(t)$ being the error, and

$$\begin{aligned}
A(\theta) &= \begin{bmatrix} 0 & 1 & 0 \\ -a_0(\theta) & -a_1(\theta) & 0 \\ 1 & 0 & 0 \end{bmatrix}, \quad B(\theta) = \begin{bmatrix} 0 \\ b_0(\theta) \\ 0 \end{bmatrix}, \\
B_r(\theta) &= \begin{bmatrix} 0 \\ 0 \\ -1 \end{bmatrix}, \quad C = \begin{bmatrix} 1 \\ 0 \\ 0 \end{bmatrix}^T, \quad K(\theta) = \begin{bmatrix} K_P(\theta) \\ K_D(\theta) \\ K_I(\theta) \end{bmatrix}^T.
\end{aligned} \tag{3.40}$$

Bolea et al. (2009), Bolea, Puig and Blesa (2013) assume that the dead time has a time-varying nature despite its estimation error dynamics is time invariant, with a constant bound. Therefore, most of the dead time is compensated and the remaining

$$\Delta\tau(\theta) = \tau(\theta) - \hat{\tau}(\theta), \tag{3.41}$$

where $\tau(\theta)$ is the time varying dead time and $\hat{\tau}(\theta)$is its real time estimation, is addressed by LTI unstructured uncertainty. This uncertainty was considered as a multiplicative output uncertainty, bounded through an uncertainty bound (weight) to the delay measurement error frequency response:

$$W_\Delta(s, \Delta\tau) = \frac{2.05\Delta\tau_{max}s}{\Delta\tau_{max}s + 1}, \quad \Delta\tau(\theta) \leq \Delta\tau_{max}. \tag{3.42}$$

The LPV PID controller is formulated as a state feedback problem considering both performance and robustness objectives organized as a mixed sensitivity problem (MSP) in such form:

$$||[W_e S \quad W_u K S \quad W_\Delta T]||_\infty^T < \gamma \leq 1, \tag{3.43}$$

where S and T are the sensitivity and complementary sensitivity transfer functions, respectively. The weight W_Δ refers to the uncertainty of the plant model, which the authors considered as the delay measurement error, the weights W_e and W_u allow to stipulate a trade-off between performance and control effort, respectively.

The following conditions were also considered to design the LPV PID controller as a state feedback and to prevent the augmented model order from not increasing:

1. performance and control effort weight functions as constants, that is $W_e = D_e$ and $W_u = D_u$,
2. a modified uncertainty weight given by

$$\tilde{W}_\Delta(s, \Delta\tau) = 2.05\Delta\tau_{max}s, \tag{3.44}$$

where $W_\Delta = \tilde{W}_\Delta G$.

Then, by using the Smith predictor structure from Figure 6, and the uncertainty weight in Equation (3.44) bounding the delay measurement error Equation (3.41), the authors proposed a reorganization of the system as an LFT LPV system represented in Figure 51, and computed such as:

$$\begin{aligned}
\dot{x}(t) &= A(\theta)x(t) + B(\theta)u(t) + B_{u_\Delta}(\theta)u_\Delta(t) \\
z(t) &= C_z(\theta)x(t) + D_{zu}(\theta)u(t) + D_{zu_\Delta}(\theta)u_\Delta(t) \\
q(t) &= C_q(\theta)x(t) + D_{qu}(\theta)u(t) + D_{qu_\Delta}(\theta)u_\Delta(t),
\end{aligned} \tag{3.45}$$

where

$$\begin{aligned}
x(t) &= \begin{bmatrix} x_1(t) \\ x_2(t) \\ x_3(t) \end{bmatrix} = \begin{bmatrix} y(t) \\ x_\Delta(t) \\ x_I(t) \end{bmatrix} = \begin{bmatrix} y(t) \\ \dot{x}(t) \\ x_I(t) \end{bmatrix}, \quad z(t) = \begin{bmatrix} y_\Delta(t) \\ \tilde{u}(t) \\ \tilde{e}(t) \end{bmatrix} \\
A(\theta) &= \begin{bmatrix} 0 & 1 & 0 \\ -a_0(\theta) & -a_1(\theta) & 0 \\ 1 & 0 & 0 \end{bmatrix}, \quad B(\theta) = \begin{bmatrix} 0 \\ b_0(\theta) \\ 0 \end{bmatrix}, \quad B_{u_\Delta}(\theta) = \begin{bmatrix} 0 \\ 0 \\ 0 \end{bmatrix}, \\
C_z(\theta) &= \begin{bmatrix} D_\Delta & C_\Delta & 0 \\ 0 & 0 & 0 \\ -D_e & 0 & 0 \end{bmatrix}, \quad C_q(\theta) = \begin{bmatrix} -1 \\ 0 \\ 0 \end{bmatrix}^T, \\
D_{zu}(\theta) &= \begin{bmatrix} 0 \\ D_u \\ 0 \end{bmatrix}^T, \quad D_{zu_\Delta}(\theta) = \begin{bmatrix} 0 \\ 0 \\ -D_e \end{bmatrix}^T, \quad D_{qu_\Delta}(\theta) = -1, \quad D_{qu}(\theta) = 0.
\end{aligned} \tag{3.46}$$

Figure 51 – MSP diagram used in Bolea et al. (2009), Bolea, Puig and Blesa (2013), Bolea and Puig (2016).

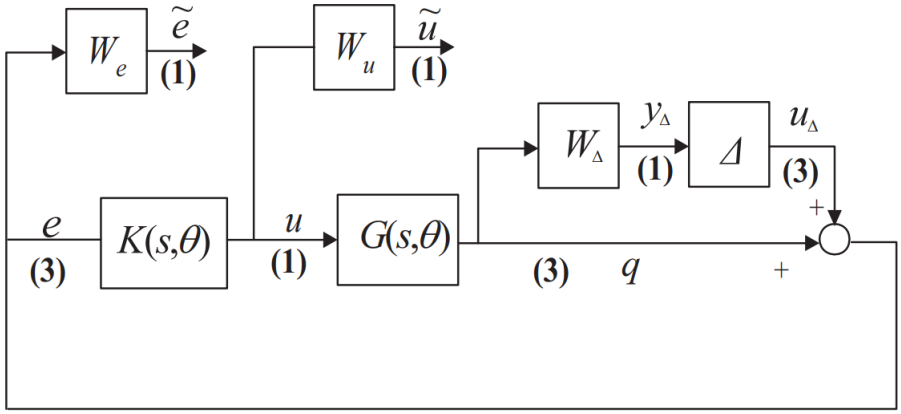

Source: Bolea et al. (2009), Bolea, Puig and Blesa (2013), Bolea and Puig (2016).

Since the system is written in LFT form, the controller gains were calculated using LMIs that use H_∞ performance and robust quadratic D-stability (PIERRE; PASCAL, 1995; APKARIAN; GAHINET; BECKER, 1995; CHILALI; GAHINET; APKARIAN, 1999).

Another approach was discussed in Oliveira and Karimi (2013), where it was proposed a design method for robust fixed order and gain-scheduling DTCs. It was considered an H_∞ robust performance condition represented by a set of convex constraints with respect to the parameters of a linearly parameterized primary controller in the Smith predictor structure. The technique showed a good performance for an uncertain time-delay simulated system and considered plants such as:

$$\mathscr{P} = G(s,\theta)e^{-\tau_i(\theta)s}, \quad i = 1,\cdots,q, \tag{3.47}$$

where the delay free model has unstructured multiplicative uncertainty, that is:

$$G(s,\theta) = G_n(s,\theta)[1+\Delta(s)W_2(s)], \tag{3.48}$$

and the scheduling vector is given by $\Theta = [\theta_1,\cdots,\theta_m]$, and it was assumed stability and performance for frozen scheduling parameters. This work considered the structure from Figure 50, where $P_0 = G_n(s,\theta)e^{-\tau(\theta)}$ is the nominal model, and had the objective of compute the primary controller $C(s\theta)$ meeting the H_∞ performance index specification.

The primary controller was linearly parameterized as $C(s,\theta) = \rho^T\phi(s)$, where $\phi(s) = [\phi_1(s),\cdots,\phi_{n_c}(s)]$ is a vector of basis functions with n_c stable transfer functions such as:

$$\phi^T(s) = \left[1, \frac{1}{s}, \frac{s}{1+T_f s}\right] \tag{3.49}$$

and where every gain $\rho^T(\theta) = [\rho_1(\theta),\rho_2(\theta),\cdots,\rho_n(\theta)]$ is a δ order polynomial function of the scheduling in the form:

$$\rho_i(\theta) = (v_{i,\delta})^T\theta^\delta + \cdots + (v_{i,1})^T\theta + v_{i,0}. \tag{3.50}$$

In order to compute the controller gains, the authors proposed the following optimization problem:

$$\begin{aligned} \min_{\rho} \quad & \gamma \\ \text{s.t.} \quad & |||W_1 S_i(s,\theta)| + |W_2 T_i(s,\theta)|||_\infty < \gamma \\ & \text{for } i = 1,\cdots,q, \forall\theta \in \Theta, \end{aligned} \tag{3.51}$$

where

$$S_i(s\theta) = \frac{1 + C(s,\theta)H(s,\theta)}{1 + C(s,\theta)(H(s,\theta) + P_i(s,\theta))} \tag{3.52}$$

and

$$T_i(s\theta) = \frac{1 + C(s,\theta)P_i(s,\theta)}{1 + C(s,\theta)(H(s,\theta) + P_i(s,\theta))}, \forall\theta \in \Theta \tag{3.53}$$

are the sensitivity and complementary sensitivity transfer functions, respectively, and $H(s,\theta) = G_n(s,\theta) - P_0(s,\theta)$. The optimization is solved by the bisection algorithm following the convex constraints:

$$\begin{aligned} &[|W_1(jw_k)[1 + C(jw_k,\theta_l)H(jw_k,\theta_l)]| + |W_2(jw_k)C(jw_k,\theta_l)P(jw_k,\theta_l)|]\,|1 + L_d(jw_k)| - \\ &Re\{[1 + L_d^*(jw_k)][1 + L_i(jw_k,\theta)]\} < 0 \quad \text{for } k = 1,\cdots,N; i = 1,\cdots,q; l = 1,\cdots,m. \end{aligned} \tag{3.54}$$

where L_d^* is the complex conjugate of a strictly proper transfer function that does not encircle the critical point.

The study from Blanchini et al. (2016) proposed a method to achieve realization and stable design of LPV-based controllers in the Smith predictor structure that ensure closed-loop stability and point-wise optimal performance. They considered stable LPV systems such as:

$$\dot{x}(t) = A(\theta)x(t) + B(\theta)u(t) \tag{3.55}$$

$$y_0(t) = C(\theta)x(t) \tag{3.56}$$

$$y(t) = y_0(t - \tau) \tag{3.57}$$

where A, B and C are continuous functions of $\theta \in \Theta$ and it is assumed that the delay is bounded by $0 \leq \tau \leq \bar{\tau}$. From the structure of SP in Figure 50, the transfer function of the controller is given by:

$$Q(s,\theta) = [I + C(s,\theta)P(s,\theta)]^{-1}C(s,\theta), \tag{3.58}$$

which has the state space realization such as:

$$\dot{z}(t) = F(\theta)z(t) + B(\theta)v(t) \tag{3.59}$$

$$u(t) = H(\theta)z(t) + K(\theta)v(t), \tag{3.60}$$

where F, G, H and K are continuous functions of $\theta \in \Theta$ and for a constant θ:

$$Q(s,\theta) = H(\theta)[sI - F(\theta)]^{-1}G(\theta) + K(\theta). \tag{3.61}$$

The control system is then represented by the diagram in Figure 52,

Figure 52 – Control scheme for the LPV-stable plant with dead time proposed in Blanchini et al. (2016).

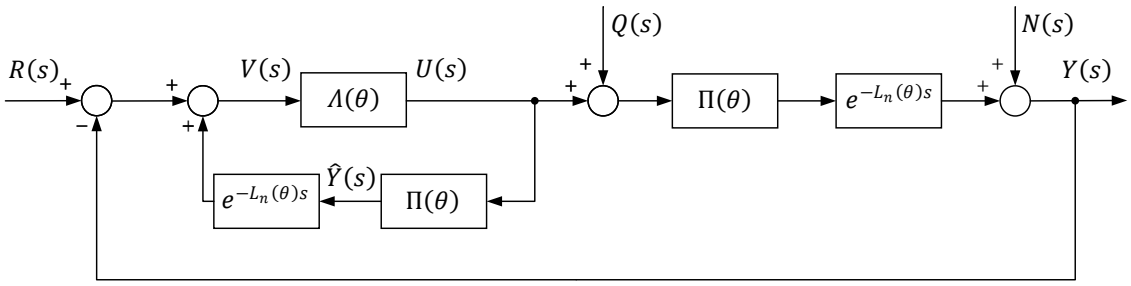

Source: The author.

where $\Pi = \{A(\theta), B(\theta), C(\theta)\}$ and $\Lambda = \{F(\theta), G(\theta), H(\theta), K(\theta)\}$. The controller gains are computed by the following online procedure:

1. Compute a realization of $Q(s,\theta)$ such as $\tilde{\Lambda} = \{\tilde{F}(\theta), \tilde{G}(\theta), \tilde{H}(\theta), \tilde{K}(\theta)\}$, where $\tilde{F}(\theta)$ is Hurwitz for all θ.

2. Calculate a positive-definite matrix $X(\theta)$ from the Lyapunov equation:

$$\tilde{F}^T(\theta)X(\theta) + X(\theta)\tilde{F}^T(\theta) = -I. \tag{3.62}$$

3. Factorize $X(\theta)$ as

$$X(\theta) = R^T(\theta)R(\theta), \tag{3.63}$$

with $R(\theta)$ as an upper triangular matrix.

4. Then realize $Q(s,\theta)$ as $\Lambda = \{F(\theta), G(\theta), H(\theta), K(\theta)\}$, with

$$\left[\begin{array}{c|c} F(\theta) & G(\theta) \\ \hline H(\theta) & K(\theta) \end{array}\right] = \begin{bmatrix} R(\theta) & 0 \\ 0 & I \end{bmatrix} \begin{bmatrix} \tilde{F}(\theta) & \tilde{G}(\theta) \\ \tilde{H}(\theta) & \tilde{K}(\theta) \end{bmatrix} \begin{bmatrix} R^{-1}(\theta) & 0 \\ 0 & I \end{bmatrix}. \tag{3.64}$$

Morato and Normey-Rico (2019) and Morato and Normey-Rico (2021) proposed an LPV-FSP controller capable of deals with time-varying dead-time systems. The structure of this controller is represented in Figure 53, where the nominal delay L_n is dealt by the predictor and the time varying $L(t)$ by the LPV feedback filter $V(s,\theta)$. With this filter is possible to set more

or less robustness to the closed-loop system considering the estimated time-varying dead time. Despite the good response in systems with time-varying delays, the paper only deals with plants with fixed transfer functions.

Figure 53 – Control scheme for the LPV Filtered Smith Predictor proposed in Morato and Normey-Rico (2019), Morato and Normey-Rico (2021).

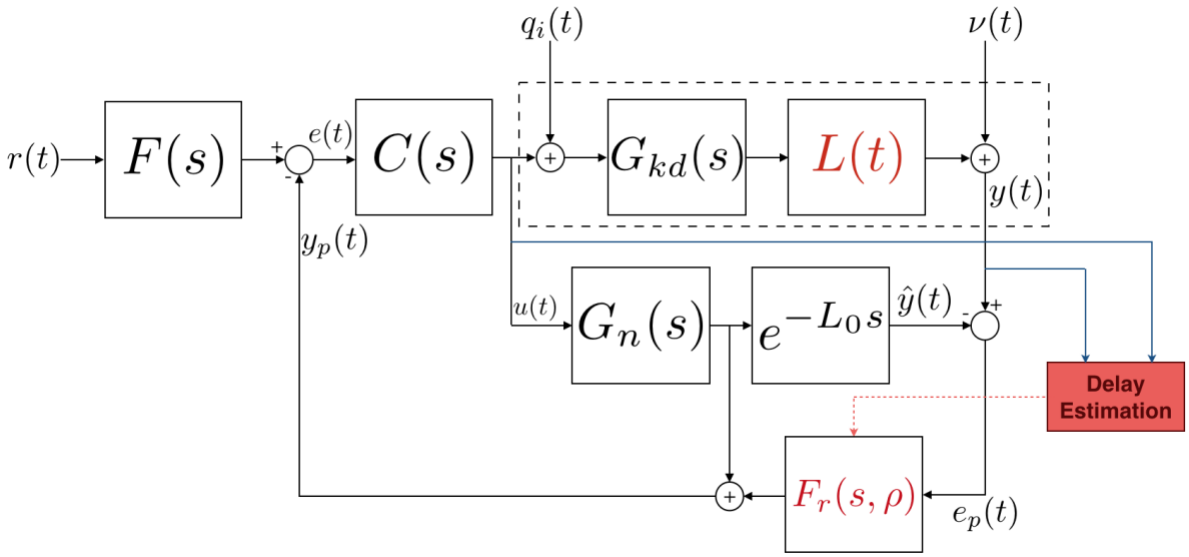

Source: (MORATO; NORMEY-RICO, 2019; MORATO; NORMEY-RICO, 2021).

This controller is implemented in discrete time and its tuning is composed by several steps (note that steps 1 and 2 are the same as described in section 2.2):

1. Considering a given reference tracking $H_{yr(z)}$, calculate a discrete primary controller $C(z)$ to stabilize the free delay model $G_n(z)$.

2. In order to deal with uncertainties $H_{yq(z)}$ and robustness disturbance $H_{yn(z)}$ responses, one have to compute a stable robustness filter $V(z)$ take in account only the nominal delay L_n.

3. To overcame the time-varying dead time, an LPV feedback filter $V(s,\theta)$ must be designed. In order to slow down the control effort when the variable delay $L(k)$ increases, the authors used a low-pass structure for the LPV filter $V(s,\theta)$, ensuring more robustness and implying greater conservatism in the closed-loop. The scheduling parameter is given by the estimated variable delay, such as:

$$\theta = \hat{L}(k) \in \Theta := [\underline{L}, \overline{L}], \tag{3.65}$$

which leads to a filter that vary according to θ from $V(z,\underline{L}) = \dfrac{1}{\underline{\tau}\dfrac{(z-1)}{t_s}+1}$ to $V(z,\overline{L}) = \dfrac{1}{\overline{\tau}\dfrac{(z-1)}{t_s}+1}$. The idea is to define safe bounds for the filter bandwidth such as $\underline{\tau} = 10\dfrac{\underline{L}}{\pi}$

and $\overline{\tau} = 10\dfrac{\overline{L}}{\pi}$ in order to deal with the minimal and maximal TV delay $\underline{L}(k)$ and $\overline{L}(k)$, respectively and then compute the filter LPV feedback filter $V(s,\theta)$ in the space state form:

$$\begin{aligned} x_V(k+1) &= \left(\frac{\tau(\theta)-t_s}{\tau(\theta)}\right)x_V(k) + \left(\frac{t_s}{\tau(\theta)}\right)e_p(k) \\ y_V(k) &= x_V(k) \\ \tau(\theta) &= \left(\frac{\overline{L}-\theta}{\overline{L}-\underline{L}}\right)\underline{\tau} + \left(\frac{\theta-\underline{L}}{\overline{L}-\underline{L}}\right)\overline{\tau}, \end{aligned} \tag{3.66}$$

where the each frozen system inside the polytope Θ must respect the stability condition of

$$||\delta P(jw)||_\infty < \left|\frac{1+C(e^{jwt_s})G_n(e^{jwt_s})}{C(e^{jwt_s})G_n(e^{jwt_s})V(e^{jwt_s})}\right|, \quad 0 \leq w < \pi/t_s, \tag{3.67}$$

with $P(z) = P_n(z)[1+\delta P(z)]$.

4. The computation of the overall robustness filter is the product of the filters $V(z)$ (regarding robustness towards uncertainties and disturbance-rejection response) and $V(z,\theta)$ (concerning the time-varying dead time). They have an independent tuning and the practical implementation is the cascade of both.

As in the LTI case, to deal with integrative and unstable plants the LPV-FSP controller has to be internally stable. Thus, the authors proposed the structure represented in Figure 54,

Figure 54 – Discrete-time equivalent implementation structure for the LPV filtered Smith predictor proposed in (MORATO; NORMEY-RICO, 2019; MORATO; NORMEY-RICO, 2021).

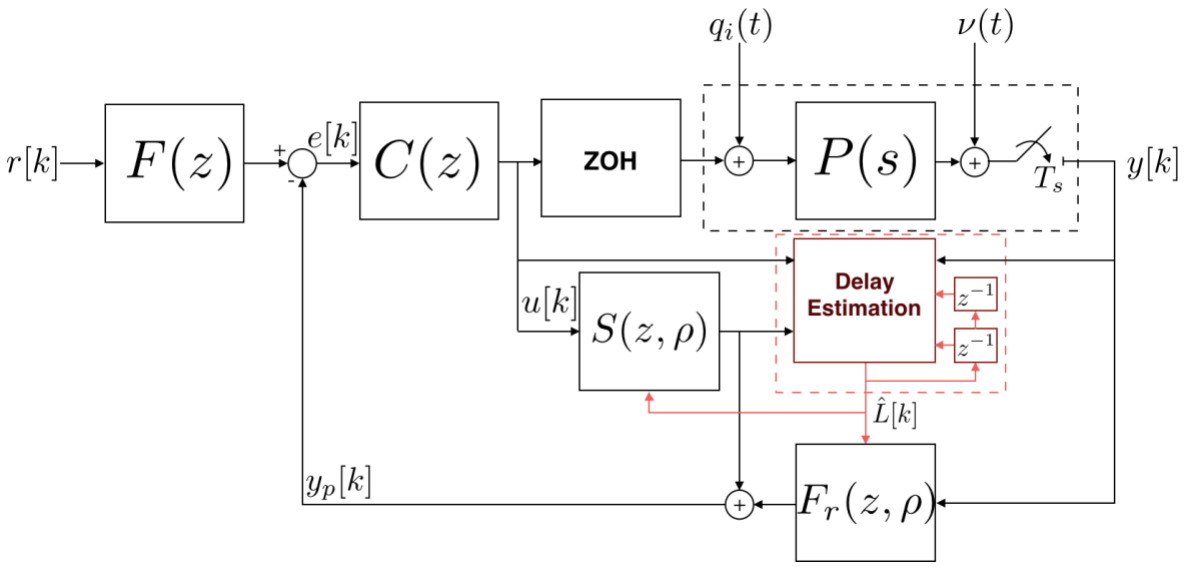

Source: (MORATO; NORMEY-RICO, 2019; MORATO; NORMEY-RICO, 2021).

with

$$S(z,\theta) = G_n(z)[1 - z^{-d_n}V(z,\theta)]. \tag{3.68}$$

The authors also proposed an estimator for the varying delay, however this escapes the scope of this work and it is implicated that the strategy is valid for any delay identification technique.

3.4.1 Discussion

The various techniques presented have several advantages in their respective field of use. However, except for the approach presented in Morato and Normey-Rico (2019), Morato and Normey-Rico (2021), all strategies use the classical Smith predictor in continuous time, that is, they are not able to work in integrative and unstable systems, because it is an internally unstable structure.

The LPV-FSP approach proposed in Morato and Normey-Rico (2019), Morato and Normey-Rico (2021), although advantageous, does not deal with problems in which the plant itself has variable dynamics, being restricted to a particular case of variable delay systems.

By considering all this context, the contribution of this work is the extension of the SFSP (TORRICO et al., 2013a; TORRICO; CORREIA; NOGUEIRA, 2016; TORRICO et al., 2018) to an LPV framework in order to deal with nonlinear dead-time systems assuring both performance and stability. The proposed controller is suitable for nonlinear dead-time systems with stable, unstable, and integrating dynamics. The method is also robust to uncertainties in the dead time, which is considered fixed.

4 SIMPLIFIED FILTERED SMITH PREDICTOR FOR SERIES CASCADE CONTROL OF DEAD-TIME PROCESSES

In this chapter it is proposed a series cascade control structure based on the simplified filtered Smith predictor (SFSP) concepts, a delay compensator, for two first-order processes plus dead time (FOPDT). In this work, the main contribution is that the controller incorporates a predictor for each process to manage unstable processes in the discrete-time domain, with the detail that each robustness filter is adjusted related to the perturbation applied to its respective loop.

4.1 Proposed control structure

The proposed control structure for series cascade processes is shown in Figure 56, where $P_1(z)$ and $P_2(z)$ represent the primary and secondary processes, respectively. $G_1(z)$ and $G_2(z)$ are the fast models while d_1 and d_2 represents the process dead time of $P_1(z)$ and $P_2(z)$, respectively. The primary controller is composed by the static gains k_r and k and the filter $F(z)$, being used to set the desired tracking dynamic. The filters $V_1(z)$ and $V_2(z)$ are tuned to guarantee stability and improve disturbance attenuation.

Figure 55 – Conceptual structure for the proposed series cascade predictor.

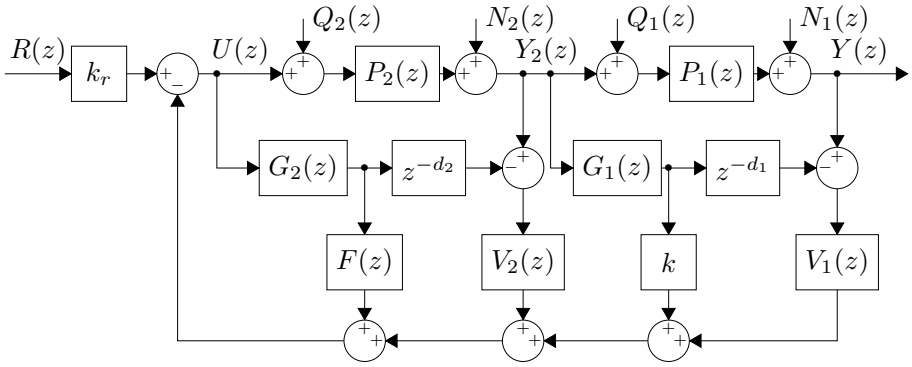

Source: The author.

This controller is designed for FOPDT models in the form:

$$P_1(z) = \frac{b_1}{z-a_1} z^{-d_1}, \tag{4.1}$$

$$P_2(z) = \frac{b_2}{z-a_2} z^{-d_2}. \tag{4.2}$$

Since the proposed controller structure presents a predictor for each process, disturbances in the loop of $P_2(z)$ are attenuated before even reach the loop of $P_1(z)$, which represents a crucial

difference in relation to the literature approaches discussed in Section 2.4. In this way, it will be possible to obtain the benefits of both control strategies:

- Good performance (faster response and no overshoot).
- Robustness with decoupling (the adjustment of each filter is related to the disturbance applied to its respective loop).
- Attenuation of disturbances in the internal loop without these reaching the external loop.
- Noise attenuation.

For the same reasons discussed in chapter 2, the conceptual structure of the proposed controller, presented in Figure 55, is not suitable for deal with unstable and/or integrative systems, as it is internally unstable. Thus, an equivalent structure for implementation is presented in Figure 56,

Figure 56 – Implementation structure for the proposed series cascade predictor.

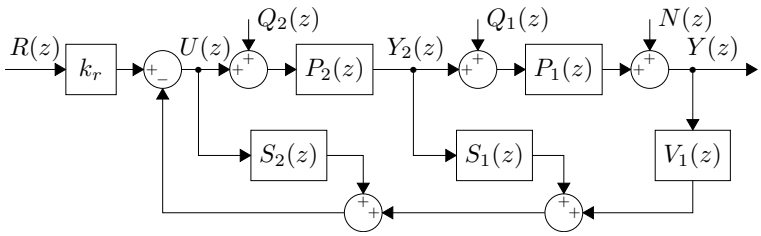

Source: The author.

where the parameters of the controller are given by:

$$S_1(z) = G_1(z)(k - V_1(z)z^{-d_1}) + V_2(z), \tag{4.3}$$

$$S_2(z) = G_2(z)(F(z) - V_2(z)z^{-d_2}). \tag{4.4}$$

The closed-loop relationships and the condition for robust stability of the proposed cascade controller are calculated considering the nominal case such as:

$$\frac{Y(z)}{R(z)} = \frac{k_r P_1(z)P_2(z)}{1 + S_2(z) + P_2(z)S_1(z) + P_1(z)P_2(z)V_1(z)}, \tag{4.5}$$

$$\frac{Y(z)}{Q_2(z)} = \left(\frac{1 + S_2(z)}{1 + S_2(z) + S_1(z)P_2(z)}\right) P_1(z)P_2(z), \tag{4.6}$$

$$\frac{Y(z)}{Q_1(z)} = \left(\frac{1 + S_2(z) + S_1(z)P_2(z)}{1 + S_2(z) + P_2(z)[S_1(z) + V_1(z)P_1(z)]}\right) P_1(z). \tag{4.7}$$

4.1.1 Setpoint tracking

The desired closed-loop transfer function for tracking may be chosen as:

$$\frac{Y(z)}{R(z)} = \frac{p_2}{\lambda_d(z)} z^{-(d_1+d_2)}, \tag{4.8}$$

where $\lambda_d(z) = z^2 + p_1 z + p_2$ is choose to obtain the desired tracking dynamics.

For the nominal case, the transfer function for tracking is reduced to:

$$\frac{Y(z)}{R(z)} = \frac{k_r b_1 b_2 z^{-(d_1+d_2)}}{(z-a_1)(z-a_2) + b_2 F(z)(z-a_1) + k b_1 b_2 z^{-d_2}}, \tag{4.9}$$

then by making an equivalence of (4.5) and (4.8) one can tune the primary controller parameters kr, k, and $F(z)$. The static gain kr is immediately computed as:

$$k_r = \frac{p_2}{b_1 b_2}, \tag{4.10}$$

and, from the equality of the denominators, the following expression is obtained

$$\lambda_d(z) = (z-a_1)(z-a_2) + b_2 F(z)(z-a_1) + k b_1 b_2 z^{-d_2}. \tag{4.11}$$

Since k is tuned to control $G_1(z)$, the static gain k is calculated by making $z = a_1$ in (4.11), one can obtain:

$$k = \frac{\lambda_d(a_1) a_1^{d_2}}{b_1 b_2}, \tag{4.12}$$

and, also from (4.11) it is possible to compute

$$F(z) = \left(\frac{\lambda_d(z) - b_1 b_2 z^{-d_2} k}{z - a_1} + z - a_2 \right) \frac{1}{b_2}, \tag{4.13}$$

or, after the polynomial division:

$$F(z) = \frac{a_1 + a_2 + p_1}{b_2} + \frac{\lambda_d(a_1)}{b_2} \sum_{n=0}^{d_2-1} a_1^n z^{-(n+1)}, \tag{4.14}$$

4.1.2 Disturbance attenuation

The robustness filters for the proposed cascade series controller are considered as:

$$V_2(z) = \frac{b_{21} z + b_{22}}{z - \alpha_2}, \tag{4.15}$$

and

$$V_1(z) = \frac{b_{11} z + b_{12}}{z - \alpha_1}, \tag{4.16}$$

where the filters coefficients b_{21}, b_{22}, b_{11} and b_{12} are calculated to achieve the design requirements of disturbances rejection at steady state and the poles α_2 and α_1 are free tuning parameters to define the dynamic disturbance attenuation of outer and inner loop, respectively.

As the poles of the processes $P_1(z)$ and $P_2(z)$ appear in (4.6) and (4.7), then it is up to the filters $V_1(z)$ and $V_2(z)$ be designed to reject step-like disturbances at steady-state. Thus, in order to fulfill these requirements they should consider two conditions: i) attenuation of disturbances and ii) cancellation of the plant model poles. For $V_2(z)$, the design conditions for $a_2 \neq 0$ are:

$$1 + S_2(z)|_{z=1} = 0, \tag{4.17}$$

$$S_2(z)|_{z=a_2} = 0, \tag{4.18}$$

and for $V_1(z)$, the conditions for $a_1 \neq 0$ are:

$$1 + S_2(z) + P_2(z)S_1(z)|_{z=1} = 0, \tag{4.19}$$

$$S_1(z)|_{z=a_1} = 0. \tag{4.20}$$

For the integrating processes with $a_1 = 1$, there is a multiplicity of roots and conditions that must be modified to:

$$\frac{d}{dz}\left[1 + S_2(z) + P_2(z)S_1(z)\right]\Big|_{z=1} = 0, \tag{4.21}$$

$$1 + S_2(z)|_{z=a_1} = 0, \tag{4.22}$$

$$S_1(z)|_{z=a_1} = 0. \tag{4.23}$$

By satisfying the set of conditions described, one can calculate the robustness filters to ensure disturbance attenuation and stability in the inner and outer loop, respectively.

4.1.3 Internal stability

The control signal of the proposed structure can be calculated such as (see Figure 56):

$$U(z) = k_r R(z) - S_2(z)U(z) - S_1(z)Y_2(z) - V_1(z)Y(z), \tag{4.24}$$

which, with Equations (4.3) and (4.4), can be written as:

$$\begin{aligned} U(z) = k_r R(z) &- \left[\frac{b_2}{z-a_2}\left(F(z) - \frac{N_{v_2}(z)}{D_{v_2}(z)}z^{-d_2}\right)\right]U(z) \\ &- \left[\frac{b_1}{z-a_1}\left(k - \frac{N_{v_1}(z)}{D_{v_1}(z)}z^{-d_1}\right) + \frac{N_{v_2}(z)}{D_{v_2}(z)}\right]Y_2(z) - \frac{N_{v_1}(z)}{D_{v_1}(z)}Y(z). \end{aligned} \tag{4.25}$$

Conditions imposed in Equations (4.18) and (4.20) allow to cancel the poles of the process $z = a_2$ and $z = a_1$ from S_2 and S_1, respectively. Using partial fraction decomposition for

$\alpha_1 \neq a_1$ and $\alpha_2 \neq a_2$, one can see that:

$$S_2(z) = \frac{N_{S_2}}{z-a_2} - \frac{N_{S_2}a_2^{d_2}}{z-a_2}z^{-d_2} - \frac{N^*_{v_2}(z)}{D_{v_2}(z)}z^{-d_2} \tag{4.26}$$

$$S_1(z) = \frac{b_1 k}{z-a_1} - \frac{b_1 k a_1^{d_1}}{z-a_1}z^{-d_1} - \frac{N^*_{v_1}(z)}{D_{v_1}(z)} + \frac{N_{v_2}(z)}{D_{v_2}(z)}, \tag{4.27}$$

where $N^*_{v_2}(z)$ and $N^*_{v_1}(z)$ are polynomials of order n_{v_2} and n_{v_1}, respectively. Considering the Diophantine equation discussed in Sanz, García and Albertos (2018):

$$1 = Q(z)(z-a) + R(z), \tag{4.28}$$

where Q and R are the quotient and remainder of the polynomial division $1/(z-a)$, it is possible to compute its solution up to d terms such as:

$$1 = \left(\sum_{i=1}^{d} a^{i-1}z^{-i}\right)(z-a) + a^d z^{-d}, \tag{4.29}$$

which can be rewrite as:

$$\frac{1}{z-a} - \frac{a^d}{z-a}z^{-d} = \sum_{i=1}^{d} a^{i-1}z^{-i}. \tag{4.30}$$

Thus, by substituting (4.29) in (4.25), the control signal can be rewrite as:

$$\begin{aligned} U(z) = k_r R(z) &- \left(\sum_{i=1}^{d_2} a_2^{i-1}z^{-i} - \frac{N^*_{v_2}(z)}{D_{v_2}(z)}z^{-d_2}\right)U(z) \\ &- \left(\sum_{i=1}^{d_1} a_1^{i-1}z^{-i} - \frac{N^*_{v_1}(z)}{D_{v_1}(z)}z^{-d_1} + \frac{N_{v_2}(z)}{D_{v_2}(z)}\right)Y_2(z) - \frac{N_{v_1}(z)}{D_{v_1}(z)}Y(z). \end{aligned} \tag{4.31}$$

From (4.31), one can observe that the poles $z = a_1$ and $z = a_2$ no longer appear in the denominator of the expression, which means that all poles now lies within the unit circle guarantying internal stability.

4.2 Numerical example

This example considers a process model presented in Bhaskaran and Rao (2020), which consists in a continuous stirred tank reactor (CSTR). The primary and secondary models of the process are described such as:

$$P_1(s) = \frac{e^{-4s}}{20s-1}, \text{ and } P_2(s) = \frac{2e^{-2s}}{20s+1}.$$

Since the results of Bhaskaran and Rao (2020) are used in this work for comparison, then a simulation of the controller applied to the discussed process model is performed and it was

found that Bhaskaran and Rao (2020) used a sampling time $T_s = 0.3$ to obtain the discretized primary and secondary models (see Appendix A), which are given by:

$$P_1(z) = \frac{0.01511}{z-1.015} z^{-14}, \text{ and } P_2(z) = \frac{0.02978}{z-0.9851} z^{-7}.$$

The tuning of the primary controller for the proposed methodology considers a pair of poles placed at $z_1 = 0.9$ and $z_2 = 0.96$ in order to obtain a faster tracking, and by using (4.10), (4.12) and (4.14) the controller is given by:

$$\begin{aligned} k_r &= 8.8887,\ k = 15.6588, \\ F(z) &= 4.709 + 0.2131z^{-1} + 0.2163z^{-2} + 0.2196z^{-3} + \\ &\quad 0.2229z^{-4} + 0.2262z^{-5} + 0.2297z^{-6} + 0.2331z^{-7}, \end{aligned}$$

and the robustness filters are designed with $\alpha_1 = 0.7$ and $\alpha_2 = 0.9$ and calculated such as:

$$V_1(z) = \frac{226.3z - 223.7}{z-0.7} \quad \text{and} \quad V_2(z) = \frac{12.69z - 12.02}{z-0.9}.$$

The simulations are performed with the same conditions presented in Bhaskaran and Rao (2020), that is, a setpoint step unit change is applied at $t = 0$ (s) and a step-like disturbance of magnitude -1 are applied to q_2 and q_1 at $t = 150$ (s) and at $t = 350$ (s), respectively. Also, a band-limited white noise of power 10^{-5} and variance 2.9695×10^{-5} is applied to n_2 at $t = 590$ (s). For a fair comparison to analyze the robustness, it is used the same model uncertainties considered in Bhaskaran and Rao (2020) where -10 % perturbations are given to the primary process time constant whereas $+10$ % perturbations are given to the primary process dead time. For the secondary process, $+10$ % perturbations are added to its gain as well as in its dead time.

The closed-loop response for the nominal is shown in Figure 57, where it can be seen that the proposed controller presents a faster response for tracking and a better disturbance attenuation of q_2, which consists exactly of the expected improvement for the series cascade controller. Regarding the perturbation of q_1, the SFSP provides a slightly faster result.

The results for the uncertainty case are presented in Figure 58. The controller in Bhaskaran and Rao (2020) presents an oscillatory response for disturbance attenuation while the response for the proposed controller is faster and with no overshoot. The SFSP still presents a faster setpoint tracking in the case with model uncertainties.

Table 1 shows the performance indices for both controllers (see Appendix A). The proposed controller has shown a better performance than the predictor proposed by (BHASKARAN; RAO, 2020) in all scenarios, except the TV index in the nominal case because the more aggressive tuning. Considering the IAE index for disturbance rejection, the SFSP presents a significant improvement in the compensation of q_2, which is precisely the expected from a cascade control system, however the proposed controller do it without any overshoot in the nominal case, i.e., the better the process model, the better the control performance it will be.

Figure 57 – Nominal case.

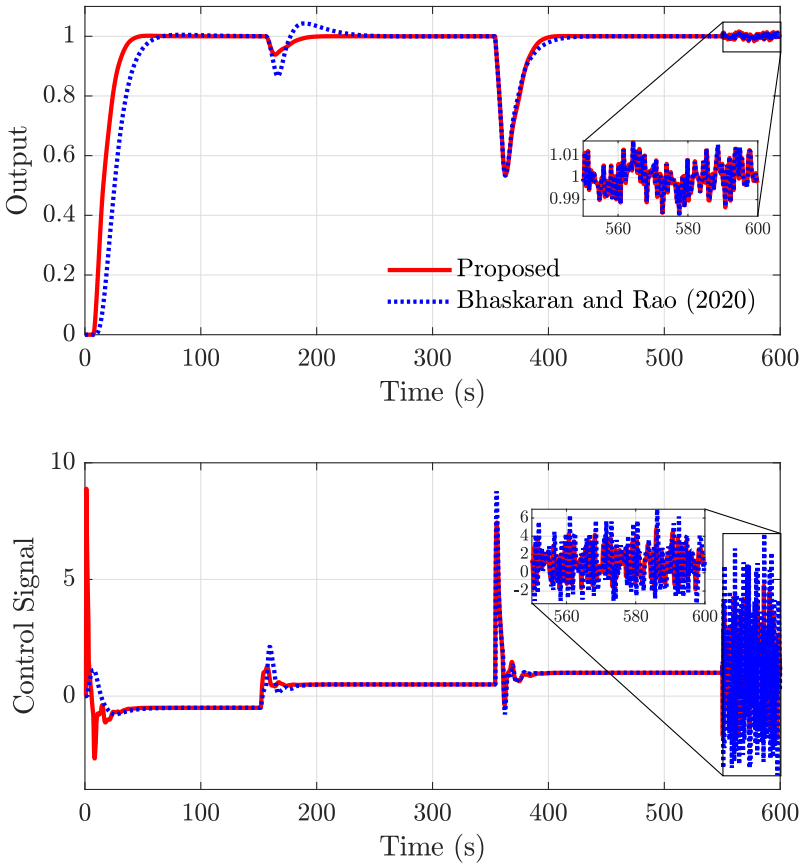

Source: The author.

Table 1 – Example 1 - Performance indices

Case	Controller	Indices				
		IAE Setpoint	IAE q_2	IAE q_1	TV	CV
Nominal	Proposed	**17.92**	**1.04**	**7.69**	45.32	**2.39**
	Bhaskaran and Rao	27.73	2.84	8.05	**30.25**	5.97
Uncertain	Proposed	**17.90**	**1.04**	**7.62**	**45.11**	**2.59**
	Bhaskaran and Rao	27.56	3.12	8.66	63.08	5.70

4.3 Discussion

In this chapter it is proposed a series cascade control structure based on the simplified filtered Smith predictor strategy to improve the response of unstable systems with delay in the discrete domain. This controller comprises a filter to guarantee the reference, two primary controllers (one gain for the primary loop and an FIR filter for the secondary loop), and two robustness filters, one for each respective loop.

A comparison was made with another controller from the literature (BHASKARAN; RAO, 2020) to prove that the proposed controller meets the expected characteristics. The proposed method presents a faster response for reference tracking, a better attenuation of the

Figure 58 – Uncertainty case.

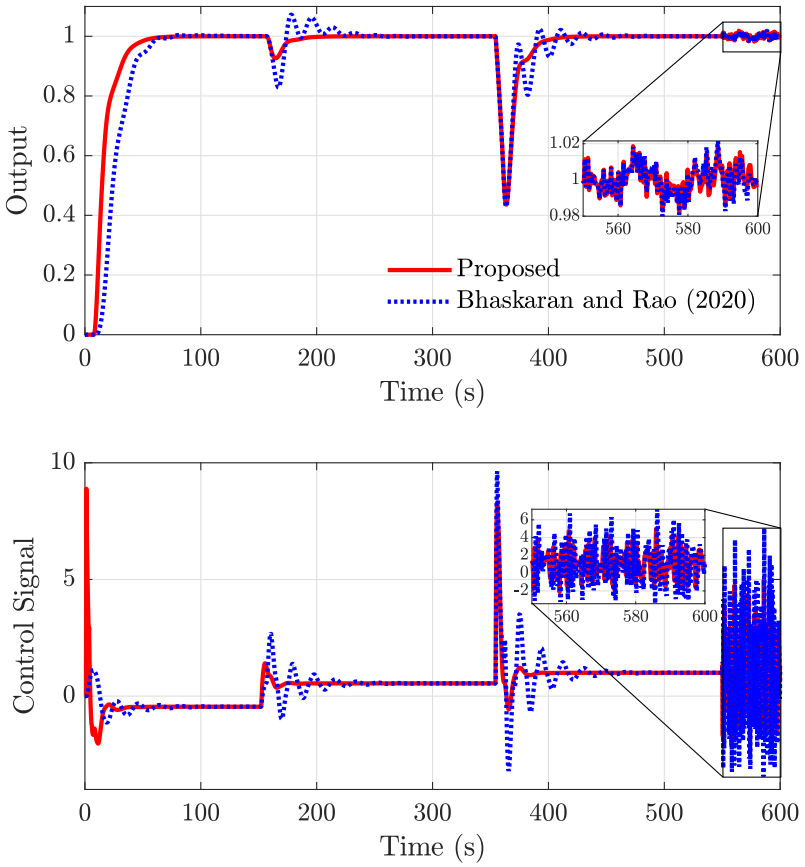

Source: The author.

disturbance q_2 in the internal loop, without overshoot, and a little better attenuation concerning the disturbance q_1 in the nominal case. Regarding the case with uncertainties, the proposed controller shows a faster Bhaskaran and Rao (2020) Bhaskaran and Rao (2020). Table 1 shows these results numerically, presenting the performance indexes in which the proposed controller gave the best values, except for the TV, due to a less smooth control signal.

5 SIMPLIFIED FILTERED SMITH PREDICTOR FOR PARALLEL CASCADE CONTROL OF DEAD-TIME PROCESSES

In this chapter, it is proposed a new parallel cascade control structure (PCCS) based on extending the discrete version of the SFSP (TORRICO et al., 2021), suitable for stable, integrating, and unstable processes. This extension is intended to develop a controller for industrial applications, similar to the SFSP for SISO systems, that does not require explicit integrating controllers in the primary controller. Robustness filters are used to reject disturbances and ensure zero steady-state error. The proposed controller aims to improve disturbance rejection for processes with dead time while maintaining a simple control structure with only four tuning parameters: the feedback gain K_2 and the robustness filter $V_2(z)$ for the inner loop, and the feedback gain K_{aug} and the robustness filter $V_{aug}(z)$ for the outer loop, unlike other controllers that require additional tuning parameters.

5.1 Parallel cascade control based on simplified FSP

The proposed parallel cascade control for dead-time systems, namely PCCS-SFSP, is presented in Figure 59.

Figure 59 – Proposed controller structure for parallel cascade SFSP.

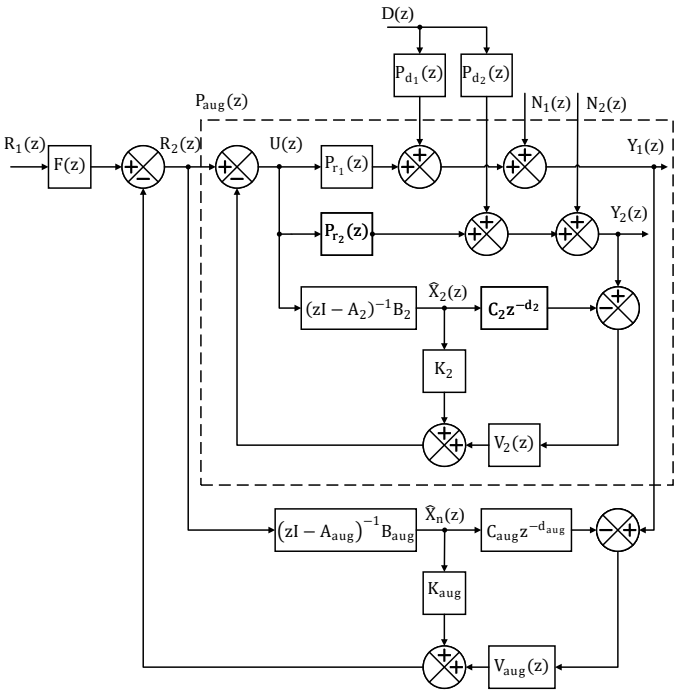

Source: The author.

where P_{r_1} and P_{r_2} represent the primary and secondary processes, and P_{d_1} and P_{d_2} represent the

disturbance models. The processes models are given by

$$P_1(z) = C_1(zI - A_1)^{-1}B_1 z^{-d_1}, \tag{5.1}$$

and

$$P_2(z) = C_2(zI - A_2)^{-1}B_2 z^{-d_2}. \tag{5.2}$$

The internal loop, which includes the process represented by Equation (5.2), is composed by a stabilizing static gain K_2 and a robustness filter $V_2(z)$ to disturbance attenuation. However, for the external loop, it is necessary to reduce the internal loop block diagram to get a higher-order process. Thus, after some manipulations, one may obtain the following augmented system to represent the external loop:

$$P_{aug}(z) = \frac{P_1(z)K_2}{1 + G_2(z)K_2} = C_{aug}(zI - A_{aug})^{-1}B_{aug}z^{-d_{aug}}, \tag{5.3}$$

and the static gain K_{aug} is designed to stabilize P_{aug} while the robustness filter V_{aug} is used for disturbance attenuation.

From the block diagram in Figure 59 and considering the nominal cases $P_2(z)$ and $P_{aug}(z)$, one can calculate the following closed-loop relations

$$H_{y_1r_1}(z) = \frac{Y_1(z)}{R_1(z)} = F_r(z)C_{aug}(zI - A_{aug} + B_{aug}K_{aug})^{-1}B_{aug}z^{-d_{aug}}, \tag{5.4}$$

$$H_{y_2r_2}(z) = \frac{Y_2(z)}{R_2(z)} = C_2(zI - A_2 + B_2K_2)^{-1}B_2 z^{-d_2}, \tag{5.5}$$

$$H_{y_1d}(z) = \frac{Y_1(z)}{D(z)} = \frac{K_g(z)[P_{d_1}(z)(1 + K_2G_2(z)) - P_{d_2}(z)P_1(z)V_2(z)]}{K_g(z)(1 + K_2G_2(z)) + P_1(z)V_{aug}(z)}, \tag{5.6}$$

$$H_{y_2d}(z) = \frac{Y_2(z)}{D(z)} = \frac{P_{d_2}(z)[K_g(z)(1 + K_2G_2(z) - P_2(z)V_2(z)) + P_1(z)V_{aug}(z)] - P_{d_1}(z)P_2(z)V_{aug}(z)}{K_g(z)(1 + K_2G_2(z)) + P_1(z)V_{aug}(z)}, \tag{5.7}$$

where

$$K_g(z) = 1 + K_{aug} - P_{aug}V_{aug}(z). \tag{5.8}$$

Regarding the robust analysis, the condition presented in Equation (2.69) remains valid for the outer loop of the PCCS-SFSP, that is

$$\overline{\delta P}(e^{j\Omega}) < I_r(\omega) = \frac{\left|1 + K_{aug}(e^{j\Omega}I - A_{aug})^{-1}B_{aug}\right|}{\left|V_{aug}(e^{j\Omega})G_{aug}(e^{j\Omega})\right|}. \tag{5.9}$$

5.1.1 Primary controllers tuning

Considering Equations (5.4) and (5.5), the tuning of the primary controllers K_{aug} and K_2 are, as in Section 2.3.3, based on pole allocation following the desired setpoint response through the characteristic polynomials

$$C_{P_{aug}} = \prod_{i=1}^{m}(z - p_i) = \det(zI - A_{aug} + B_{aug}K_{aug}) \tag{5.10}$$

and

$$C_{P_2} = \prod_{j=1}^{m}(z - p_j) = \det(zI - A_2 + B_2K_2) \tag{5.11}$$

where p_i and p_j represents the desired closed-loop poles for P_{aug} and P_2, respectively.

In order to guarantee unitary static gain to tracking, the reference filter is defined as

$$F(z) = \left[C_{aug}(I - A_{aug} + B_{aug}K_{aug})^{-1}B_{aug}\right]^{-1}, \tag{5.12}$$

however if a better tracking is expected, then poles and zeros can be added to $F(z)$ maintaining the same static gain.

5.1.2 Robustness filter proposed design

The robustness filters $V_2(z)$ and $V_{aug}(z)$ are designed in two steps. First, one should consider the internal loop, which can be reduced to a 2DOF structure with an equivalent controller, such as

$$C_{2_{eq}}(z) = \frac{V_2(z)}{1 + S_2(z)}, \tag{5.13}$$

where

$$S_2 = (K_2 - z^{-d_2}V_2(z)C_2)(zI - A_2)^{-1}B_2. \tag{5.14}$$

In order to (i) cancel the undesired poles of $P_2(z)$ and (ii) reject steps, ramps, or sinusoidal, the following conditions must be satisfied

$$\begin{cases} 1 + S_2(z)|_{z=p_{2i}\neq 1} = 0, \\ 1 + S_2(z)|_{z=e^{\pm j\omega_{2k}}} = 0, \\ \dfrac{d^k}{dz^k}(1 + S_2(z))|_{z=1} = 0, k = 0, \ldots, m_2 - 1, \end{cases} \tag{5.15}$$

where p_{2i} represent the poles of the process $P_2(z)$ and ω_{2k} are the frequencies for sinusoidal disturbances. The parameter $m_2 = m_{21} + m_{22}$ is the sum of the number of model poles m_{21} at $z = 1$ and the disturbance order m_{22}. The number of poles for $V_2(z)$ are defined to satisfy the inequality $n_{v2} \leq n_{u2} + 1$, where $n_{u2} + 1$ is the number of equations in (5.15).

Next, a similar analysis can be made to the external loop, where the equivalent controller is given by

$$C_{n_{eq}}(z) = \frac{V_{aug}(z)}{1 + S_{aug}(z)}, \tag{5.16}$$

with

$$S_{aug} = (K_{aug} - z^{-d_{aug}} V_{aug}(z) C_2)(zI - A_{aug})^{-1} B_{aug}, \tag{5.17}$$

and where the conditions for $V_{aug}(z)$ design are analogous, that is: (i) the undesired zeros of $S_{aug}(z)$, which came from the poles of $P_{aug}(z)$, must be canceled and (ii) the filter should reject disturbances at steady state. Therefore, one can derive the equations

$$\begin{cases} 1 + S_{aug}(z)|_{z=p_{aug_i} \neq 1} = 0, \\ 1 + S_{aug}(z)|_{z=e^{\pm j\omega_{nk}}} = 0, \\ \dfrac{d^k}{dz^k}(1 + S_{aug}(z))|_{z=1} = 0, k = 0, ..., m_{aug} - 1, \end{cases} \tag{5.18}$$

with p_{aug_i} as the poles of the process $P_{aug}(z)$, and ω_{nk} as the frequencies for any sinusoidal disturbances, and $m_{aug} = m_{aug_1} + m_{aug_2}$ as the sum of the number of model poles m_{aug_1} at $z = 1$ and the disturbance order m_{aug_2}. The number of poles for $V_{aug}(z)$ is calculated from the inequality $n_{vn} \leq n_{un} + 1$, where $n_{un} + 1$ is the number of equations in (5.18).

The robustness filters are defined as

$$V_2(z) = \frac{N_{v_2}}{D_{v_2}} = \frac{v_{20} + v_{21}z^{-1} + ... + v_{2n_{u2}}z^{-n_{u2}}}{(1 - \alpha_{21}z^{-1})(1 - \alpha_{22}z^{-1})...(1 - \alpha_{2n_{v2}}z^{-1})} \tag{5.19}$$

and

$$V_{aug}(z) = \frac{N_{v_{aug}}}{D_{v_{aug}}} = \frac{v_{n0} + v_{n1}z^{-1} + ... + v_{nn_{un}}z^{-n_{un}}}{(1 - \alpha_{n1}z^{-1})(1 - \alpha_{n2}z^{-1})...(1 - \alpha_{nn_{vn}}z^{-1})}. \tag{5.20}$$

where the coefficients of the filter $V_2(z)$ are calculated by a linear system derived from (5.15) and (5.19), and the coefficients of $V_{aug}(z)$ by another linear system from (5.18) and (5.20). The robustness filters poles, $\alpha_{21}...\alpha_{2n_{v2}}$ and $\alpha_{n1}...\alpha_{nn_{v2}}$ are free parameters for tuning.

5.1.3 Stable implementation structure for PCCS-SFSP

Likewise in Section 2.3.3, the controller structure from Figure 59 is only meant for open loop stable processes, which means that is only a conceptual structure for analysis. Thus, the controller is modified to an implementation structure, which is internally stable and can be used to control any process with dead time, including unstable and integrating processes. This controller structure for implementation is represented in Figure 60.

Figure 60 – Proposed SFSP structure for parallel cascade control for unstable and integrating process.

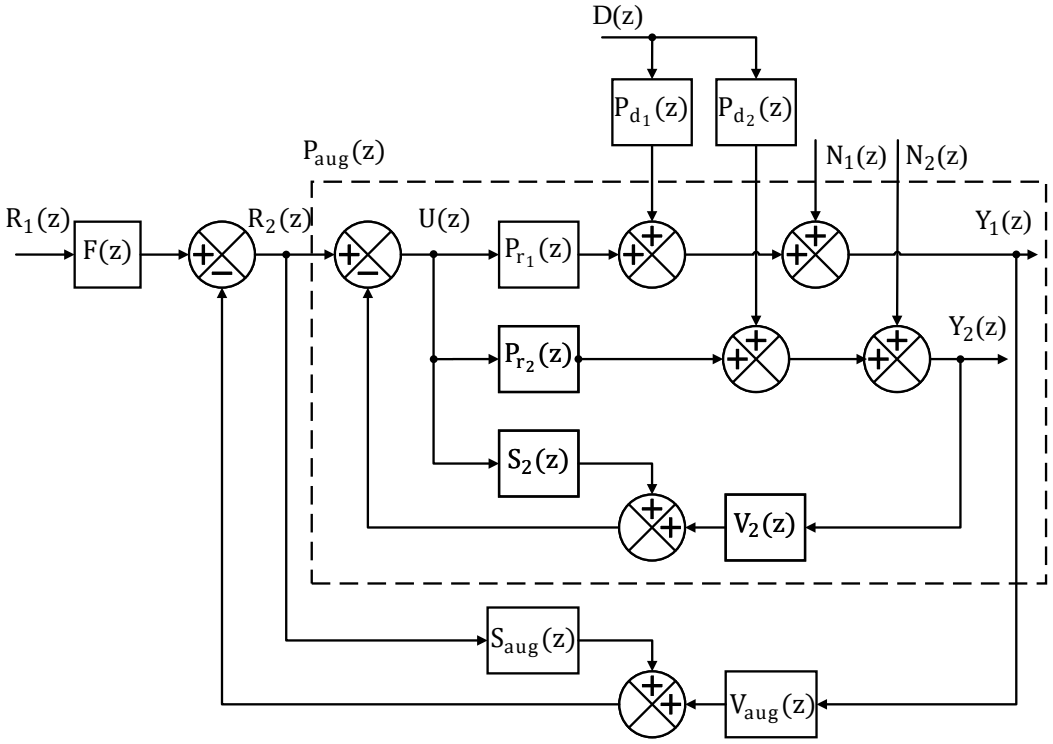

Source: The author.

A similar analysis to what is discussed in Section 2.3.3.4 can be done to calculate $S_2(z)$ and $S_{aug}(z)$ in order to guarantee the internal stability of the PCCS-SFSP. Therefore, $S_2(z)$ and $S_{aug}(z)$ can be rewrite, respectively, as:

$$S_2(z) = \sum_{i=1}^{d_2} K_2 A_2^{i-1} B_2 z^{-i} + V_2^*(z) z^{-d_2} \tag{5.21}$$

$$S_{aug}(z) = \sum_{i=1}^{d} K_{aug} A_{aug}^{i-1} B_{aug} z^{-i} + V_{aug}^*(z) z^{-d_{aug}} \tag{5.22}$$

where

$$V_2^*(z) = \frac{N_{v_2}^*(z)}{D_{v_2}(z)} \tag{5.23}$$

$$V_{aug}^*(z) = \frac{N_{v_{aug}}^*(z)}{D_{v_{aug}}(z)}. \tag{5.24}$$

$N_v^*(z)$ and $N_{v_{aug}}^*(z)$ can be obtained from the following partial decompositions, respec-

tively:

$$G_2(z)V_2(z) = \frac{N_{g_2}(z)N_{v_2}(z)}{D_{g_2}(z)D_{v_2}(z)} = \frac{N_g^*(z)}{D_{v_2}(z)} + \frac{N_{v_2}^*(z)}{D_{g_2}(z)},\ D_{g_2}(z) \neq D_{v_2}(z) \tag{5.25}$$

$$G_{aug}(z)V_{aug}(z) = \frac{N_{g_{aug}}(z)N_{v_{aug}}(z)}{D_{g_{aug}}(z)D_{v_{aug}}(z)} = \frac{N_{g_{aug}}^*(z)}{D_{v_{aug}}(z)} + \frac{N_{v_{aug}}^*(z)}{D_{g_{aug}}(z)},\ D_{g_{aug}}(z) \neq D_{v_{aug}}(z), \tag{5.26}$$

and thus, from (5.21) and (5.22), it is possible to see that the poles of $G_2(z)$ and $G_{aug}(z)$ are no longer part of $S_2(z)$ and $S_{aug}(z)$, respectively, which means that this structure guarantees internal stability.

5.2 Numerical examples

The proposed SFSP structure for Parallel cascade control is applied to processes recently studied in the literature in order to evaluate the controller. The examples are compared with the strategy proposed in Pashaei and Bagheri (2019) and disturbances rejection are analyzed.

5.2.1 Example 1 - stable case

A liquefied petroleum gas splitter plant studied in Pashaei and Bagheri (2019) is considered for this example. The process model is given by the following transfer functions:

$$\begin{aligned} P_{r_1}(s) &= \frac{-0.0067e^{-300s}}{105.8s+1}, \quad P_{r_2}(s) = \frac{-5.217}{101.6s+1}, \\ P_{d_1}(s) &= \frac{0.0584e^{-300s}}{115.5s+1}, \quad P_{d_2}(s) = \frac{44.15}{109.5s+1}. \end{aligned} \tag{5.27}$$

The discretized processes, with sampling time of T = 1.0 s, are given by:

$$\begin{aligned} P_{r_1}(z) &= \frac{-6.303\times10^{-5}}{z-0.9906}z^{-300}, \quad P_{r_2}(z) = \frac{-0.0511}{z-0.9902}, \\ P_{d_1}(z) &= \frac{0.0005034}{z-0.9914}z^{-300}, \quad P_{d_2}(z) = \frac{0.4014}{z-0.9909}. \end{aligned} \tag{5.28}$$

The PCCS-SFSP is tuned according to the following sequence: First, for the internal loop, a closed-loop pole at $z = 0.85$ is chosen and a feedback gain $K_2 = -2.7439$ is obtained. The robustness filter $V_2(z)$ is tuned with poles at $\alpha_{21} = \alpha_{22} = 0.1$, which leads to

$$V_2(z) = \frac{-18.57 + 16.19z^{-1}}{1 - 0.2z^{-1} + 0.01z^{-2}}. \tag{5.29}$$

Next, the feedback gain $K_{aug} = [-13510.848 \quad -15878.169]$ is calculated for the external loop to achieve closed-loop poles at $z_{aug_1} = z_{aug_2} = 0.99$. For disturbance rejection, the robustness filter $V_{aug}(z)$ is tuned with $\alpha_{aug_1} = \alpha_{aug_2} = 0.94$, so it is calculated as

$$V_{aug}(z) = \frac{-411.6 + 757.6z^{-1} - 346.6z^{-2}}{1 - 1.88z^{-1} + 0.8836z^{-2}}. \tag{5.30}$$

The reference filter calculated is given by:

$$F(z) = -161.991 \frac{(1-\gamma_1 z^{-1})(1-\gamma_2)}{(1-\gamma_2 z^{-1})(1-\gamma_1)} \tag{5.31}$$

where $\gamma_1 = 0.99$ and $\gamma_2 = 0.98$.

For this example, the simulation performed in Pashaei and Bagheri (2019) used an unit setpoint change applied at $t = 0$ s and a step disturbance of magnitude 100 at $t = 1000$ s. Also, a band-limited white noise of power 10^{-3} and variance 1.6344×10^{-4} is applied at $t = 2500$ s. The closed-loop response and control signal for the nominal case are shown in Figure 61.

Figure 61 – Example 1 - Nominal case

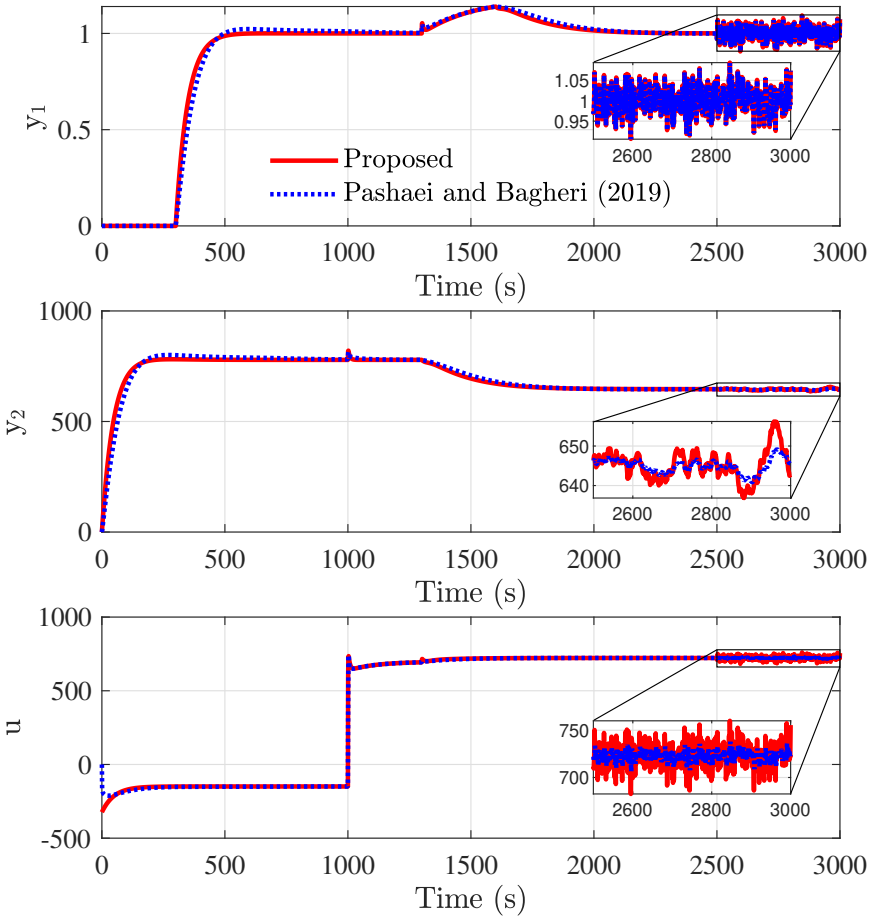

Source: The author.

It is also considered the uncertainties proposed in Pashaei and Bagheri (2019) where is applied +20 % in the gain of the primary and secondary process models, +5 % perturbations on the dead time of $P_{r_1}(s)$ and $P_{d_1}(s)$ and +10 % uncertainties in the time constants of $P_{r_1}(s)$, $P_{r_2}(s)$, $P_{d_1}(s)$ and $P_{d_2}(s)$. The results for the closed-loop response are shown in Figure 62, where it can be seen the better performance of the PCSS-SFSP.

Figure 62 – Example 1 - Uncertain case

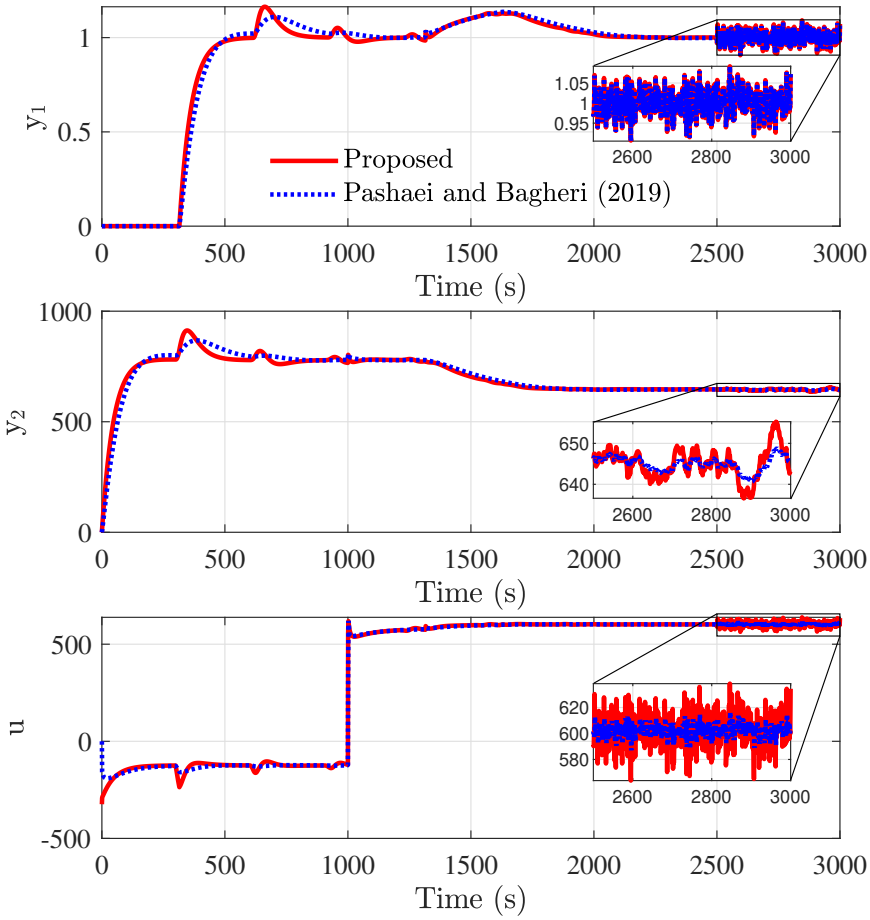

Source: The author.

Table 2 show the performance indices for both controllers where it can be seen that the proposed method shows better results in six out of eighth scenarios. The proposed controller presents worse TV for the uncertain case due a more aggressive tuning and the proposed structure also shows worse noise attenuation. However, the IAE is significantly improved in both cases caused by the fast action of the robustness filters in disturbance compensation, which shows the advantage of using the PCSS-SFSP.

Table 2 – Example 1 - Performance indices.

Case	Controller	Indices			
		IAE setpoint	IAE Pertubation	TV	CV
Nominal	PCCS-SFSP	**347.57**	**54.172**	**1243**.2	170.74
	Pashaei and Bagheri (2019)	366.83	62.772	1335.7	**27.36**
Uncertain	PCCS-SFSP	**380.21**	**56.964**	1586.2	167.43
	Pashaei and Bagheri (2019)	397.87	63.065	**1227.4**	**24.36**

5.2.2 Example 2 - unstable case

Consider the isothermal continuous stirred tank reactor, discussed in Pashaei and Bagheri (2019), with model given by

$$P_{r_1}(s) = P_{d_1}(s) = \frac{3.433e^{-20s}}{103.1s-1}, \quad P_{r_2}(s) = P_{d_2}(s) = \frac{e^{-0.5s}}{3s+1}, \tag{5.32}$$

which is discretized, with a sampling time of $T = 0.1$ s, and computed as:

$$P_{r_1}(z) = P_{d_1}(z) = \frac{0.003331}{z-1.001}z^{-200}, \quad P_{r_2}(z) = P_{d_2}(z) = \frac{0.03278}{z-0.9672}z^{-5}. \tag{5.33}$$

For the tuning of the PCCS-SFSP, the desired closed-loop pole is choose as $z = 0.7$ and the internal loop feedback gain obtained is $K_2 = 8.1508$. The reference filter is calculated as $F(z) = 3.3054$ and the robustness filter $V_2(z)$ is tuned with a pole $\alpha_{21} = 0.7$, leading to

$$V_2(z) = \frac{27.5 - 24.76z^{-1}}{1 - 0.7z^{-1}}. \tag{5.34}$$

The external loop is set to achieve closed-loop poles at $z_{aug_1} = z_{aug_2} = 0.981$ with a computed feedback gain $K_{aug} = [218.0951 \quad 306.4978]$. The robustness filter $V_{aug}(z)$ is tuned with $\alpha_{aug_1} = 1$, so it is calculated as the FIR filter:

$$V_{aug}(z) = 14.32 - 10.02z^{-1} \tag{5.35}$$

The control system simulation discussed in Pashaei and Bagheri (2019) considered an unit step setpoint at $t = 0$ s and a step disturbance of magnitude 5 at $t = 150$ s. To evaluate noise attenuation, at $t = 300$ s it is applied a band-limited white noise of power 10^{-5} and variance 2.4754×10^{-5}. The nominal case is shown in Figure 63, where it can be seen that there is no overshoot for the PCCS-SFSP, followed by an improvement in disturbance compensation. The controller from Pashaei and Bagheri (2019), presented an unstable control signal in the presence of noise, which is not shown in Figure 63 so that the control signals can be better visualized, while the PCCS-SFSP maintain a stable system with good noise attenuation.

Figure 63 – Example 2 - Nominal case

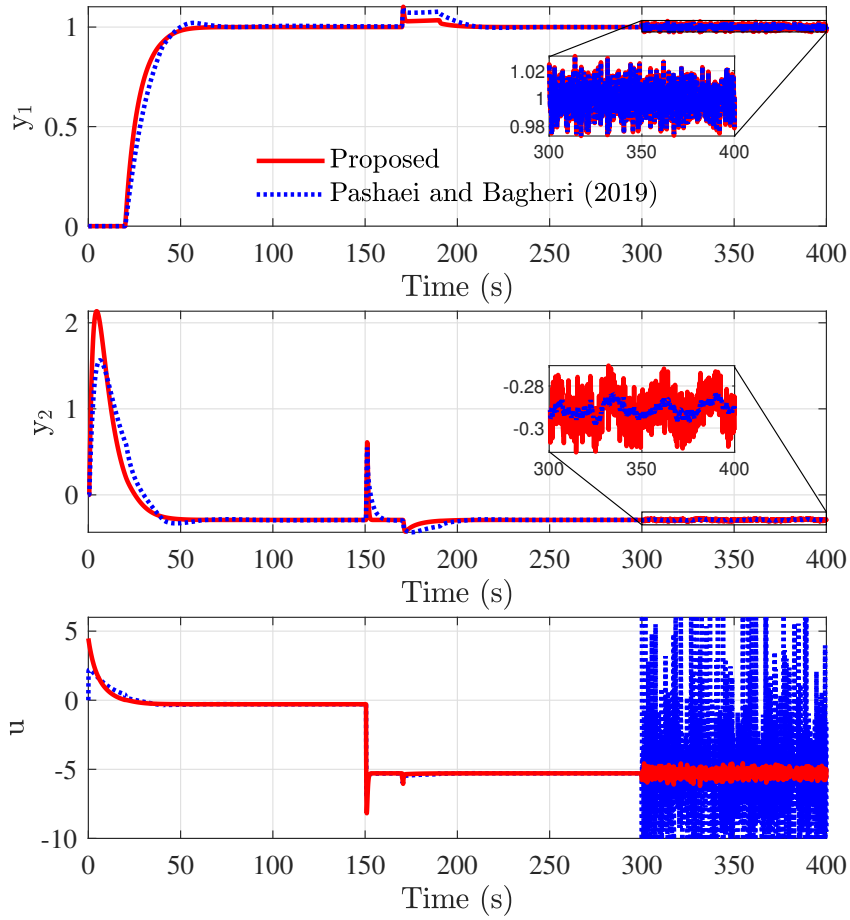

Source: The author.

For the uncertain case is applied $+10$ % in the dead time of the primary and secondary process models and disturbance transfer functions, and $+20$ % uncertainty is considered in the time constants and in the gains of $P_{r_1}(s)$, $P_{r_2}(s)$, $P_{d_1}(s)$ and $P_{d_2}(s)$. The results for the closed-loop response, in the uncertain case, are shown in Figure 64 where it can be seen that the PCCS-SFSP still presents better disturbance and noise attenuation.

Figure 64 – Example 2 - Uncertain case

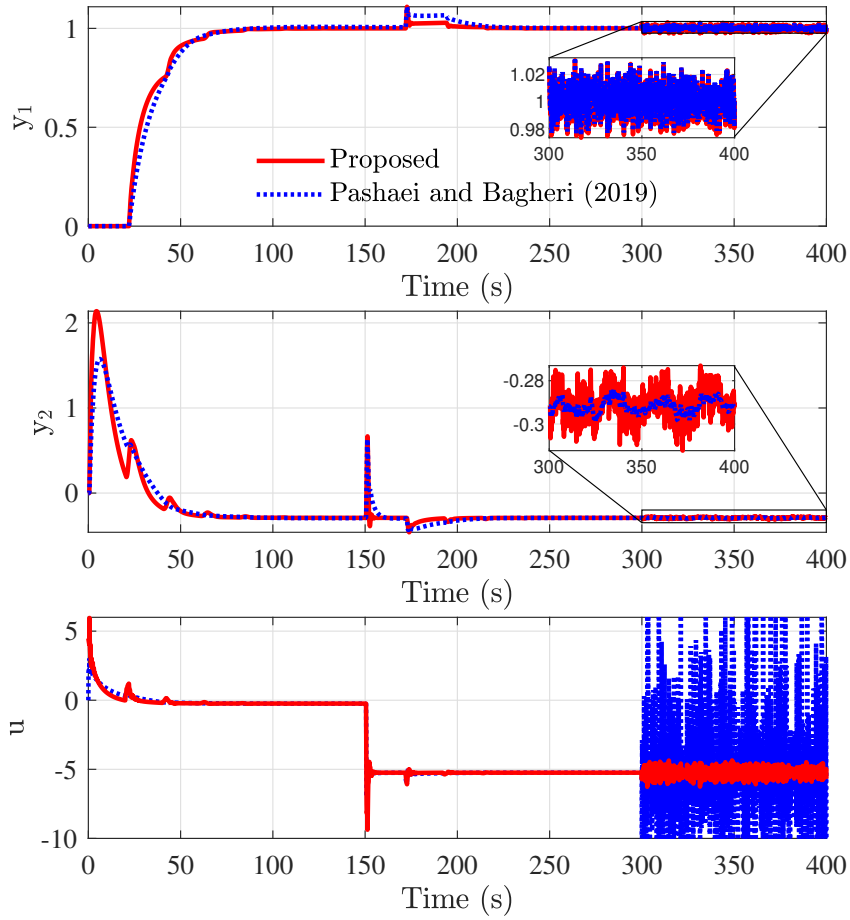

Source: The author.

Table 3 shows the performance indices for both controllers, where it can be seen that the proposed method shows better results in all scenarios, except in the TV index due to the more aggressive tuning. Both controllers show similar IAE for tracking, however it should be noted that the PCCS-SFSP improved the IAE for disturbance rejection in 61.43 % while maintain stability in noise environment.

Table 3 – Example 2 - Performance indices.

Case	Controller	Indices			
		IAE setpoint	IAE Pertubation	TV	CV
Nominal	PCCS-SFSP	**27.497**	**0.85927**	16.333	**0.058281**
	Pashaei and Bagheri (2019)	30.19	2.2276	**12.873**	4.0765×10^{17}
Uncertain	PCCS-SFSP	**33.286**	**0.86337**	32.883	**0.097923**
	Pashaei and Bagheri (2019)	35.679	2.6354	**24.82**	4.0765×10^{17}

5.2.3 Example 3 - integrative case

In this example, it is discussed a process studied in Pashaei and Bagheri (2019) with a second-order integrating plus large time delay (SOIPTD) as the primary system P_{r_1} and a stable FOPTD process as the secondary system P_2, which are given by:

$$P_{r_1}(s) = P_{d_1}(s) = \frac{e^{-6.5672s}}{s(3.4945s+1)}, \quad P_{r_2}(s) = P_{d_2}(s) = \frac{2e^{-2s}}{s+1}. \tag{5.36}$$

The processes are discretized with sample time $T = 0.1$ s, and the obtained transfer functions are show as in the following:

$$P_{r_1}(z) = P_{d_1}(z) = \frac{0.001417z + 0.001404}{z^2 - 1.972z + 0.9718} z^{-66}, \quad P_{r_2}(z) = P_{d_2}(z) = \frac{0.1903}{z - 0.9048} z^{-20}. \tag{5.37}$$

The tuning for tracking of the PCCS-SFSP is set for a desired closed-loop pole at $z = 0.87$, which gives an internal loop feedback gain $K_2 = 0.1830$. The reference filter is computed as $F(z) = 0.2384$ and the robustness filter $V_2(z)$ is tuned with a pole $\alpha_2 = 0.82$, leading to

$$V_2(z) = \frac{1.27 - 1.147z^{-1}}{1 - 0.82z^{-1}}. \tag{5.38}$$

The closed-loop poles for the outer loop are chosen at $z_{aug_1} = z_{aug_2} = z_{aug_3} = 0.96$, where it can be obtained a feedback gain $K_{aug} = [516.0428 \;\; 583.7878 \;\; 661.6658]$. The robustness filter $V_{aug}(z)$ is tuned with $\alpha_{aug_1} = 1$ and $\alpha_{aug_2} = 0.96$, so it is calculated as:

$$V_{aug}(z) = \frac{2.59 - 4.77z^{-}1 + 2.189z^{-}2}{1 - 1.96z^{-}1} \tag{5.39}$$

To perform the simulation an unit setpoint change is applied at $t = 0$ s, a step disturbance of magnitude -0.2 at $t = 125$ s and a band-limited white noise of power 10^{-5} and variance 1.6344×10^{-4} is applied at $t = 300$ s. The closed-loop response and control signal for the nominal case are shown in Figure 61 where it can be seen that the controller from Pashaei and Bagheri (2019) presents overshoot and a small error at steady state, while the PCCS-SFSP shows a faster response with zero error at steady state and no overshoot. Also, the proposed controller maintain stability when noise is applied.

Figure 65 – Example 3 - Nominal case

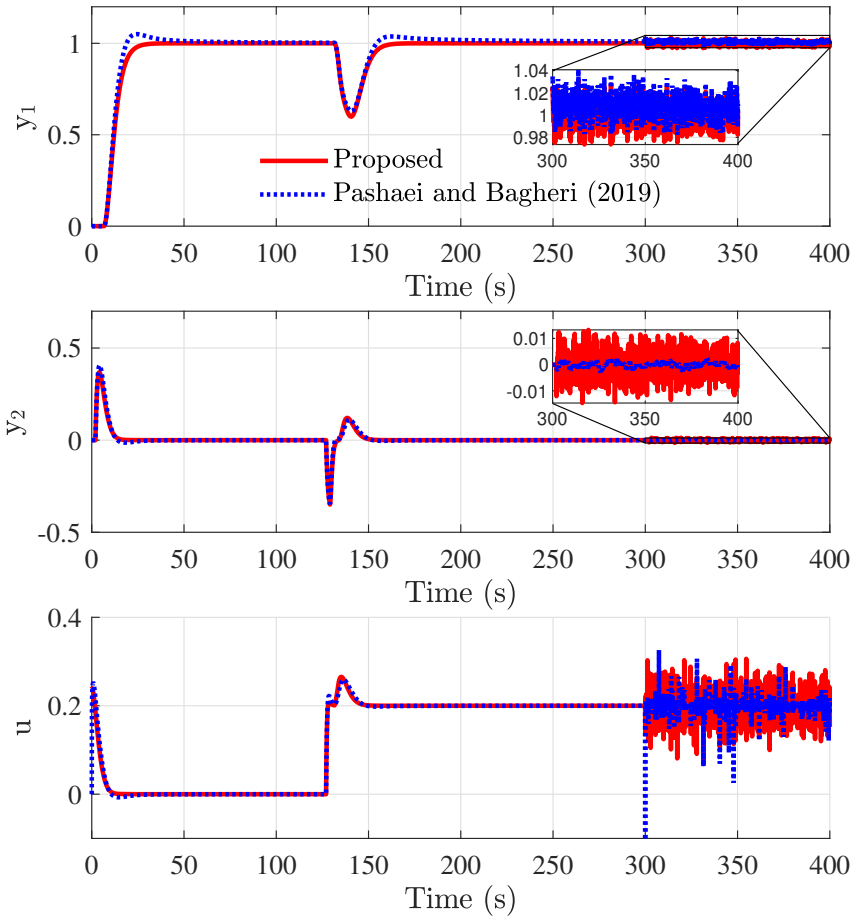

Source: The author.

For robustness analysis, $+20$ % uncertainty is applied in the dead time of the primary and secondary process models and primary and secondary disturbance transfer functions, -20 % perturbation is considered in time constant of $P_{r_1}(s)$ and $P_{d_1}(s)$, -10 % uncertainty is considered in gain of $P_{r_1}(s)$ and $P_{d_1}(s)$, and $+20$ % in the gain of $P_2(s)$ and $P_{d_2}(s)$. The simulation shows that even in this uncertain condition the PCCS-SFSP maintain a faster tracking and disturbance rejection as well as stability in the control signal when noise is applied. The results for both controllers are shown in Figure 66.

Figure 66 – Example 3 - Nominal case

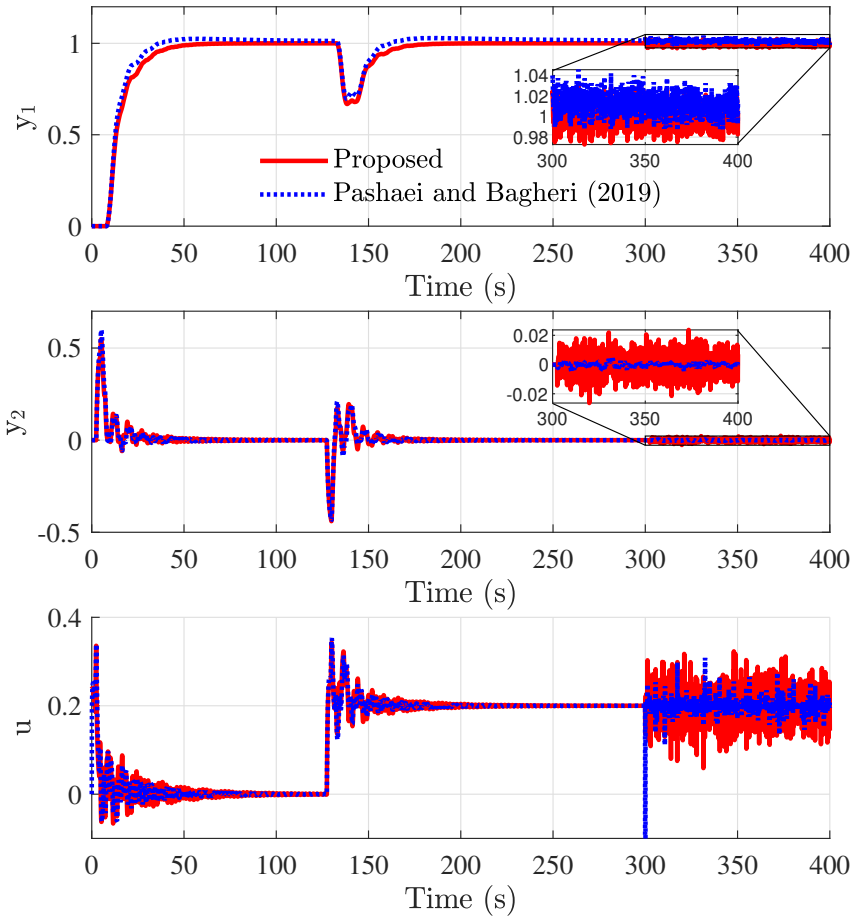

Source: The author.

Table 4 show the performance indices for both controllers, where it can be seen that the proposed method shows better results in the majority of scenarios. Although the aggressive tuning used results in higher TV indices, it is worth highlighting that the TVs presented by PCCS-SFSP are close and have the same order of magnitude as those presented by Pashaei and Bagheri (2019). This is rewarded by gains in IAE indices and by maintaining stability in the presence of noise with good CV results.

Table 4 – Example 3 - Performance indices.

Case	Controller	Indices			
		IAE setpoint	IAE Pertubation	TV	CV
Nominal	PCCS-SFSP	**12.974**	**5.1934**	0.57065	**0.001215**
	Pashaei and Bagheri (2019)	13.377	7.1557	**0.62485**	4.4158×10^{12}
Uncertain	PCCS-SFSP	16.725	**5.1972**	7.3395	**0.001465**
	Pashaei and Bagheri (2019)	**16.586**	6.9796	**5.5783**	4.4158×10^{12}

5.3 Discussion

In this chapter, a new parallel cascade control structure for the simplified filtered Smith predictor for high-order dead-time process was presented.

Simulation results show better performance compared to other recently published work in terms of IAE, TV and CV indices for the majority of scenarios. The IAE index for perturbation of the proposed controller, was up to 15.88 % for Example 1, and was up to 61.43 % for Example 2, and was up to 34.30 % for Example 3 in the nominal case when compared with the other structure.

6 DEAD-TIME COMPENSATOR FOR TITO PROCESSES BASED ON PREDICTIVE CONTROL

In this chapter, a modification to the state-space based GPC structure is proposed for improving the output disturbance rejection. In order to prove usefulness, the proposed scheme is applied to the control of a TITO system with multiple delays and output disturbance.

The main contribution of this work is to use the design predictions of the GPC controller to include an FIR filter in order to compensate output disturbances in process with dead time. Thus, through a simple modification of the traditional GPC algorithm in state space for systems with dead time, it is possible to present better performance in the control of industrial plants.

6.1 Generalized predictive control for TITO Model

Consider a TITO process with multiple dead time and output disturbances modeled as

$$\begin{bmatrix} Y_1(s) \\ Y_2(s) \end{bmatrix} = \begin{bmatrix} G_{11}(s)e^{-L_{11}s} & G_{12}(s)e^{-L_{12}s} \\ G_{21}(s)e^{-L_{21}s} & G_{22}(s)e^{-L_{22}s} \end{bmatrix} \begin{bmatrix} U_1(s) \\ U_2(s) \end{bmatrix} + \begin{bmatrix} G_{q1}(s)e^{-L_{q1}s} \\ G_{q2}(s)e^{-L_{q2}s} \end{bmatrix} D(s). \tag{6.1}$$

with input disturbance $D(s)$ applied for both models simultaneously, as presented in Figure 67, with $P_{ij}(s) = G_{ij}(s)e^{-L_{ij}s}$.

Figure 67 – Block Diagram of TITO system.

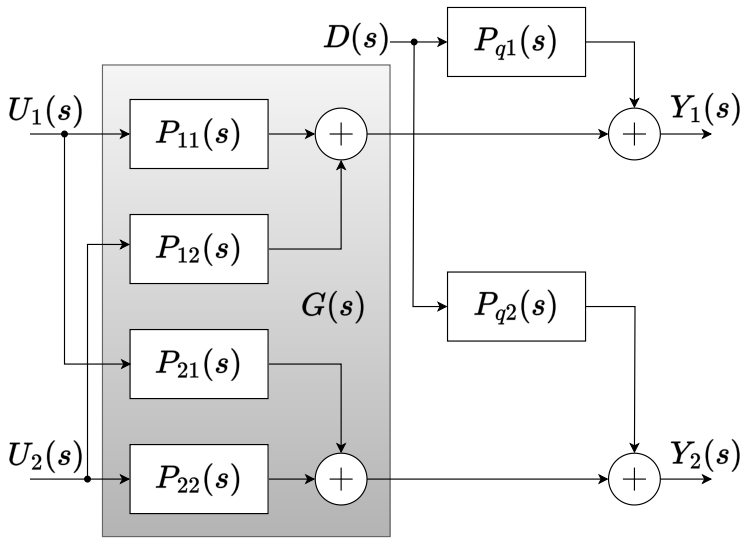

Source: The author.

Consider to define

$$E_1(s) = e^{-L_{q1}s}D(s) \tag{6.2}$$

as a L_{q1} pure delayed version of the disturbance $D(s)$. It is worth to highlight that $E_1(s)$ preserves the same properties of $D(s)$. In this work it is considered that $L_{q2} > L_{q1}$, so that output 2 presents a dead time greater than that of the output 1. If $L_{q1} > L_{q2}$ then the following analysis may be readily switched. Thus, it is possible to find a proper relationship between $E_2(s)$ with $E_1(s)$ as

$$\begin{aligned} E_2(s) &= \alpha e^{-(L_{q2}-L_{q1})s} E_1(s) \\ &= \alpha e^{-L_q s} E_1(s), \end{aligned} \tag{6.3}$$

where α is a tuning parameter. The importance of this modification is that in this way the predictions of the signal $E_1(s)$ can be used to predict the behavior of $E_2(s)$, so that it can be included in the controller design.

Therefore, block diagram presented in Figure 67 might be slightly modified for the one presented in Figure 68.

Figure 68 – Block Diagram of the equivalent system.

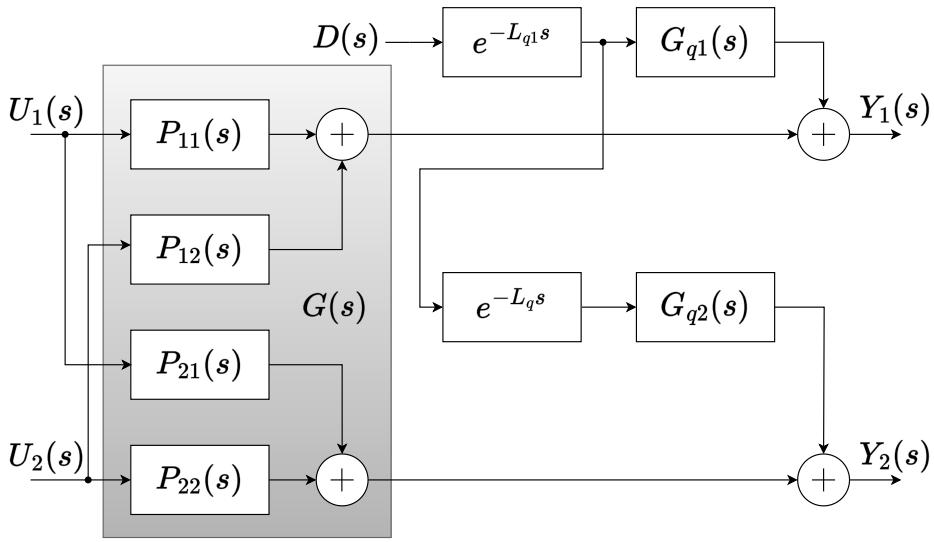

Source: The author.

For design the GPC, the following discrete model can be used

$$\begin{aligned} Y_1(z) = &\frac{b_{11}(z)}{a_{11}(z)} z^{-d_{11}} U_1(z) + \frac{b_{12}(z)}{a_{12}(z)} z^{-d_{12}} U_2(z) + \frac{c_1(z)}{\Delta(z) a_1(z)} E_1(z) \\ Y_2(z) = &\frac{b_{21}(z)}{a_{21}(z)} z^{-d_{21}} U_1(z) + \frac{b_{22}(z)}{a_{22}(z)} z^{-d_{22}} U_2(z) + \frac{c_2(z)}{\Delta(z) a_2(z)} E_2(z) \end{aligned} \tag{6.4}$$

where d_{ij} denotes the dead time of the i-output and j-input model

$$\begin{aligned} b_{ij}(z) =& b_{ij1} z^{-1} + b_{ij2} q^{-2} + \cdots + b_{ijn} q^{-n} \\ a_{ij}(z) =& 1 + a_{ij1} z^{-1} + a_{ij2} q^{-2} + \cdots + a_{ijn} q^{-n} \\ c_i(z) =& 1 + c_{i1} z^{-1} + c_{i2} q^{-2} + \cdots + c_{in} q^{-n} \\ a_i(z) =& 1 + a_{i1} z^{-1} + a_{i2} q^{-2} + \cdots + a_{in} q^{-n} \\ \Delta(z) =& 1 - z^{-1} \end{aligned}$$

Although the system (6.4) can be used to design the GPC controller, a state-space representation for multivariable systems simplifies the controller design process. For the TITO system considered here, such representation can be written as:

$$\begin{cases} x_{11}(k+1) = A_{11}x_{11}(k) + B_{11}u_1(k-d_{11}) \\ \quad y_{11}(k) = C_{11}x_{11}(k) \end{cases} \tag{6.5}$$

$$\begin{cases} x_{12}(k+1) = A_{12}x_{12}(k) + B_{12}u_2(k-d_{12}) \\ \quad y_{12}(k) = C_{12}x_{12}(k) \end{cases} \tag{6.6}$$

$$\begin{cases} x_{21}(k+1) = A_{21}x_{21}(k) + B_{21}u_1(k-d_{21}) \\ \quad y_{21}(k) = C_{21}x_{21}(k) \end{cases} \tag{6.7}$$

$$\begin{cases} x_{22}(k+1) = A_{22}x_{12}(k) + B_{22}u_2(k-d_{22}) \\ \quad y_{22}(k) = C_{22}x_{22}(k) \end{cases} \tag{6.8}$$

$$\begin{cases} x_{13}(k+1) = A_{13}x_{13}(k) + B_{13}e_1(k) \\ \quad y_{13}(k) = C_{13}x_{13}(k) + e_1(k) \end{cases} \tag{6.9}$$

$$\begin{cases} x_{23}(k+1) = A_{23}x_{12}(k) + B_{23}e_2(k) \\ \quad y_{23}(k) = C_{23}x_{23}(k) + e_2(k) \end{cases} \tag{6.10}$$

where, $y_{ij}(k)$ stands for the $ij-th$ output of the process, $u_1(k)$ and $u_2(k)$ are the set of two process inputs, $e(k)$ is a zero mean white noise disturbance. Matrices $A_{ij} \in \mathbb{R}^{n\times n}$, $B_{ij} \in \mathbb{R}^{n\times 2}$ and $C_{ij} \in \mathbb{R}^{1\times n}$; $i = 11, 12, 21, 22$, are in observable canonical form, describing TITO linear system dynamics in discrete time framework. Moreover, in a discrete-time framework and for better writings one might consider $d_{q_1} = \mathscr{Z}\{e^{-L_{q1}s}\}$ and $d_{q_2} = \mathscr{Z}\{e^{-L_{q2}s}\}$, which allows (6.3) to be written as

$$e_2(k) = \alpha e_1(k-d_q), \tag{6.11}$$

where $d_q = d_{q_2} - d_{q_1}$ is the relative delay between disturbance models for loops 1 and 2 respectively. Since the proposed method considers $d_{q_2} > d_{q_1}$, thus the predictions of $e_2(k)$ are approximated by the relation (6.11) and included in the controller designed such as described in the following section.

6.2 Proposed controller

This section presents the output predictions when the relation (6.11) takes place and its implications to obtain a modified GPC control law. Lately, it is shown the block diagram for the closed loop system.

6.2.1 Prediction outputs

By recursively applying (6.5) to (6.8) one can finds future outputs.The predictions considering $d_1 = \min\{d_{11}, d_{12}, \dots\}$, $d_2 = \min\{d_{21}, d_{22}, \dots\}$ and $d_3 = \min\{d_{31}, d_{32}, \dots\}$ are given by:

$$
\begin{aligned}
x_{ij}(k+d_{ij}+1) &= A_{ij}x_{ij}(k+d_{ij}) + B_{ij}u_j(k) \\
x_{ij}(k+d_{ij}+2) &= A_{ij}^2 x_{ij}(k+d_{ij}) + A_{ij}B_{ij}u_j(k) + B_{ij}u_j(k+1) \\
&\vdots \\
x_{ij}(k+d_i+N) &= A_{ij}^{h_{ij}} x_{ij}(k+d_{ij}) + A_{ij}^{h_{ij}-1} B_{ij}u_j(k) + \cdots + B_{ij}u_j(k+N_{ij}-1)
\end{aligned}
$$

where $h_{ij} = d_i + N - d_{ij}$.

Using the state's prediction, it can be obtained

$$
Y_i = G_{ij}U_j + Gp_i u_i(k) + F_{ij}x_{ij}(k+d_{ij}) \tag{6.12}
$$

where,

$$
F_{ij} = \begin{bmatrix} Iz^{-d_{ij}+d_i} \\ \vdots \\ Iz^{-1} \\ C_{ij}A_{ij} \\ C_{ij}A_{ij}^2 \\ \\ C_{ij}A_{ij}^{h_{ij}} \end{bmatrix}, \qquad I = \begin{cases} C_{ij}A_{ij} & \text{if } d_{ij} \neq d_i \\ \nexists & \text{if } d_{ij} = d_i \end{cases} \tag{6.13}
$$

$$
G_{ij} = \begin{bmatrix} \mathbf{0}_{d_i-d_{ij}\times 1} & \mathbf{0}_{d_i-d_{ij}\times 1} & \dots & \mathbf{0}_{d_i-d_{ij}\times 1} & \dots & \mathbf{0}_{d_i-d_{ij}\times 1} \\ C_{ij}B_{ij} & 0 & \dots & 0 & \dots & 0 \\ C_{ij}A_{ij}Bij & C_{ij}B_{ij} & & 0 & \dots & 0 \\ & \vdots & \cdots & 0 & \vdots & 0 \\ C_{ij}A_{ij}^{h_{ij}-1}Bij & C_{ij}A_{ij}^{h_{ij}-2}Bij & \dots & C_{ij}B_{ij} & & 0 \end{bmatrix}, \; U_j = \begin{bmatrix} u_j(k) \\ u_j(k+1) \\ \vdots \\ u_j(k+N-1) \end{bmatrix} \tag{6.14}
$$

$$
Gp_i = \begin{bmatrix} C_{ij}B_{ij}z^{-d_{ij}+d_i} \\ \vdots \\ C_{ij}B_{ij}z^{-1} \\ \mathbf{0}_{(h_{ij}-1\times 1)} \end{bmatrix} \tag{6.15}
$$

.

The predictions of the disturbance model can be computed using (6.9) and (6.10) such as

$$\begin{aligned}
x_{i3}(k+1) &= A_{i3}x_{i3}(k) + B_{i3}e_i(k)\\
x_{i3}(k+2) &= A_{i3}^2 x_{i3}(k) + A_{i3}B_{i3}e_1(k) + B_{i3}e_i(k+1)\\
&\vdots\\
x_{i3}(k+d_i+N) &= A_{i3}^{d_i+N}x_{i3}(k) + A_{i3}^{N+d_i-1}B_{i3}e_i(k) + \cdots + B_{i3}e_i(k+N+d_i-1)
\end{aligned}$$

$$Y_{i3} = F_{i3}x_{i3}(k) + D_i e_i(k) + Dq_i e_i(k) \tag{6.16}$$

where,

$$F_{i3} = \begin{bmatrix} C_{i3}A_{i3}^{d_i+1} \\ \vdots \\ C_{i3}A_{i3}^{d_i+N} \end{bmatrix} \tag{6.17}$$

$$D_i = \begin{bmatrix} C_{i3}A_{i3}^{d_i}B_{i3} \\ \vdots \\ C_{i3}A_{i3}^{d_i+N-1}B_{i3} \end{bmatrix} \tag{6.18}$$

$$D_{q_i} = I \begin{bmatrix} C_{i3}A_{i3}^{d_i-1}B_{i3} + C_{i3}A_{i3}^{d_i-2}B_{i3}z^{-1} + \cdots + C_{i3}A_{i3}^{d_i-d_q}B_{i3}z^{dq-1} \\ \vdots \\ C_{i3}A_{i3}^{N+d_i-2}B_{i3} + C_{i3}A_{i3}^{N+d_i-3}B_{i3}z^{-1} + \cdots + C_{i3}A_{i3}^{N+d_i-1-d_q}B_{i3}z^{dq-1} \end{bmatrix}, \tag{6.19}$$

$$I = \begin{cases} 0 & \text{if } d_i = d_3 \\ 1 & \text{if } d_i \neq d_3. \end{cases} \tag{6.20}$$

A compact form of predictions can be written by merging matrices, for both loops, in single matrices representations. In this case, the output predictions, including the using of the relation (6.11), may be written such as

$$\mathbf{Y} = \mathbf{G}\mathbf{U}(z) + \mathbf{G}_p(z)\mathbf{U}(z) + \mathbf{F}_1\mathbf{X}(z) + \mathbf{F}_2(z)\mathbf{X}(z) + \mathbf{F}_e\mathbf{X}_e(z) + \mathbf{D}\mathbf{E}(z) + \mathbf{D}_q(z)E_1(z), \tag{6.21}$$

where $\mathbf{U} = [U_1(k)\ U_2(k)]^T$, $\mathbf{X}(z) = \begin{bmatrix} X_{11}(z) & X_{12}(z) \\ X_{21}(z) & X_{22}(z) \end{bmatrix}$,

$\mathbf{E}(z) = [E_1(z)\ E_2(z)]^T, \mathbf{X}_e(z) = [X_{13}(z)\ X_{23}(z)]^T$,

$\mathbf{G} = \begin{bmatrix} G_{11} & G_{12} \\ G_{21} & G_{22} \end{bmatrix}$, $\mathbf{G}_p(z) = \begin{bmatrix} G_{p_1}(z) & 0 \\ 0 & G_{p_2}(z) \end{bmatrix}$, $\mathbf{F}_1 = \begin{bmatrix} 0 & F_{12} \\ F_{21} & 0 \end{bmatrix}$,

$\mathbf{F}_2(z) = \begin{bmatrix} F_{11}(z) & 0 \\ 0 & F_{22}(z) \end{bmatrix}$, $\mathbf{F}_e = \begin{bmatrix} F_{13} & 0 \\ 0 & F_{23} \end{bmatrix}$, $\mathbf{D} = \begin{bmatrix} D_1 & 0 \\ 0 & D_2 \end{bmatrix}$,

$\mathbf{D}_q(z) = \begin{bmatrix} D_{q_1}(z) & 0 \\ 0 & \alpha D_{q_2}(z) \end{bmatrix}$.

The free parameter α is used to improve the output disturbance response respecting the trade-off between performance and robustness.

6.2.2 Control law

The basic algorithm of GPC states that only the first element of $\mathbf{U}_1$ and $\mathbf{U}_2$ are used, thus the optimal control is given by

$$\mathbf{U}(z) = \mathbf{K}(\mathbf{W} - \mathbf{f}), \tag{6.22}$$

where $\mathbf{W}$ represents the future reference vector and $\mathbf{K}$ contains the first and the $N+1$ rows of $\left(\mathbf{G}^T\lambda\mathbf{Q}\mathbf{G}\right)^{-1}\mathbf{G}^T$, with $\mathbf{Q}$ as an identity matrix. The free response is given by

$$\mathbf{f} = \mathbf{G}_p(z)\mathbf{U}(z) + \mathbf{F}_1\mathbf{X}(z) + \mathbf{F}_2(z)\mathbf{X}(z) - \mathbf{F}_e\mathbf{X}_e(z) - \mathbf{D}E(z) - \mathbf{D}_q(z)E_1(z), \tag{6.23}$$

and the control signal is calculates as

$$\begin{aligned}\mathbf{U}(z) = \mathbf{K}_r R(z) - \mathbf{K}_p(z)\mathbf{U}(z) - \mathbf{K}_{F_1}\mathbf{X}(z) - \mathbf{K}_{F_2}(z)\mathbf{X}(z) \\ - \mathbf{K}_{F_e}\mathbf{X}_e(z) - \mathbf{K}_D E(z) - \mathbf{K}_{D_q}(z)E_1(z),\end{aligned} \tag{6.24}$$

where $\mathbf{K}_p = \mathbf{K}\mathbf{G}_p(z)$, $\mathbf{K}_{F_1} = \mathbf{K}\mathbf{F}_1$, $\mathbf{K}_{F_2}(z) = \mathbf{K}\mathbf{F}_2(z)$, $\mathbf{K}_{F_e} = \mathbf{K}\mathbf{F}_e$, $\mathbf{K}_D = \mathbf{K}\mathbf{D}$, $\mathbf{K}_{D_q}(z) = \mathbf{K}\mathbf{D}_q(z)$ and $\mathbf{K}_r$ is computed from $\mathbf{K}\mathbf{W}$ considering the reference tracking for steady-state. A block diagram representation of the proposed controller is shown in Figure 69.

6.3 Numerical example

To evaluate the usefulness of the proposed GPC, a case study was carried out on the stable open-loop process of *Wood-Berry* column distillation, which is described by:

$$P_n(s) = \begin{bmatrix} \dfrac{12.8e^{-s}}{16.7s+1} & \dfrac{-18.9e^{-3s}}{16.7s+1} \\ \dfrac{6.6e^{-7s}}{10.9s+1} & \dfrac{-19.4e^{-3s}}{14.4s+1} \end{bmatrix}, \quad P_q(s) = \begin{bmatrix} \dfrac{3.8e^{-8.1s}}{14.9s+1} \\ \dfrac{4.9e^{-3.4s}}{13.2s+1} \end{bmatrix}, \tag{6.25}$$

where $\mathbf{Y}(s) = \mathbf{P}_n(s)\left(\mathbf{U}(s) + \mathbf{D}_u(s)\right) + \mathbf{P}_q(s)d_y(s)$. The output disturbance in this case is given by $\mathbf{D}_y(s) = \mathbf{P}_q(s)d_y(s)$ with $d_y(s)$ as an unmeasurable scalar disturbance. The output $Y_1(s)$ represents the overhead product mole fraction of methanol and $Y_2(s)$ defines the bottom product mole fraction of methanol, $U_1(s)$ describes the reflux flow rate, $U_2(s)$ expresses the reboiler steam flow rate, $d_y(s)$ defines the feed flow rate, $\mathbf{D}_u(s) = [D_{u_1}(s)\ D_{u_2}(s)]^T$ is used to represents a reflux flow rate ($D_{u_1}(s)$) or an steam flow rate disturbance ($D_{u_2}(s)$) and the time measurement unit is in minutes. In order to satisfy the $Lq_1 < Lq_2$ condition, the following process model was considered

$$P_n(s) = \begin{bmatrix} \dfrac{6.6e^{-7s}}{10.9s+1} & \dfrac{-19.4e^{-3s}}{14.4s+1} \\ \dfrac{12.8e^{-s}}{16.7s+1} & \dfrac{-18.9e^{-3s}}{16.7s+1} \end{bmatrix}, \quad P_q(s) = \begin{bmatrix} \dfrac{4.9e^{-3.4s}}{13.2s+1} \\ \dfrac{3.8e^{-8.1s}}{14.9s+1} \end{bmatrix}. \tag{6.26}$$

Figure 69 – Block diagram of the system.

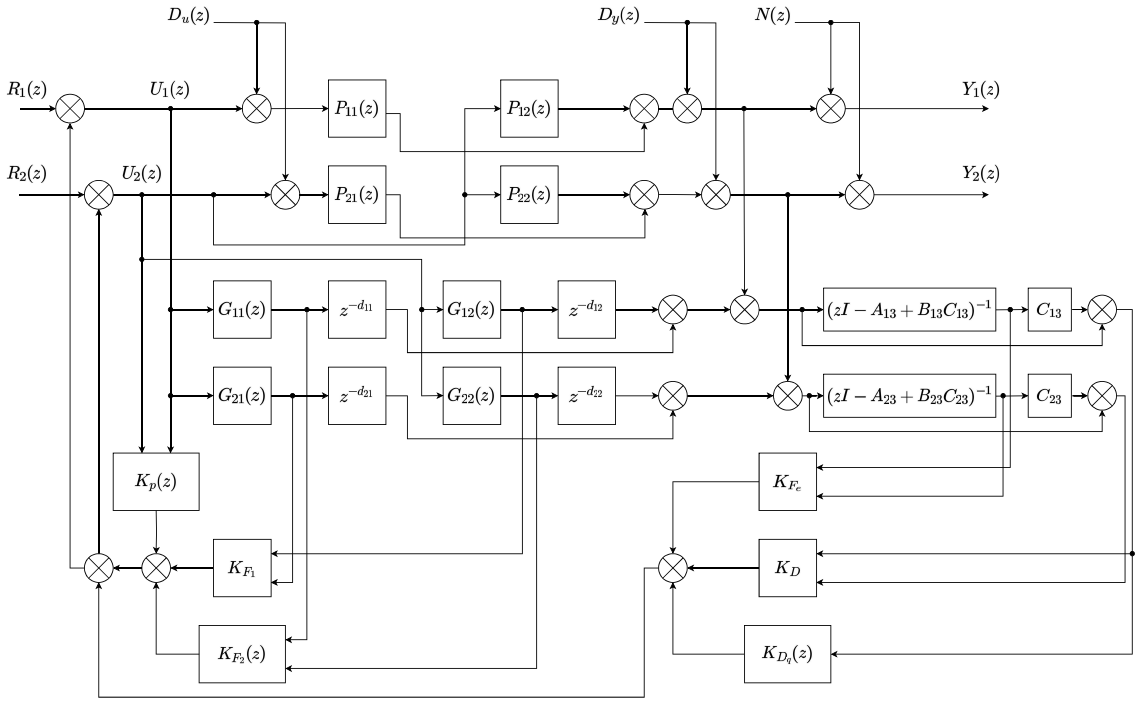

Source: The author.

The discrete-time model of system presented in Equation (6.26) is obtained with sampling time of $T_s = 1$ min:

$$P_n(z) = \begin{bmatrix} \dfrac{0.5786z^{-7}}{z-0.9123} & \dfrac{-1.302z^{-3}}{z-0.9329} \\ \dfrac{0.744z^{-1}}{z-0.9419} & \dfrac{-0.8789z^{-3}}{z-0.9535} \end{bmatrix}, \quad P_q(z) = \begin{bmatrix} \dfrac{0.3575z^{-3}}{z-0.927} \\ \dfrac{0.2467z^{-9}}{z-0.9351} \end{bmatrix}. \tag{6.27}$$

A step disturbance with amplitude of -0.1 is applied at the feed flow rate at $t = 150$ min and a step disturbance with amplitude 0.1 is added at the reflux rate at $t = 250$ min. Also, a band-limited white noise of power 10^{-3} and variance 1.4018×10^{-4} is applied at $t = 350$ min. First, it is evaluated the influence of parameter α in the attenuation of $D_y(s)$. Figures 70 and 71 show the outputs and control signals, respectively, obtained for the nominal model of the plant where the GPC is tuned with with $N = 5$ and $\lambda = 1$, while α assumed three different values,

0.50, 0.70 and 0.9. The GPC parameters are given by:

$$\mathbf{K}_r = \begin{bmatrix} -0.1455 & 0.4211 \\ -0.2387 & 0.0295 \end{bmatrix} \tag{6.28}$$

$$\mathbf{K}_p = \begin{bmatrix} -0.02619z^{-1} - 0.02031z^{-2} - 0.014z^{-3} - 0.007244z^{-4} & -0.0578z^{-1} - 0.02976z^{-2} \\ -0.03722z^{-1} - 0.02886z^{-2} - 0.0199z^{-3} - 0.0103z^{-4} & -0.01221z^{-1} - 0.00629z^{-2} \end{bmatrix} \tag{6.29}$$

$$\mathbf{K}_{F_1} = \begin{bmatrix} -0.1156 & 0.3417 \\ -0.1868 & 0.0262 \end{bmatrix} \tag{6.30}$$

$$\mathbf{K}_{F_2} = \begin{bmatrix} -0.02592 - 0.04129z^{-1} - 0.03202z^{-2} - & 0.2908 + 0.0627z^{-1} + 0.03229^{-2} \\ \quad -0.02208z^{-3} - 0.01142z^{-4} & \\ -0.06591 - 0.05869z^{-1} - 0.04551z^{-2} - & 0.008143 + 0.01325z^{-1} + 0.006824^{-2} \\ \quad -0.03138z^{-3} - 0.01624z^{-4} & \end{bmatrix} \tag{6.31}$$

$$\mathbf{K}_{F_e} = \begin{bmatrix} -0.8477 & -0.7575 & 1.9974 & 1.6858 \\ -1.4208 & -1.2751 & 0.1060 & 0.0818 \end{bmatrix} \tag{6.32}$$

$$\mathbf{K}_D = \begin{bmatrix} -0.0468 & 0.1356 \\ -0.0771 & 0.0091 \end{bmatrix} \tag{6.33}$$

$$\mathbf{K}_{D_q} = \begin{bmatrix} 0 & 0.1315 + 0.1271z^{-1} + 0.1224z^{-2} + 0.1174z^{-3} + 0.1121z^{-4} \\ 0 & 0.008733 + 0.008393z^{-1} + 0.00803z^{-2} + 0.007641z^{-3} + 0.007225z^{-4} \end{bmatrix} \tag{6.34}$$

Figure 70 – Output response of proposed GPC for different static gains α.

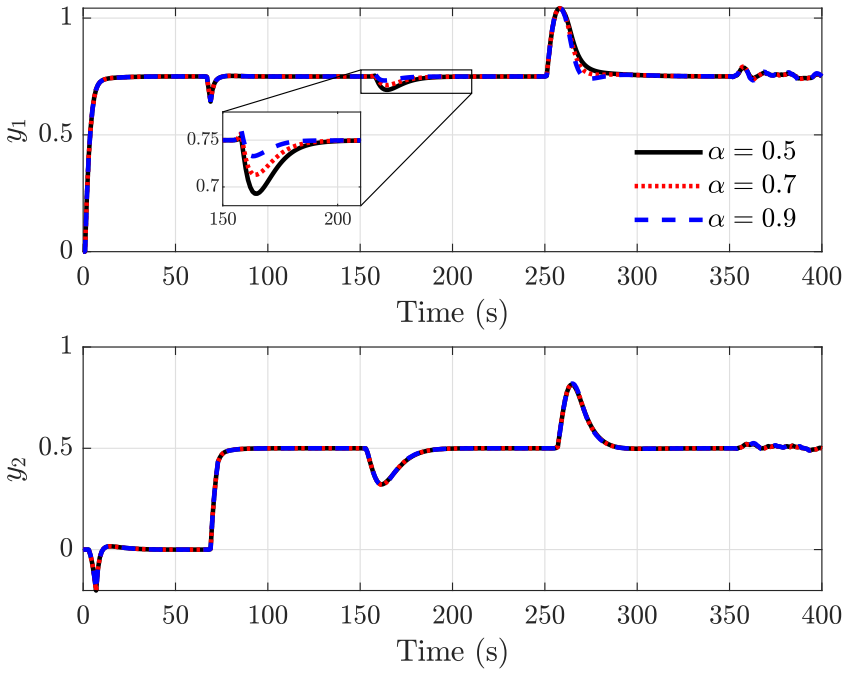

Source: The author.

As can be seen, the rejection of the perturbation $D_y(s)$ becomes faster as α increases, without changes in the tracking. It is also noted that the rejection of $D_u(s)$ is affected, becoming faster. This improvement in disturbance rejection occurs without a significant increase in control effort, as can be seen in Figure 71.

Figure 71 – Control signal of proposed GPC for different static gains α.

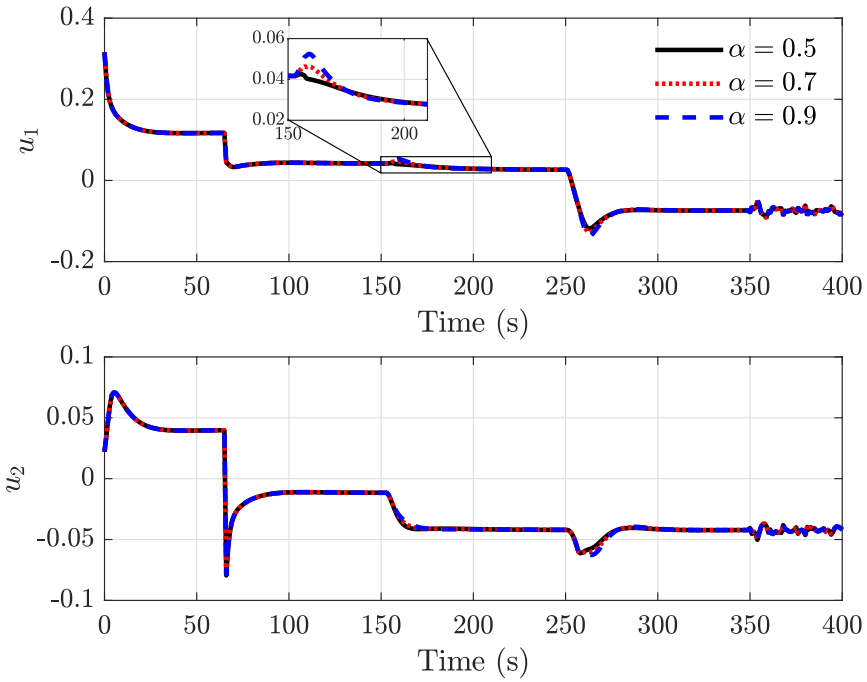

Source: The author.

The proposed GPC is also compared with controllers from literature, which are the MIMO-FSP from Flesch et al. (2011) and the MIMO-SFSP from Santos, Torrico and Normey-Rico (2016). The previous simulation conditions are applied to the controllers and the same tuning for the GPC is used, with $\alpha = 0.9$. The closed-loop response the nominal case are shown in Figure 72 where it can be seen that the proposed GPC presents a fast tracking with no overshoot or oscillations in both y_1 and y_2. However, it should be emphasized the better result of the GPC for disturbance rejection, mostly for $D_y(s)$ where is precisely where it is designed to act.

Figure 72 – Output response for the nominal case.

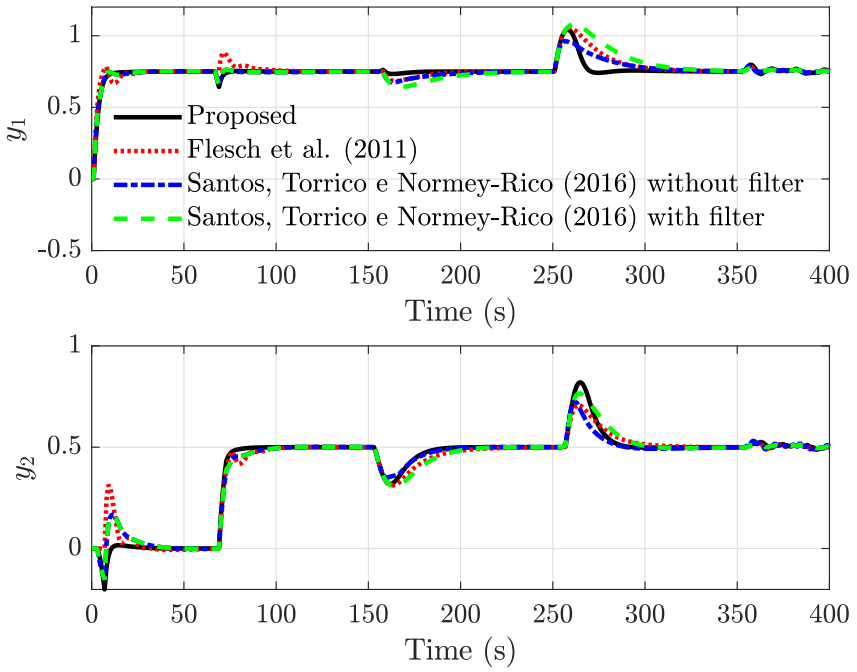

Source: The author.

This better performance is provided with little control effort compared with the control signal from Flesch et al. (2011) and Santos, Torrico and Normey-Rico (2016), which can be seen in 73, however the control signal for D_{u_1} is higher for the proposed GPC, showing an aggressive tuning and that α must be tuned considering the trade off between robustness and stability.

Figure 73 – Control signal for the nominal case.

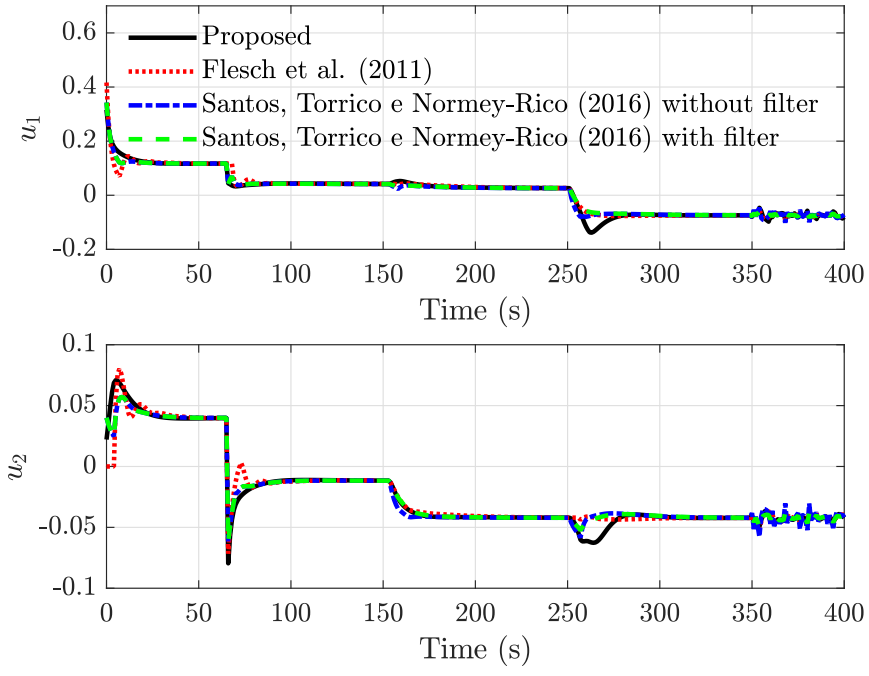

Source: The author.

As proposed in Santos, Torrico and Normey-Rico (2016), for robustness analysis it is applied +30 % of uncertainty in all delays, time-constants and gains of the transfer functions from the system in Equation (6.26). The simulation results are shown in Figure 74 and Figure 75.

Figure 74 – Output response for the uncertain case.

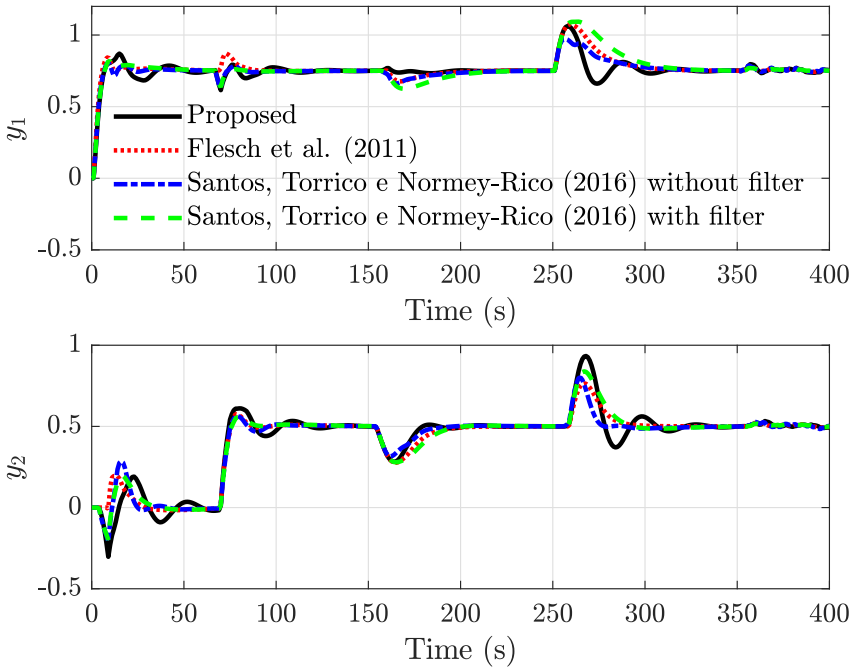

Source: The author.

Despite the slightly more oscillatory response, the proposed GPC still maintain better results for disturbance rejection and the control signal in Figure 75 also shows a similar behavior in relation to the nominal one, indicating that the proposed tuning, including for the gain α, have provided good stability margins.

Figure 75 – Control signal for the uncertain case.

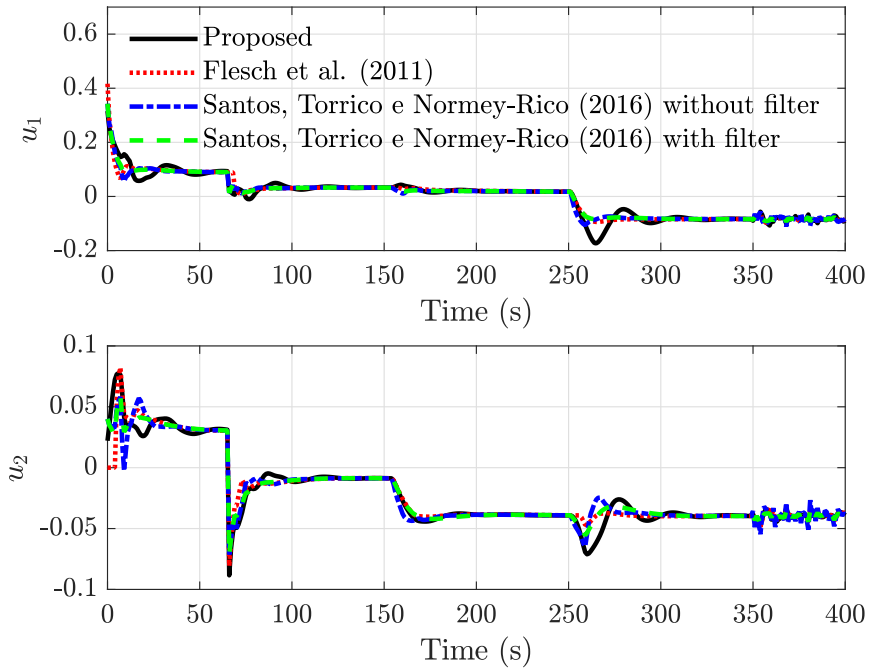

Source: The author.

Quantitative results for the nominal case are shown in Table 5. The proposed controller presents better results for all IAE indices of $Y_1(s)$, while the other indices remain in the same order of magnitude as the compared controllers, which indicates the advantages of using the FIR filter with the gain α in GPC design.

Table 5 – TITO example - Performance indices for the nominal case.

Example	Controller	Indices				
		IAE setpoint	IAE D_y	IAE D_{u_1}	TV	CV
Nominal $Y_1(s)$	Proposed	**3.0078**	**0.24304**	**3.465**	0.56857	8.5364×10^{-5}
	Flesch et al. (2011)	4.038	1.3991	7.3397	0.729	4.7323×10^{-5}
	Santos, Torrico and Normey-Rico (2016) without filter	3.1975	1.9241	5.5771	0.55126	0.00012622
	Santos, Torrico and Normey-Rico (2016) with filter	3.1986	3.359	10.412	**0.50875**	$\mathbf{2.0762 \times 10^{-5}}$
Nominal $Y_2(s)$	Proposed	36.112	3.0208	4.501	0.34632	5.8424×10^{-6}
	Flesch et al. (2011)	**34.814**	4.4684	4.1698	0.39784	8.8764×10^{-6}
	Santos, Torrico and Normey-Rico (2016) without filter	35.183	**2.961**	**3.11**	0.28886	2.8015×10^{-5}
	Santos, Torrico and Normey-Rico (2016) with filter	35.189	4.7809	5.3436	**0.27444**	$\mathbf{4.764 \times 10^{-6}}$

Table 6 show the performance indices for the uncertain case. The proposed controller maintain better IAE results for disturbance rejection in $Y_1(s)$ showing the robustness of the GPC. The advantage of the proposed method is that only by adjusting the α parameter is it possible

to obtain better responses to disturbances in the outputs, whether they are more robust or more aggressive.

Table 6 – TITO example - Performance indices for the uncertain case.

Example	Controller	Indices				
		IAE setpoint	IAE D_y	IAE D_{u_1}	TV	CV
Uncertain $Y_1(s)$	Proposed	5.9284	**0.43523**	**5.1958**	1.0995	8.2543×10^{-5}
	Flesch et al. (2011)	4.1912	1.4817	7.3936	0.68273	4.5259×10^{-5}
	Santos, Torrico and Normey-Rico (2016) without filter	**3.7668**	1.9186	5.6135	0.752	0.00012662
	Santos, Torrico and Normey-Rico (2016) with filter	4.2325	3.3892	10.518	**0.5682**	$\mathbf{2.0575 \times 10^{-5}}$
Uncertain $Y_2(s)$	Proposed	38.399	3.3258	7.3331	0.5178	6.5454×10^{-6}
	Flesch et al. (2011)	**35.442**	4.4676	4.1667	0.4068	8.0619×10^{-6}
	Santos, Torrico and Normey-Rico (2016) without filter	35.848	**3.1281**	**3.2606**	0.51118	2.8392×10^{-5}
	Santos, Torrico and Normey-Rico (2016) with filter	35.823	5.062	5.8364	**0.34403**	$\mathbf{4.6841 \times 10^{-6}}$

6.4 Discussion

In this work, a modification to the GPC was proposed in order to improve the output disturbance rejection of a TITO system with multiple delay.

A comparison was made with others controllers from the literature (FLESCH et al., 2011; SANTOS; TORRICO; NORMEY-RICO, 2016) to prove that the proposed controller meets the expected characteristics of output disturbance rejection. In the nominal case, the proposed method presents faster tracking and better attenuation for both $D_y(s)$ and D_{u_1} without overshoot in $Y_1(s)$, and other indices with the same order of magnitude that the compared controllers present. Regarding the case with uncertainties, the proposed controller presents similar results, indicating a good trade off between robustness and stability with the addition of only a FIR filter and a simple one-parameter adjustment.

7 SIMPLIFIED FILTERED SMITH PREDICTOR FOR LPV SYSTEMS

Consider the following discrete system represented by an auto-regressive with exogenous input (ARX) LPV model (ARX-LPV) (NOGUEIRA et al., 2018),

$$y(k) = \frac{B(z, \boldsymbol{\theta}(k))}{A(z, \boldsymbol{\theta}(k))} z^{-d} + e(k), \tag{7.1}$$

where $y(k)$ and $u(k)$ are the system input and output, respectively, $\boldsymbol{\theta}(k) = [\theta_1(k) \quad \theta_2(k) \quad \cdots \quad \theta_p(k)]$ is a vector with scheduling parameters, z is the forward-shift operator, $e(k)$ is the measurement noise, and d is the equivalent discrete dead time, which has a fixed value but unknown in the interval set $\{d_1,\ d_2,\ ...,\ d_{n_d}\}$.

For one scheduling variable $\theta_1(k) := \theta$, $B(z,\theta)$ and $A(z,\theta)$ are parameterized polynomials with coefficient $b(\cdot)$ and $a(\cdot)$ respectively, so that

$$B(z,\theta) = b_0 + b_1(\theta)z^{-1} + \cdots + b_{n_b}(\theta)z^{-n_b}, \tag{7.2}$$

$$A(z,\theta) = a_0 + a_1(\theta)z^{-1} + \cdots + a_{n_a}(\theta)z^{-n_a}, \tag{7.3}$$

where n_b and n_a are the order of the parameterized polynomials. For this thesis, are considered functions with polynomial dependence on θ such as

$$b_i(\theta) = b_{i1} + b_{i2}\theta + \cdots + b_{iN}\theta^N, i = 1, \cdots, n_b, \tag{7.4}$$

$$a_j(\theta) = a_{j1} + a_{j2}\theta + \cdots + a_{jN}\theta^N, j = 1, \cdots, n_a, \tag{7.5}$$

One may select $N = 1$ for affine dependence on θ, however it should be mentioned that when $N = 0$, the resulting model is a conventional ARX model.

A suitable choice to compose θ is to use variables that influence the change of operating points of the system, which means that they must necessarily be measurable by sensors or calculated in real-time so that they can be used in the adaptation algorithm of the controller. Since the dynamics of the dead-time system from Equation (7.1) change as the scheduling parameter changes, it is reasonable to assume that a SP-based controller extended to an LPV framework can show a good performance both in reference tracking and in disturbance rejection for all operating points of the system.

7.1 LPV-SFSP synthesis

The original SFSP, proposed in Torrico, Correia and Nogueira (2016), may be seen as a particular case of the LPV system illustrated in Figure 76 when there is no dependency on θ. The transfer function $P(z,\theta)$ represents the real process, $P_n(z,\theta) = G_n(z,\theta)z^{-d_n(\theta)}$ is the nominal

process model, $G_n(z,\theta)$ is the nominal process fast model, and d_n is the nominal dead-time. In order to properly analyze the closed-loop system properties, the input-output relationships are computed:

$$H_{yr}(z,\theta) = \frac{Y(z)}{R(z)} = \frac{F_r(\theta)P_n(z,\theta)}{1+F_1(z,\theta)+G_n(z,\theta)F_2(z,\theta)}, \tag{7.6}$$

$$H_{yq}(z,\theta) = \frac{Y(z)}{Q(z)} = P_n(z,\theta)\left[1 - \frac{P_n(z,\theta)V(z,\theta)}{1+F_1(z,\theta)+G_n(z,\theta)F_2(z,\theta)}\right], \tag{7.7}$$

$$H_{un}(z,\theta) = \frac{U(z)}{N(z)} = \frac{-V(z,\theta)}{1+F_1(z,\theta)+G_n(z,\theta)F_2(z,\theta)}, \tag{7.8}$$

where $H_{yr}(z,\theta)$, $H_{yq}(z,\theta)$, and $H_{un}(z,\theta)$ are the input–output transfer functions related to the setpoint to output, disturbance to output, and noise to control action channels. $U(z)$, $Y(z)$, $R(z)$, $N(z)$, and $Q(z)$ are, respectively, the Z-transform of the control action, process output, reference, measurement noise, and input disturbance signals.

The forms $F_r(\theta)$, $F_1(z,\theta)$, and $F_2(z,\theta)$ represent an LPV gain and finite impulse response (FIR) LPV filters, respectively, which are tuned in order to obtain a desired setpoint tracking. The filter $V(z,\theta)$ is designed to cancel the effect of slow or unstable poles in the disturbance rejection $H_{yq}(z,\theta)$ and to attenuate the effect of measurement noise.

It is also possible to calculate the robustness index $I_r(\omega)$, which may be given by

$$I_r(\theta,\omega) = \left|\frac{1+F_1(z,\theta)+G_n(z,\theta)F_2(z,\theta)}{G_n(z,\theta)V(z,\theta)}\right|_{z=e^{j\omega T_s}} > \overline{\delta P}(e^{j\omega T_s}), \tag{7.9}$$

where, T_s is the sampling time (with $0 < \omega < \pi/T_s$) and $\overline{\delta P}(e^{j\omega T_s})$ is the upper bound of the multiplicative uncertainty norm.

Figure 76 – SFSP-LPV structure.

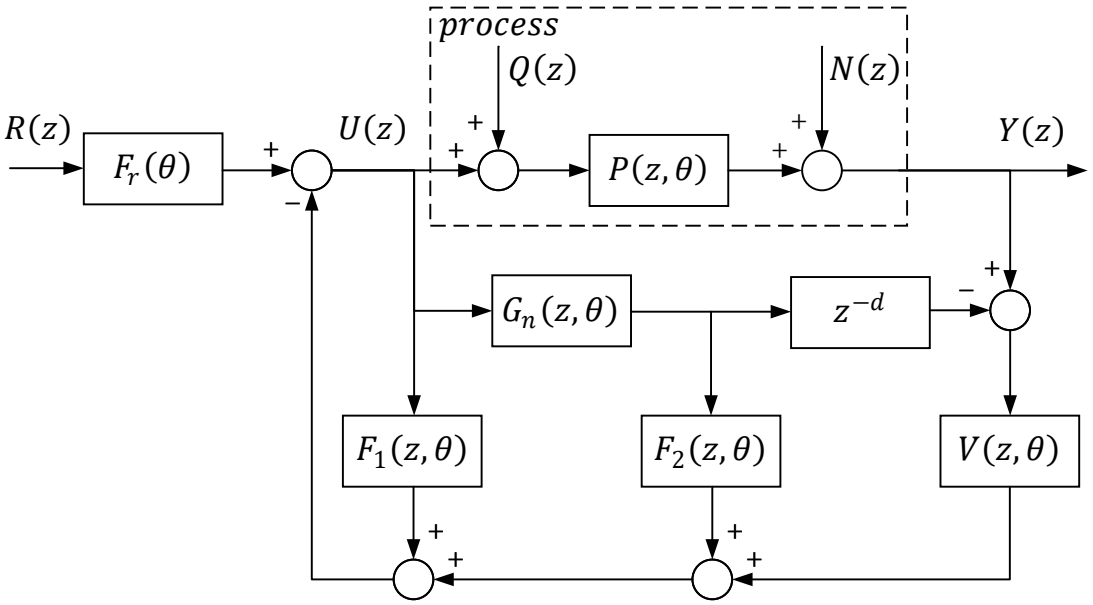

Source: The author.

For open-loop processes with integrating and unstable poles, the structure from Figure 76 needs to be modified to an equivalent structure in order to obtain an internally stable implementation of the predictor, which is presented in Figure 77, where

$$S(z,\theta) = F_1(z,\theta) + G_n(z,\theta)(F_2(z,\theta) - V(z,\theta)z^{-d_n}). \tag{7.10}$$

It can be notice from Equation (7.10) that $S(z,\theta)$ is designed to cancel both integrating and unstable poles of $G_n(z,\theta)$, thus ensuring internal stability.

Figure 77 – SFSP-LPV stable implementation structure.

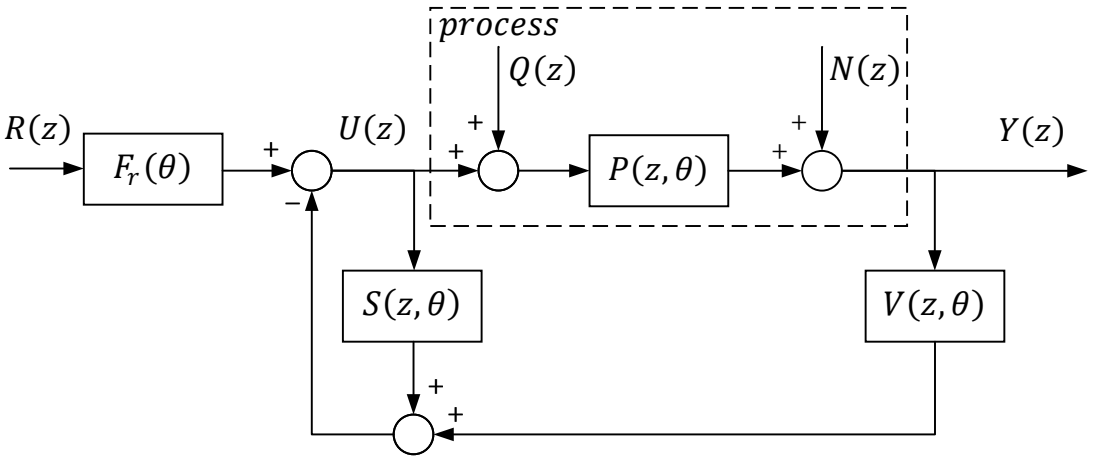

Source: The author.

7.2 Design of $F_r(\theta)$, $F_1(z,\theta)$ and $F_2(z,\theta)$

The SFSP-LPV primary controller is defined by the forms $F_r(\theta)$, $F_1(z,\theta)$, and $F_2(z,\theta)$, which should be designed in order to obtain a desired setpoint tracking. In order to obtain a setpoint tracking with zero steady-state error, the reference filter $F_r(\theta)$ is calculated as an extended version of the LTI case (TORRICO et al., 2018; TORRICO et al., 2021)

$$F_r(\theta) = K_r(\theta)\frac{(1-\beta_f)^{n_{\beta_f}}}{(1-\beta_f z^{-1})^{n_{\beta_f}}}\frac{(1-\alpha_f z^{-1})^{n_{\alpha_f}}}{(1-\alpha_f)^{n_{\alpha_f}}}, \tag{7.11}$$

where β_f and α_f are free tuning parameters in order to achieve a desired tracking response, while n_{β_f} and n_{α_f} are the filter order. The LPV gain $K_r(\theta)$ is given as

$$K_r(\theta) = \frac{1+F_1(\theta,1)+G_n(\theta,1)F_2(\theta,1)}{P_n(\theta,1)}. \tag{7.12}$$

It should be noted that $K_r(\theta)$ is the inverse of $H_{yr}(z,\theta)$, so $z=1$ because the gain has an effect in the steady state. This has to do with the fact that there is no integrator controller (TORRICO; CORREIA; NOGUEIRA, 2016).

Since the plant is LPV, i.e., its parameters belongs to a polytope, one may consider $F_1(z,\theta)$ and $F_2(z,\theta)$ as FIR LPV filters such as

$$F_1(z,\theta) = f_{1_1}(\theta)z^{-1} + f_{1_2}(\theta)z^{-2} + \cdots + f_{1_n}(\theta)z^{-n+1}, \tag{7.13}$$

$$F_2(z,\theta) = f_{2_0} + f_{2_1}(\theta)z^{-1} + \cdots + f_{2_n}(\theta)z^{-n+1}, \tag{7.14}$$

where $n = n_a$ and

$$f_{1_i}(\theta) = (f_{1_{i1}} + f_{1_{i2}}\theta + \cdots + f_{1_{iN}}\theta^{N-1}),\ i = 1,\cdots,n, \tag{7.15}$$

$$f_{2_i}(\theta) = (f_{2_{i1}} + f_{2_{i2}}\theta + \cdots + f_{2_{iN}}\theta^{N-1}),\ i = 1,\cdots,n, \tag{7.16}$$

are polynomial functions dependent on θ.

The scheduling parameters are inside a space Ω which belongs to a semi-algebraic set defined as

$$\Omega = \{\theta \in \mathbb{R}^p : g_i(\theta) \geq 0, i = 1,\cdots,n_\theta\}, \tag{7.17}$$

where $g_i(\theta)$ are polynomials with dependence on θ. The control problem is to compute $F_1(z,\theta)$ and $F_2(z,\theta)$ in order to guarantee the closed-loop performance and stability for the whole parameter space.

One possible way to deal with such problem is by defining the discrete-time closed-loop fast transfer function as

$$M(z,\theta) = \frac{N_{dz}(z,\theta)}{D_{dz}(z,\theta)} = \frac{G_n(z,\theta)}{1+F_1(z,\theta)+G_n(z,\theta)F_2(z,\theta)}, \tag{7.18}$$

where

$$D_{dz}(z,\theta) = \sum_{\alpha\in\mathbb{N}^p} D_{dz_\alpha}(z)\theta^\alpha = \sum_{\alpha\in\mathbb{N}^p}\sum_{i=0}^{dz} d_{dz_i} z^i \theta^\alpha, \text{ and}$$

$$N_{dz}(z,\theta) = \sum_{\alpha\in\mathbb{N}^p} N_{dz_\alpha}(z)\theta^\alpha = \sum_{\alpha\in\mathbb{N}^p}\sum_{i=0}^{dz} n_{dz_i} z^i \theta^\alpha$$

are polynomials of degree dz of the z-domain. Considering $Y_M(z)/U_M(z) = N_{dz}(z)/D_{dz}(z)$, where $Y_M(z)$ and $U_M(z)$ are, respectively, the Z-transforms of the input $u_M(k)$ and output $y_M(k)$ signals sequences, one can define a state-vector as $x(k) = [y_M(k)\ y_M(k-1)\ \cdots\ y_M(k-dz+1)]^T$ and $\xi(k) = [x(k)\ y_M(k-dz)]^T$.

By using the notation $x(k) = \Pi_2\xi(k)$ and $x(k+1) = \Pi_1\xi(k)$, it is possible to consider a quadratic Lyapunov function $V = x^*(k)Px(k) = \xi^*(k)\Pi_2^* P\Pi_2\xi(k)$ where

$$\Pi_1 = \begin{bmatrix} 0 & 1 & & \\ \vdots & & \ddots & \\ 0 & & & 1 \end{bmatrix}, \quad \Pi_2 = \begin{bmatrix} 1 & & & 0 \\ & \ddots & & \vdots \\ & & 1 & 0 \end{bmatrix}.$$

The well known conditions to asymptotic stability are given by $V(k) > 0$ and $\Delta V(x(k)) \triangleq V(x(k+1)) - V(x(k)) \leq 0$. The latter is equivalent to $\xi^*(k)F_{dz}(P)\xi(k) \leq 0$, where $F_{dz}(P) = \Pi_1^* P\Pi_1 - \Pi_2^* P\Pi_2$ is a linear mapping chosen in order to ensure that all closed-loop roots are within the unit circle (GILBERT et al., 2010). Thus, polynomial D_{dz} is stable if and only if, for a given a discrete stable polynomial C_{dz}, exists a symmetric matrix P so that

$$C_{dz}(z)^* D_{dz}(z) + D_{dz}(z)^* C_{dz}(z) - F_{dz}(P) \succeq 0 \tag{7.19}$$

where the symbol $\succeq$ means positive semidefinite, that is, all eigenvalues are non-negative and real; $C_{dz}(z)$ is a polynomial of free choice by the designer, with the constraint that it must be stable, being directly connected to the desired location for closed-loop poles and usually named central polynomial.

7.2.1 Control problem formulation

Assuming that $D_{dz}(z,\theta)$ is affected by an additive norm bounded uncertainty

$$D_{dz_\delta}(z,\theta) = D_{dz}(z,\theta) + \delta N_{dz}(z,\theta), \quad ||\delta||_\infty \leq \gamma^{-1}$$

with δ as an unknown matrix whose maximum singular value does not exceed a certain positive threshold γ^{-1} and using the definition contained in Theorem 1, the control problem can be defined as a parameterized LMI (PLMI) that includes the H_∞ performance constraint (GILBERT et al., 2010).

Theorem 1. *(GILBERT et al., 2010) By considering a stable discrete polynomial $C(z)$, the transfer function $M(z,\theta)$ is stable and its H_∞ norm is less than a given bound γ, for all trajectories of $\theta \in \Omega$, if there are a scalar λ and a symmetric matrix P_∞ such that*

$$\begin{bmatrix} C^*D(\theta) + D^*(\theta)C - F(P_\infty) - \lambda C^*C & N^*(\theta) \\ N(\theta) & \lambda\gamma^2 \end{bmatrix} \succeq 0. \tag{7.20}$$

As discussed in (HENRION, 2013) and (GILBERT et al., 2010), it is also possible to formulate the control problem to deal with H_2 performance. The idea is that for the transfer function $M(z,\theta)$, with input signal u and output signal y, the generalized H_2 norm can be defined as an energy to peak norm $||M||_2 = \sup ||y||_\infty / ||u||_2$, which represents the maximum possible output peak due to an arbitrary excitation with unit energy (KNOBLACH; LOOYE, 2017). Thus, Lemma 1 for the LPV case and robust stability may state that (HENRION, 2013)

Lemma 1. *(HENRION, 2013) Given a stable polynomial $C(z)$, rational polynomial $D^{-1}(z,\theta)N(z,\theta)$ is stable with generalized H_2 norm less than or equal to γ if there exists a symmetric matrix P_2 such that*

$$\begin{aligned} &C^*D(\theta)+D^*(\theta)C - F(P_2) - C^*C \succeq 0, \\ &\begin{bmatrix} P_2 & N(\theta)^* \\ N(\theta) & \gamma^2 I \end{bmatrix} \succeq 0. \end{aligned} \tag{7.21}$$

7.2.2 H_2/H_∞ mixed control

This paper proposes a strategy of mixed H_2/H_∞ in order to minimize the generalized H_2 norm of $M(z,\theta)$ and minimize the H_∞ norm constraint. In this way, the controller H_2/H_∞ has the multi-objective of minimizing the effects of uncertainties in $D_{dz}(z,\theta)$, as well as minimizing the maximum output peak that occurs for an arbitrary excitation with unit energy.

The LMIs (7.20) and (7.21) are combined for a scalar λ and a symmetric matrix P. The LMI $L(\eta,\theta)$ is positive semidefinite for a multiobjective H_2/H_∞ control performance if

$$L(\eta,\theta) = \begin{bmatrix} M_1 & \mathbf{0} & \mathbf{0} \\ \mathbf{0} & M_2 & \mathbf{0} \\ \mathbf{0} & \mathbf{0} & M_3 \end{bmatrix} \succeq 0, \tag{7.22}$$

holds for all $\theta \in \Omega$, with

$$M_1 = \begin{bmatrix} C^*D(\theta) + D^*(\theta)C - F(P) - \lambda C^*C & N^*(\theta) \\ N(\theta) & \lambda\gamma^2 \end{bmatrix},$$

$$M_2 = C^*D(\theta) + D^*(\theta)C - F(P) - C^*C,$$

$$M_3 = \begin{bmatrix} P & N(\theta)^* \\ N(\theta) & \gamma^2 I \end{bmatrix}.$$

The vector η gathers all decision variables of the problem, i.e., controller parameters, the matrices that form P, and scalar λ. The solution of PLMI (7.22) consists of searching for adequate values for the decision variables in order to ensure a positive semidefinite result, for all $\theta \in \Omega$. However, there are infinite numerical possibilities that suit θ inside the semi-algebraic space, so it is clear that (7.22) includes an infinite set of LMIs.

7.2.3 Sum-of-squares relaxation

It can be stated that the solution of PLMI $L(\eta,\theta) \succeq 0$ is equivalent to test the PLMI global positivity. In order to perform this test is possible to relax the polynomial matrices by writing them as a polynomial sum-of-squares (SOS). The result is a relaxed system which can be solved as a semidefinite program (SDP) problem (APKARIAN; TUAN, 2000; SCHERER; HOL, 2006; BLEKHERMAN; PARRILO; THOMAS, 2012).

For a polynomial matrix $S_r(x)$ to be considered as SOS, there must be a polynomial matrix $T_r(x)$ so that $S_r(x) = T_r^*(x)T_r(x)$, where $x \in \mathbb{R}^N$. It is possible to find out if a matrix is SOS by a computational procedure that consists basically on finding a matrix $X_r = [X_{r_1} \cdots X_{r_n}]$ in the equation

$$T_r(x) = X_{r_1}u_{r_1}(x) + \cdots + X_{r_n}u_{r_n}(x) = X_rU_r(x), \tag{7.23}$$

where $U_r = [I \times u_{r_1}(x) \cdots I \times u_{r_n}(x)]^*$. So, through (7.23), the matrix $S_r(x)$ can be rewritten as

$$S_r(x) = U_r^*(x)(X_r^*X_r)U_r(x). \tag{7.24}$$

Based on SOS decomposition, the term $X_r^*X_r$ can be replaced by $Q_r = X_r^*X_r$ and the positiveness of $S_r(x)$ can be relaxed by Theorem 2 (SCHERER, 2006; SCHERER; HOL, 2006; BLEKHERMAN; PARRILO; THOMAS, 2012).

Theorem 2. *(SCHERER; HOL, 2006) The polynomial matrix $S_r(x)$ is SOS if exists a symmetric and positive semidefinite matrix Q_r, for a given monomial base $U_r(x)$, such that*

$$S_r(x) = U_r^*(x)Q_rU_r(x) \quad \textit{and} \quad Q_r \succeq 0. \tag{7.25}$$

The result of the expression $S_r - U_r^*Q_rU_r$ should be an empty matrix, although, in practical situations this outcome is generally infeasible due to numerical problems in floating-point variables and the ending criteria in the SDP solvers. One way to deal with these calculations is by the SOS package functions of YALMIP, which ensures the semidefinite constraint of Q_r (LOFBERG, 2009). Despite its non-negativeness, the polynomial resultant from the SOS decomposition is not identical to the considered in the problem (LOFBERG, 2009; NOGUEIRA et al., 2018).

The SOS relaxation for LPV systems, that is, when the matrix $S_r(\theta)$ is parameterized on θ, which belongs to a semi-algebraic set as defined in (7.17), has its positiveness relaxed by Theorem (3) (SCHERER, 2006; GILBERT et al., 2010).

Theorem 3. *(GILBERT et al., 2010) Suppose $L(\eta,\theta) \succeq 0$ is equivalent to $L(\eta,\theta) \succ 0$, then there is a η so that $L(\eta,\theta) \succ 0$ for all $\theta \in \Omega$ if and only if it exists SOS polynomial matrices $S_{r_i}(\theta)$ so that*

$$L(\eta,\theta) = S_{r_0}(\theta) + \sum_{i=1}^{n+1} g_i(\theta) S_{r_i}(\theta). \tag{7.26}$$

It must be noted that the restriction $L(\eta,\theta) \succ 0$ is a linear combination of several SOS polynomial matrices. Thus, it can be described as an LMI with these same SOS matrices and all the decision variables reunited in the vector η configuring the decision variables referring to the optimization problem.

7.3 Design of filter $V(z,\theta)$

The robustness filter is designed under certain conditions to ensure predetermined specifications of disturbance rejection. As in Torrico et al. (2013a), the system is rearranged into a 2DOF structure with an equivalent controller in the form

$$C_{eq}(z,\theta) = \frac{V(z,\theta)}{1+S(z,\theta)}, \tag{7.27}$$

which can be combined with (7.10) to adjust $V(z,\theta)$ to meet the design specifications of (i) to eliminate unstable or slow modes of $P(z,\theta)$ with

$$1+S(z,\theta)\big|_{z=p_i\neq 1} = 0, \tag{7.28}$$

and (ii) to guarantee proper disturbance rejection with

$$\begin{aligned} &\frac{d^{n_1}}{dz^{n_1}}(1+S(z,\theta))\big|_{z=1} = 0, \\ &n_1 = 1,\cdots,m-1, \end{aligned} \tag{7.29}$$

where p_i are poles of the plant model, $m = m_1 + m_2$, with m_1 representing the poles at $z = 1$, and m_2 can take on values according to the order of disturbance, thus, has a value of 1 for steps, 2 for ramps, etc. Furthermore, for sinusoidal disturbances, with

$$1+S(z,\theta)\big|_{z=e^{\pm j\omega_n T_s}} = 0, \tag{7.30}$$

where w_n are the sinusoidal disturbances frequencies.

Then, the filter can be computed as

$$V(z,\theta) = \frac{v_0(\theta) + v_1(\theta)z^{-1} + \cdots + v_n(\theta)z^{-n_s}}{(1-\alpha_1 z^{-1})(1-\alpha_2 z^{-1})\cdots(1-\alpha_v z^{-1})}, \tag{7.31}$$

where $n_s + 1$ is equal to number of equations in (7.28), (7.29) and (7.30), $n_v = n_s$ is the number of poles and α_i are free tuning parameters (different from the poles of $G_n(z,\theta)$) that define disturbance rejection dynamics.

Considering that filter $V(z,\theta)$ depends on θ as

$$v_i(\theta) = (v_{i1} + v_{i2}\theta + \cdots + v_{iN}\theta^{N-1}),\ i = 1,\cdots,n, \tag{7.32}$$

then the filter numerator must be computed at each iteration, according to the scheduling parameter, following the procedure in (TORRICO et al., 2021) in order to properly deal with the disturbance rejection for all operation points.

7.4 Simulations results

In order to properly evaluate the performance of the proposed technique, two examples are used. The first simulation is a comparison to the works from Oliveira and Karimi (2013) and Bolea, Puig and Blesa (2013) which proposed PID controllers for dead-time LPV processes, while the second one simulates an unstable process of an aero-pendulum model proposed in Habib et al. (2017). The disturbances and noise measurement in the output response are applied separately in order to provide a better analysis of the effects.

7.4.1 Example 1 - Stable case

Consider the following simulated system studied in Oliveira and Karimi (2013):

$$P_n(s,\theta) = G(s,\theta)e^{-\tau s} \tag{7.33}$$

where $G(s,\theta) = G_n(s,\theta)[1 + \Delta(s)W_2(s)]$, $\Delta(s)$ is an unknown stable transfer function with $||\Delta||_\infty < 1$, and

$$G_n(s,\theta) = \frac{(2+0.2\theta)^2}{s^2 + 0.2(2+0.2\theta)s + (2+0.2\theta)^2)}, \tag{7.34}$$

$$W_2(s) = 0.8\frac{1.1337s^2 + 6.8857s + 9}{(s+1)(s+10)} \tag{7.35}$$

and $\theta \in [-1,1]$. The dead-time is within the interval $\tau \in [2.7, 3.3]$, however its exact value is unknown during runtime.

The system is identified by using the algorithm from Bamieh and Giarre (2002) with sample time of $T_s = 0.05$ s. Thus, the discrete system is given as

$$G_n(z,\theta) = \frac{(0.00498 + 0.00098\theta)z^{-1} + (0.00495 + 0.00095\theta)z^{-2}}{1 + (-1.97008 + 0.00322\theta)z^{-1} + (0.98003 - 0.00126\theta)z^{-2}}. \tag{7.36}$$

The purpose of central polynomial $C(z)$ is pole allocation, as the closed-loop poles of the system tend towards its roots (GILBERT, 2008; NOGUEIRA et al., 2018), which means that the desired behavior for the LPV closed-loop system can be specified through a proper choice of it. For the system presented in Equation (7.34), the control objectives are a nominal response without overshoots and faster tracking relative to the compared controllers. Thus, in order to properly fulfill this specification, the central polynomial is choose as

$$C(z,\theta) = 1 - 2.4z^{-1} + 1.91z^{-2} - 0.504z^{-3}. \tag{7.37}$$

Characteristics of polynomial $C(z)$, such as damping, frequency and time constant are shown in Table 7.

Table 7 – Example 1. $C(z)$ polynomial characteristics.

Pole	Damping	Frequency (rad/s)	Time constant (s)
0.7	1	2.11	0.475
0.8	1	4.46	0.224
0.9	1	7.13	0.140

The SFSP-LPV primary controller is tuned, according to Equation (7.22), as

$$F_1(z,\theta) = -(0.4720 + 8.8273 \times 10^{-4}\theta)z^{-1}, \tag{7.38}$$

$$F_2(z,\theta) = (8.6244 - 1.9230\theta) + (-8.5290 + 1.8123\theta)z^{-1} \tag{7.39}$$

and the reference filter $F_r(\theta)$ parameters in Equation (7.11) are choose as $\beta_f = 0.85$, $\alpha_f = 0.8$, $n_{\beta_f} = 2$, $n_{\alpha_f} = 2$, and the LPV gain $K_r(\theta)$ is given through Equation (7.12).

The open and closed-loop poles for several values of the scheduling parameter can be seen by the pole map in Figure 78. This map is a powerful tool for analyzing the robustness of LPV controllers. As can be observed, the closed-loop poles of the system are confined in a small region which is close to the central polynomial poles, as well as inside the 0.9 damping curve in the z-plane. This result may indicate of low sensitivity against variations in the closed-loop LPV system operating conditions. The proposed SFSP-LPV controller has been able to meet a good trade-off for both stability and performance specifications considering all operating points.

Figure 78 – Example 1. Closed-loop poles for several values of $\theta \in [-1, 1]$.

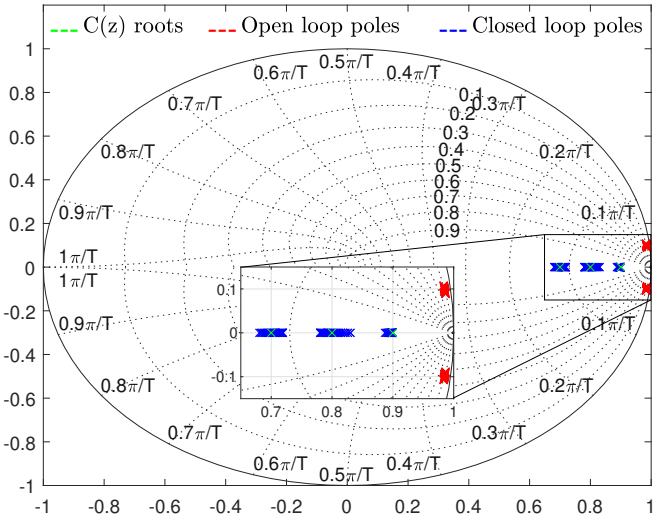

Source: The author.

Regarding to the tuning of the robustness filter $V(z, \theta)$ in Equation (7.32) it is desired a good balance between noise attenuation and robustness for the dynamic of disturbance response, thus the poles $\alpha_0 = 0.8$, $\alpha_1 = 0.9$ and $\alpha_2 = 0.9$ are chosen.

The time responses to a unit step reference for several values of $\theta \in [-1, 1]$, using the continuous system, are shown in Figure 79. A negative step disturbance of magnitude 0.1, is applied at the process input at $t = 40$ s and white noise, with zero mean and a variance of 5×10^{-5}, is added to the measured output at $t = 75$ s.

The response of SFSP-LPV is compared with the PID-LPV proposed by Bolea, Puig and Blesa (2013) and by Oliveira and Karimi (2013). Although they all have similar tracking responses, the SFSP-LPV is less oscillatory and the control signal has a smaller amplitude at the beginning since there is not a derivative portion.

An uncertainty situation is also considered, where the nominal case has dead time $t_d = 3$ s and the real plant $t_d = 3.3$ s and result showed in Figure 80. The SFSP-LPV exhibit a faster tracking and disturbance rejection with less oscillations. The control signal, as well in the nominal case, has a smaller amplitude at the beginning.

A 0.1 constant disturbance at $t = 40$ s is applied to the system. It should be observed that from $t = 40$ s to approximately $t = 48.3$ s the dead time dynamic prevents any controller from taking any action on the system, but after that only SFSP-LPV shows a non oscillatory response. The controllers also present a similar response to noise attenuation, however in the SFSP-LPV the control signal is far less affected by noise.

Figure 79 – Example 1. Nominal case for several values of $\theta \in [-1, 1]$.

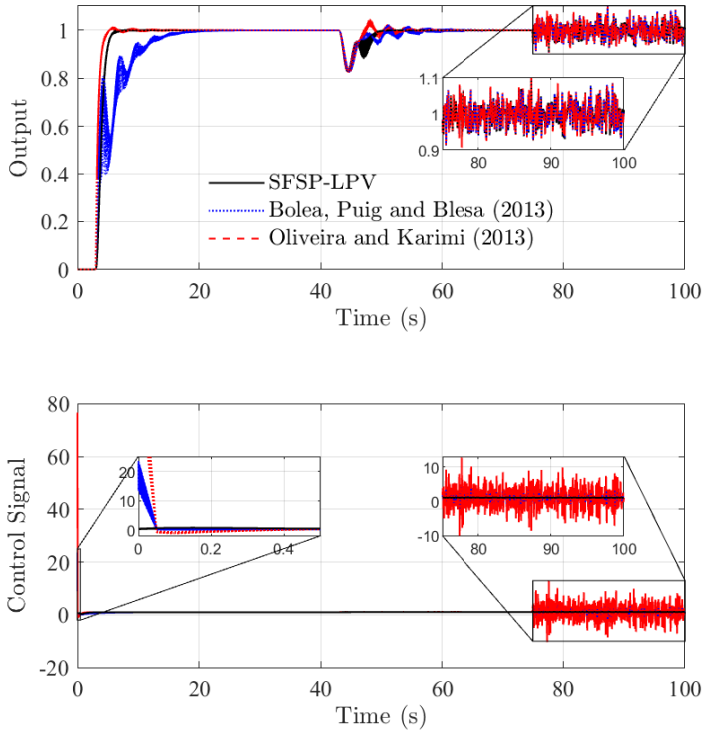

Source: The author.

Figure 80 – Example 1. Case with model uncertainties for several values of $\theta \in [-1, 1]$.

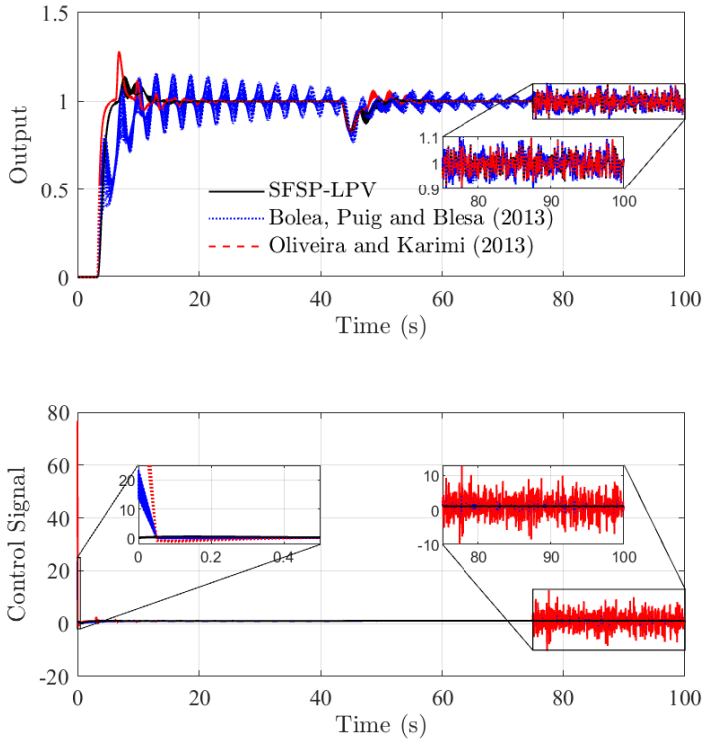

Source: The author.

The curves for robustness index are presented in Figure 81 for the controllers. It is

important to note that them, for all controllers, do not touch the multiplicative uncertainty curve, which indicates their stability through the considered delay uncertainties. However, at high frequencies, SFSP-LPV has better noise attenuation as its curve is steeper.

Figure 81 – Example 1. Robustness Index for several values of $\theta \in [-1, 1]$.

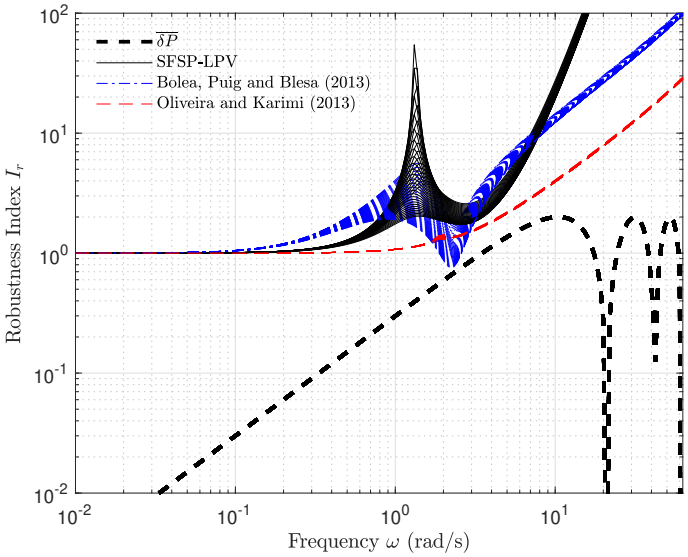

Source: The author.

Considering the LPV case, it is reasonable that one should compute the performance indices for at least a range of operations points in order to properly analyze the controllers behavior. Thus the results are shown in a graphic form. For Example 1, the nominal case is presented in Figure 82. The controller from Oliveira and Karimi (2013) present better IAE indices for both tracking and disturbance rejection, however this is done for a response with overshoot. The SFSP-LPV is tuned for fast tracking without overshoot, thus presenting intermediate IAE indices considering the compared controllers, but still with lower TV values in all scheduling ranges. Also the proposed SFSP-LPV shows better noise attenuation in all scenarios. For the uncertain case, Figure 83, the SFSP-LPV presents less oscillatory results, which is confirmed when analyzing the performance indices. For tracking, the proposed controller still presents intermediate results, considering the entire scheduling range, but for the IAE index for disturbance rejection, the SFSP-LPV presents better results than the compared controllers and even with lower TV indices, which means that better results are obtained with less control efforts. The SFSP-LPV maintains the best noise attenuation even in the case with uncertainty.

Figure 82 – Example 1. Controllers performance for the nominal case.

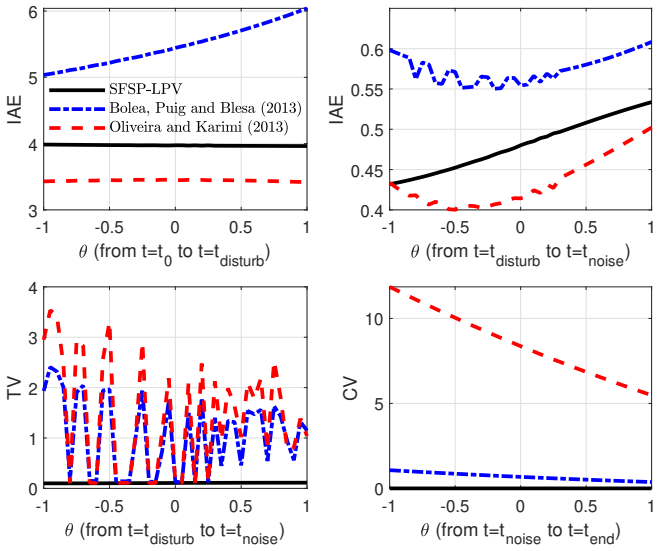

Source: The author.

Figure 83 – Example 1. Controllers performance for the uncertain case.

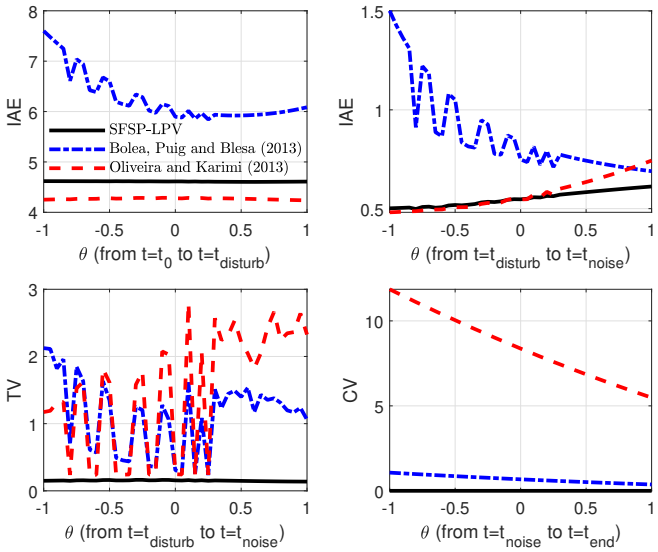

Source: The author.

7.5 Example 2 - Unstable case

On this example it is discussed the application of SFSP-LPV in a nonlinear model of an aero-pendulum. In addition to the nonlinearities, this system has the characteristic of having a stable and an unstable region, which can bring additional difficulties to the design of a controller. By comparing with other LPV controllers, it is possible to clearly verify the advantages of using the proposed approach.

7.5.1 System model decryption and modification for unstable region control

The herein aero-pendulum model was proposed by Habib et al. (2017). By disregarding the electrical dynamics of the actuator, the motion equations for the aero-pendulum are derived from Euler-Lagrange method.

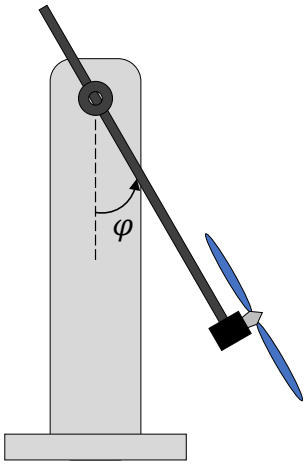

Figure 84 – Aero-pendulum physical diagram.

The Lagrangian function may be given by

$$L = \frac{1}{2} I_{pp} \dot{\varphi}^2 + \frac{1}{2} I_{prop} \dot{\theta}^2 + m_{pp} g l_{pend} \cos(\varphi), \tag{7.40}$$

where

- I_{pp} - pendulum-propeller moment of inertia regarding the pivot point;
- φ - pendulum angular position;
- I_{prop} - propeller moment of inertia regarding its center;
- θ - propeller angular position;
- m_{pp} - pendulum-propeller mass;
- g - acceleration of gravity;
- l_{pend} - center of gravity of the pendulum and axis of rotation distance.

By means of the Euler-Lagrangian method, one may get

$$\begin{cases} I_{pp}\ddot{\varphi} + m_{pp} g l_{pend} \sin(\varphi) = -c_{l_{pend}} \dot{\varphi} - c_{q_{pend}} \dot{\varphi}|\dot{\varphi}| - c_{fri_{pend}}(\dot{\varphi}) \dfrac{\dot{\varphi}}{|\dot{\varphi}|} + l_{pp} \tilde{F}_{prop}(\dot{\theta}) \\ I_{prop}\ddot{\theta} = -c_{l_{prop}} \dot{\theta} + \tilde{\tau}_{PWM} \end{cases} \tag{7.41}$$

with

- $c_{l_{pend}}$ - air drag linear damping coefficient on the pendulum;
- $c_{q_{pend}}$ - air drag quadratic damping coefficient on the pendulum;
- $c_{fri_{pend}}$ - dry friction coefficient on the pendulum;
- l_{pp} - distance between the axes of rotation of the pendulum and of the propeller;
- $\tilde{F}_{prop}$ - reaction force provided by the propeller;
- $c_{l_{prop}}$ - linear damping coefficient on the propeller;
- $\tilde{\tau}_{PWM}$ - torque from the motor, which is related to the PWM signal provided by the controller.

The nonlinear state space system is then given by

$$\begin{cases} \ddot{\varphi} + 2\delta_l \omega_n \dot{\varphi} + \delta_q \dot{\varphi}|\dot{\varphi}| + C(\dot{\varphi})\dfrac{\dot{\varphi}}{|\dot{\varphi}|} + \omega_n^2 \sin(\varphi) = F_{prop}(\Omega) \\ \dot{\Omega} = -\dfrac{\Omega}{\lambda} + \dfrac{\tau_{PWM}}{\lambda} \end{cases} \tag{7.42}$$

where

- $\delta_l = \dfrac{c_{l_{pend}}}{2\sqrt{m_{pp} g l_{pend} I_{pp}}}$ is the linear damping coefficient;
- $\omega_n = \sqrt{\dfrac{m_{pp} g l_{pend}}{I_{pp}}}$ is the natural frequency;
- $\delta_q = \dfrac{c_{q_{pend}}}{I_{pp}}$ is the quadratic damping coefficient;
- $C(\dot{\varphi}) = c_{fri_{pend}}(\dot{\varphi}) = \mu_{fri}(1 + \alpha e^{-\beta|\dot{\varphi}|})$ is the dry friction model;
- Ω is the propeller velocity;
- $F_{prop}(\Omega) = \dfrac{l_{pp}\tilde{F}_{prop}(\omega_n)}{I_{pp}}$;
- $\lambda = \dfrac{I_{prop}}{c_{l_{prop}}}$ is the propeller time constant;
- $\tau_{PWM} = \dfrac{\tilde{\tau}_{PWM}}{c_{l_{prop}}}$.

Habib et al. (2017) then identified the real system for the stable region, with angles from 0° to 90° and a PWM signal from -127 to 127. However, for the purposes of this work the system has to be modified in order to include the unstable region, i.e., angles from 90° to 180° and a more general control signal, only related to PWM signal.

The modified version for the aero-pendulum model is given by

$$\begin{cases} \ddot{\varphi} + 2\delta_l \omega_n \dot{\varphi} + \delta_q \dot{\varphi}|\dot{\varphi}| + C(\dot{\varphi})\dot{\varphi} + \omega_n^2 \sin(\varphi) = a\omega_n^2 \Omega \\ \dot{\Omega} = -\dfrac{\Omega}{\lambda} + \dfrac{u}{\lambda} \end{cases} \tag{7.43}$$

where a is a constant to approximate $F_{prop}(\Omega)$ for all angle range and u is the control signal, which is related to the PWM signal. The parameters values of Equation (7.43) are given in Table 8.

Table 8 – Aero-pendulum nonlinear system parameters.

Parameter	Value
Linear Damping coefficient δ_l	0 rad^{-1}
Natural frequency ω_n	6.9 rad/s
Quadratic Damping coefficient δ_q	0.028 rad^{-1}
Constant μ_{fri}	2.6 rad/s^2
Constant α	0.77
Constant β	2
Constant a	10
Propeller time constant λ	0.28 s

In order to linearize the system, one may follow the approach from Isidori (1995), Habib et al. (2017), where the dry friction is replaced with a linear damping. The value used for this work is $\delta_{ld} = 0.2$ rad^{-1} and it is also used the approximation $\sin(\varphi) \approx \sin(\varphi_{op}) + (\varphi - \varphi_{op})\cos(\varphi_{op})$, with φ_{op} indicating the angular position at the point of operation. Thus, the linearized system is given by

$$\begin{cases} \ddot{\varphi} + 2\delta_{ld} \omega_n \dot{\varphi} + \omega_n^2 (\sin(\varphi_{op}) + (\varphi - \varphi_{op})\cos(\varphi_{op})) = a\omega_n^2 \Omega \\ \dot{\Omega} = -\dfrac{\Omega}{\lambda} + \dfrac{u}{\lambda} \end{cases} \tag{7.44}$$

It should be noted that the quadratic damping term δ_q only interferes in large amplitudes, that is, basically in the first complete oscillation of the pendulum. Thus, this term could be disregarded in the linearized model (HABIB et al., 2017).

7.5.2 LPV modeling for the Aero-pendulum system

The system from (7.44) can be rewrite as

$$\begin{cases} \ddot{\varphi} + 2\delta_{ld} \omega_n \dot{\varphi} + \omega_n^2 \cos(\varphi_{op})\varphi = a\omega_n^2 \Omega - \omega_n^2 (\sin(\varphi_{op}) - \varphi_{op}\cos(\varphi_{op})) \\ \dot{\Omega} = -\dfrac{\Omega}{\lambda} + \dfrac{u}{\lambda}, \end{cases} \tag{7.45}$$

so that convenient considerations for LPV modeling can be stipulated.

Since the term $-\omega_n^2(\sin(\varphi_{op}) - \varphi_{op}\cos(\varphi_{op}))$ is a constant value for each operation point, it can be disregarded from the modeling and left to be handled by the LPV controller.

However, one may consider the approximation $\omega_n^2 \cos(\varphi_{op}) = \Gamma(\varphi_{op}) = \Gamma(\theta)$, where $\theta = \varphi_{op}$ is the scheduling variable.

It should be noted that in order for $\Gamma(\theta)$ to be considered a good approximation for $\omega_n^2 \cos(\varphi_{op})$, a structure for it must be chosen. Thus, for this work, it is used a polynomial structure in the form

$$\Gamma(\theta) = \Gamma_1 + \Gamma_2\theta + \Gamma_3\theta^2 + \cdots + \Gamma_{n_\Gamma}\theta^{n_\Gamma} \tag{7.46}$$

where by considering angle positions from 0° to 180°, it is possible to calculate the parameters of $\Gamma(\theta)$ through the least squares algorithm as in

$$\begin{pmatrix} \Gamma_1 \\ \Gamma_2 \\ \vdots \\ \Gamma_{n_\Gamma} \end{pmatrix} = \begin{pmatrix} 1 & \theta_1 & \theta_1^2 & \cdots & \theta_1^{n_\Gamma} \\ 1 & \theta_2 & \theta_2^2 & \cdots & \theta_2^{n_\Gamma} \\ \vdots & \vdots & & & \\ 1 & \theta_{n_\Gamma} & \theta_{n_\Gamma}^2 & \cdots & \theta_{n_\Gamma}^{n_\Gamma} \end{pmatrix}^{-1} \begin{pmatrix} \omega_n^2 \cos(\varphi_1) \\ \omega_n^2 \cos(\varphi_2) \\ \vdots \\ \omega_n^2 \cos(\varphi_{n_\Gamma}) \end{pmatrix}, \tag{7.47}$$

which is given as

$$\Gamma(\theta) = 47.1798 + 4.0461\theta - 32.5456\theta^2 + 6.9064\theta^3 \quad \text{with} \quad \theta \in [0, \pi]. \tag{7.48}$$

The comparison between $\omega_n^2 \cos(\varphi_{op})$ and $\Gamma(\theta)$ is showed in Figure 85.

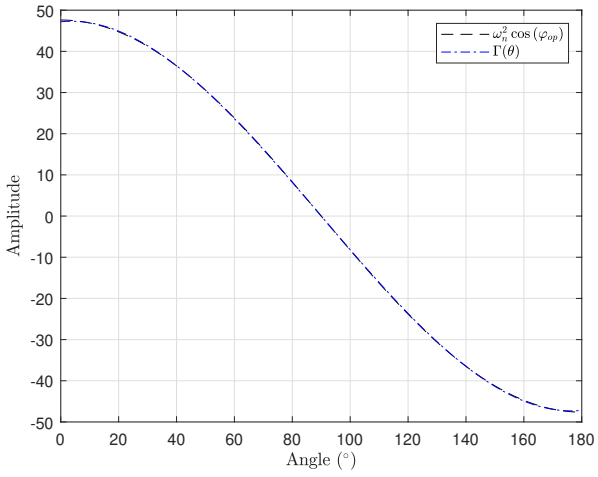

Figure 85 – Comparison between $\omega_n^2 \cos(\varphi_{op})$ and $\Gamma(\theta)$.

Finally, the system from (7.45) can be rewritten in an LPV framework as

$$\begin{cases} \ddot{\varphi} + 2\delta_{ld}\omega_n\dot{\varphi} + \Gamma(\theta)\varphi = a\omega_n^2\Omega \\ \dot{\Omega} = -\dfrac{\Omega}{\lambda} + \dfrac{u}{\lambda}, \end{cases} \tag{7.49}$$

which can take the form of an LPV transfer function such

$$P_n(s,\theta) = \frac{1700.35714}{(s^2 + 2.76s + \Gamma(\theta))(s + 3.5714)} e^{-0.15s}, \tag{7.50}$$

where the delay can represents communication issues as discussed in Habib et al. (2017).

The discretization, with $T_s = 0.01$ s, leads to the following discrete LPV transfer function (TÓTH, 2010)

$$P_n(z,\theta) = \frac{0.00170035z^{-3}}{(1-1.9724z^{-1}+(0.0001\Gamma(\theta)+0.9724)z^{-2})(1-0.9643z^{-1})}z^{-15} \tag{7.51}$$

and the comparison between (7.43), (7.50) and (7.51) is shown in Figure 86.

Figure 86 – Comparison between nonlinear model and LPV models of the aero pendulum system.

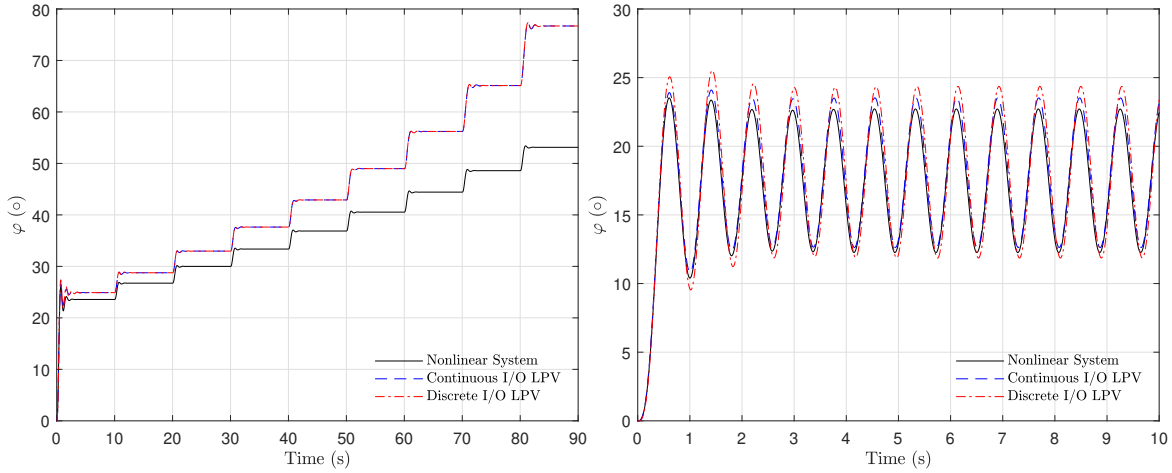

Source: The author.

In Figure 86a a set of step inputs ranging from $u = 0.04$ to $u = 0.08$ is applied, demonstrating the divergence, mainly in amplitude magnitude, of the LPV models when compared to the nonlinear model. In Figure 86b, the outputs of the models for $u = 0.03 + 0.015\sin(8t)$ are presented, in order to compare the oscillations present in the responses.

The dynamics of the nonlinear system (7.43) is characterized by stable $\varphi = (...0,\ 2\pi,\ 4\pi...)$ and unstable $\varphi = (...\pi,\ 3\pi,\ 5\pi...)$ equilibrium points. In the stable regions, any initial condition leads to a convergent trajectory to the respective equilibrium point, while for regions near unstable equilibrium points there is a jump to the next stable region. This behavior can be seen in the system phase portrait, shown in Figure 87.

In Figure 87a it is possible to observe the different equilibrium points of the nonlinear system, as previously described. However, in Figure 87b it is possible to observe that the approximation of the system by an LPV model leads to only four equilibrium points, of which two are stable $\varphi = (0,\ 4\pi/3)$ and two are unstable $\varphi = (-\pi/3,\ \pi/2)$. The other regions presented by the phase portrait of the LPV system show divergent trajectories. It is also possible to verify that the stable region close to the equilibrium point $(0,0)$ is smaller for the LPV system, which can be explained due to the chosen modeling, which opts to use the interpolation of the linearized system in the stable region.

Figure 87 – Phase portraits of the nonlinear system and the LPV approximation.

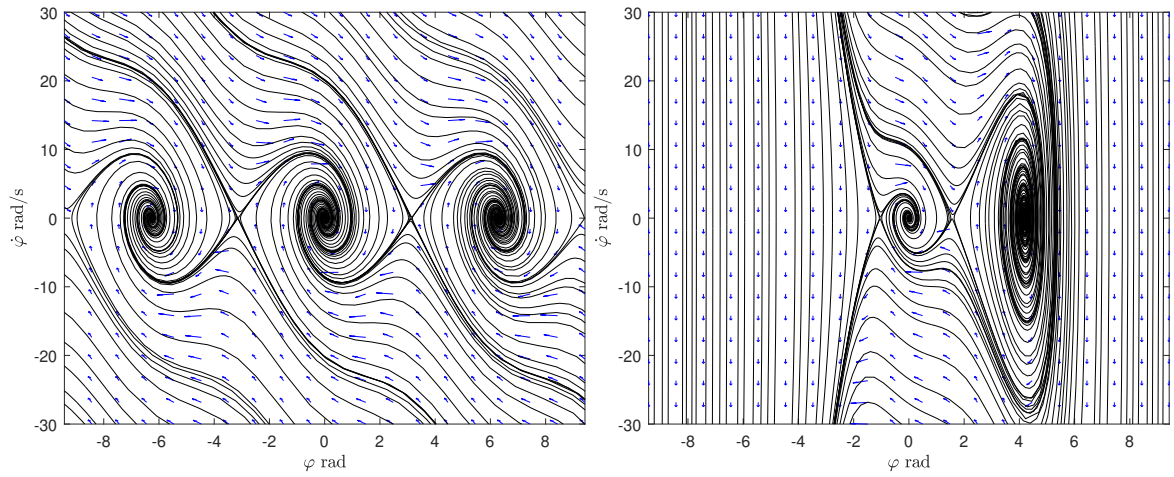

(a) Nonlinear system.

(b) LPV system.

Source: The author.

The LMI (3.25) with a Lyapunov function of the type $V = x^T Px$ are also used to calculate a region of attraction in which the system (7.49) is quadratically and asymptotically stable. A feasible result is found for the angles between $\varphi = -0.82030$ rad to $\varphi = 1.18682$ rad, where

$$P = \begin{pmatrix} 121.615 & 5.59220 & -907.181 \\ 5.59220 & 3.68789 & 200.329 \\ -907.181 & 200.329 & 31629.7 \end{pmatrix}. \tag{7.52}$$

7.6 SFSP-LPV Controller aero-pendulum

The central polynomial is set to

$$C(z,\theta) = 1 - 1.996z^{-1} + 1.073z^{-2} - 0.07668z^{-3} + 0.001579z^{-4} - 9.177 \times 10^{-6}z^{-5}. \tag{7.53}$$

with damping, frequency and time constant of polynomial $C(z)$ shown in Table 9.

Table 9 – Example 2. $C(z)$ polynomial characteristics.

Pole	Damping	Frequency (rad/s)	Time constant (s)
0.01	1	461	0.00217
0.02	1	391	0.00256
0.05	1	300	0.00334
0.95	1	5.13	0.195
0.966	1	3.46	0.289

The SFSP-LPV primary controller is tuned, as

$$\begin{aligned} F_1(z,\theta) = {} & (0.9388 + 0.0014\theta - 0.0013\theta^2 + 2.6969 \times 10^{-4}\theta^3)z^{-1} \\ & + (0.9525 + 0.0023\theta + 7.7813 \times 10^{-4}\theta^2 - 2.1848 \times 10^{-4}\theta^3)z^{-2} \end{aligned} \tag{7.54}$$

$$F_2(z,\theta) = (564.3375 + 1.6398\theta + 3.5226\theta^2 - 0.8209\theta^3) +$$
$$(-1091.6 - 3.1403\theta - 1.9481\theta^2 + 0.4969\theta^3)z^{-1} +$$
$$(527.7826 + 1.5003\theta - 1.3327\theta^2 + 0.2515\theta^3)z^{-2}. \quad (7.55)$$

It should be noted that in the same way that the LPV model of the plant needs higher-order terms in the scheduling polynomial to represent the nonlinearities, the FIR filters $F_1(z,\theta)$ and $F_2(z,\theta)$ also need more terms for a more adequate compensation. The reference filter $F_r(\theta)$ is parameterized with $\beta_f = 0.8$, $\alpha_f = 0.75$, $n_{\beta_f} = 2$, $n_{\alpha_f} = 2$, and the LPV gain $K_r(\theta)$ is computed through (7.12). The robustness filter $V(z,\theta)$ is tuning with poles $\alpha_0 = 0.93$, $\alpha_1 = 0.9$, $\alpha_2 = 0.9$ and $\alpha_3 = 0.8$.

In Figure 88 are shown the open and closed-loop poles for several values of the scheduling parameter. As can be seen, although the open loop presents an unstable or a very oscillatory (for stable operation points) system, the SFSP-LPV is able to place the closed-loop poles into a small region close to the central polynomial poles.

Figure 88 – Example 2. Closed-loop poles for several values of $\theta \in [0, \pi]$.

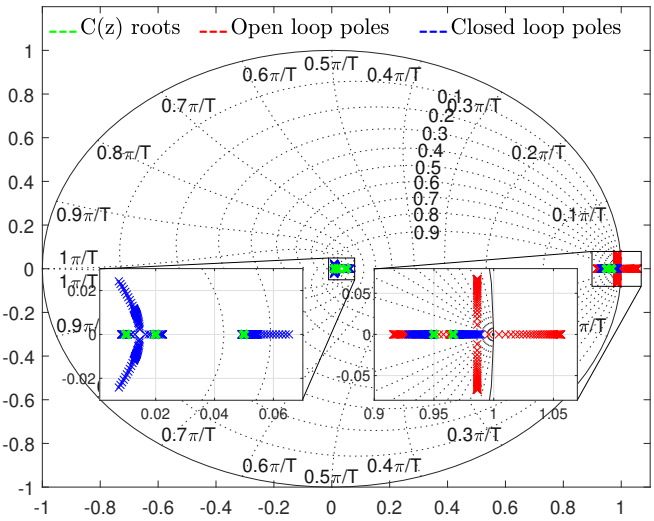

Source: The author.

The nonlinear system is then simulated in order to verify the SFSP-LPV performance when compared to the PID-LPV and PI-LPV proposed by Bolea, Puig and Blesa (2013) and Oliveira and Karimi (2013), respectively. A time response to a unit step reference is shown in Figure 89 with a negative step disturbance of magnitude 0.005 and an additive white noise, with zero mean and variance of 5×10^{-5}, in the measured output.

The controllers from Bolea, Puig and Blesa (2013) and Oliveira and Karimi (2013) are only able to act in the stable region of the system since the classical Smith predictor structure is internally unstable (NORMEY-RICO; CAMACHO, 2007). This can be confirmed by Figure

89 at $t = 400$ s where the system response for these controllers became unstable, while the SFSP-LPV can control the system all over the range. It can also be observed that the proposed controller has better rejection of disturbances, reaching the steady state faster.

Figure 89 – Example 2. Nominal case.

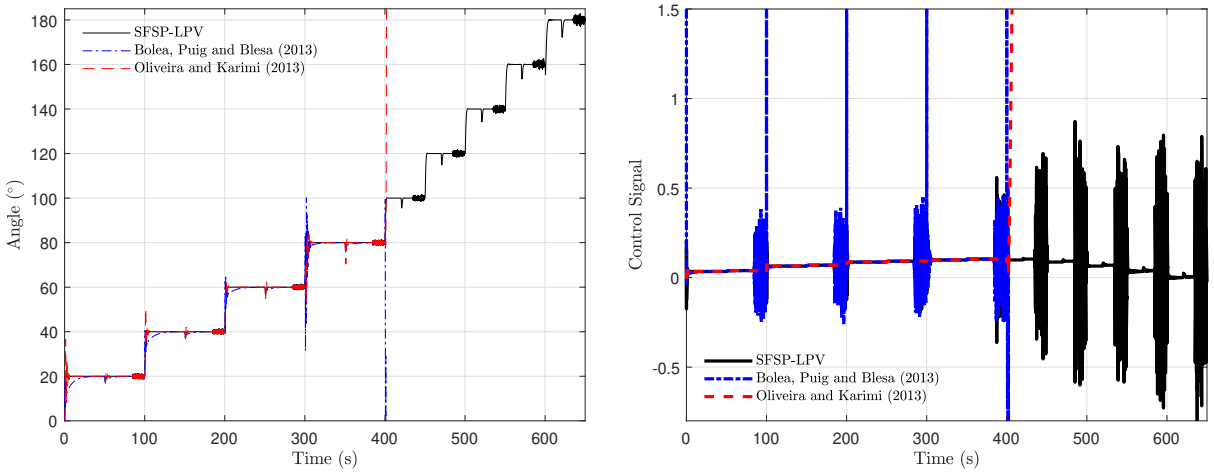

(a) (b)

Source: The author.

An uncertainty situation is also considered for a nominal dead time of $t_d = 0.15$ s and the a real plant with $t_d = 0.17$ s. The result is shown in Figure 90. Once again, the SFSP-LPV is able to control throughout the whole range with fast tracking and disturb rejection. The control signal has a good response to a noisy situation.

Figure 90 – Example 2. Case with model uncertainties.

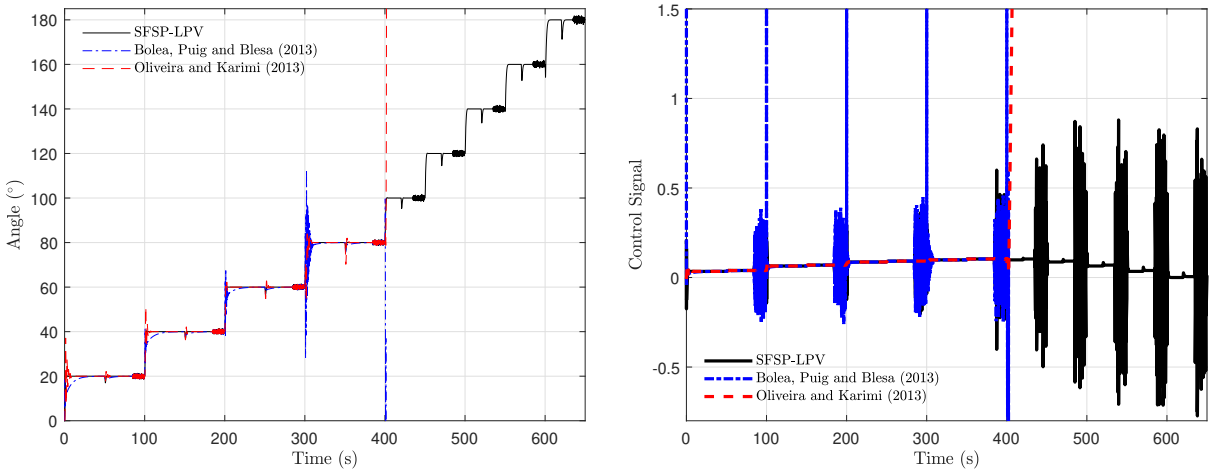

(a) (b)

Source: The author.

The graphs for the robustness index are presented in Figure 91 for several values of θ. Despite showing an aggressive tuning, the SFSP-LPV does not touch the multiplicative

uncertainty curve, which indicates its stability through the considered delay uncertainties. The same cannot be said of PID LPV controllers, as the robustness curves touch the uncertainty index curve for some operating points, that is, stability cannot be guaranteed.

Figure 91 – Example 2. Robustness Index for several values of $\theta \in [0, \pi]$.

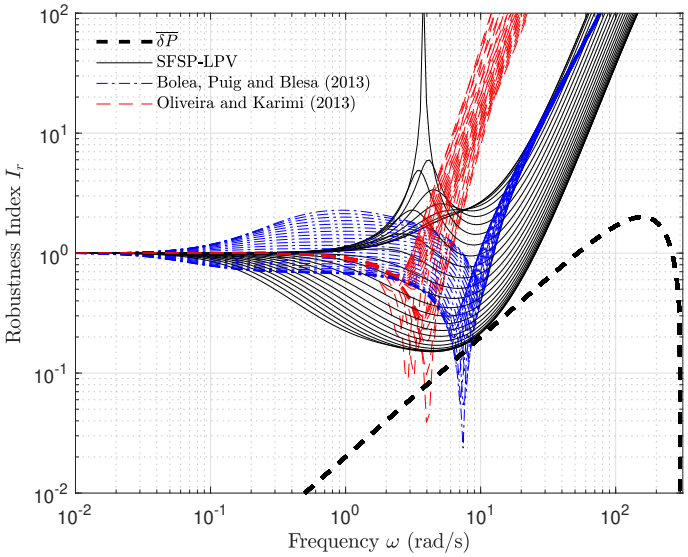

Source: The author.

Regarding the performance indices for example 2, the nominal and uncertain cases are shown in Figure 92 and 93, respectively. The proposed controller presents better IAE for both tracking and disturbance rejection while still maintaining stability across the entire scheduling range. Higher TV values, for the SFSP-LPV, indicate an aggressive tuning, however this is justified because the behavior of the system changes as the angle increases, going from a stable system to an unstable one, therefore they show that as the angle grows, the greater the control effort. Finally, the CV index shows that the SFSP-LPV has an intermediate noise attenuation considering the controllers compared.

Figure 92 – Example 2. SFSP performance for the nominal case.

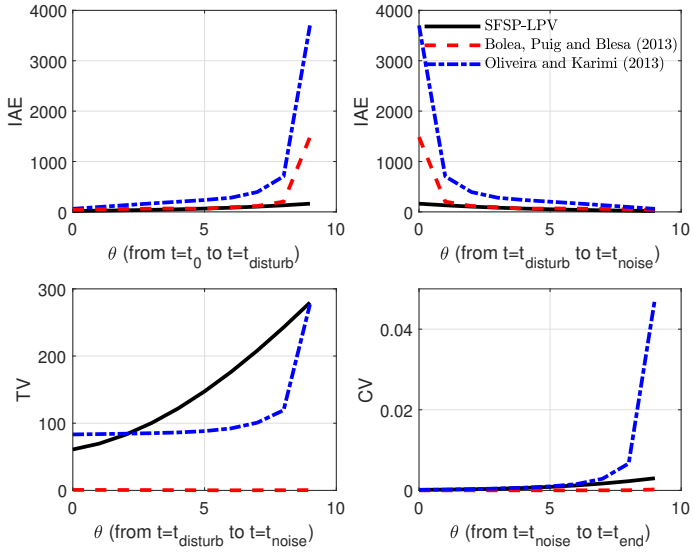

Source: The author.

Figure 93 – Example 2. SFSP performance for the uncertain case.

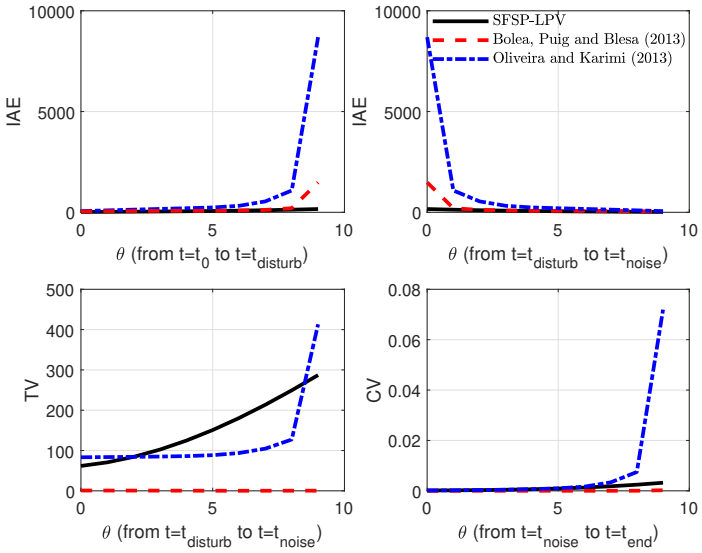

Source: The author.

8 CONCLUSIONS

This thesis proposed proposed a series cascade control structure based on the simplified filtered Smith predictor strategy to improve the response of unstable systems with delay in the discrete domain. This controller comprises a filter to guarantee the reference, two primary controllers (one gain for the primary loop and an FIR filter for the secondary loop), and two robustness filters, one for each respective loop.

In this way, it will be possible to obtain the benefits of both control strategies:

- Good performance (faster response and no overshoot).
- Robustness with decoupling (the adjustment of each filter is related to the disturbance applied to its respective loop).
- Attenuation of disturbances in the internal loop without these reaching the external loop.
- Noise attenuation.

A comparison was made with another controller from the literature proposed in Bhaskaran and Rao (2020) to prove that the proposed controller meets the expected characteristics. The proposed method presents a faster response for reference tracking, a better attenuation of the disturbance q2 in the internal loop, without overshoot, and a little better attenuation concerning the disturbance q1 in the nominal case. Regarding the case with uncertainties, the proposed controller shows a faster response without oscillations, contrary to what is noted by Bhaskaran and Rao (2020). Table 1 shows these results numerically, presenting the performance indexes in which the proposed controller gave the best values, except for the TV, due to a less smooth control signal.

It is also proposed a parallel cascade control structure based on SFSP with the purpose of stabilize and control stable, unstable and integrating FOPDT models with long dead time. On the three examples presented, the simpler tuning rules of the SFSP made possible to obtain parameters for set-tracking reference, disturbance rejection and noise attenuation more easily, and it also made possible for the systems to obtain good performance. The results showed similar behavior and responses in transient and steady states to recent papers and a better noise attenuation. This feature is of interest for practical applications.

In this thesis, a modification to the GPC was presented and its improvement to the output disturbance rejection of a TITO system with multiple delay was studied. From the numerical case simulated it was shown that the proposed GPC was able to reject output disturbances even in the uncertain scenario.

This thesis proposed the generalization of the simplified filtered Smith predictor (SFSP) for LPV systems by combining H_2/H_∞ into an LMI framework. The primary controller was computed in order to achieve the desired tracking response and the robustness filter was tuned regarding an intended trade-off between robustness and performance. The strategy preserved the main advantages of the original SFSP, such as simplicity in its structure, robustness to disturbance and noise, and good tracking performance.

Two examples from the literature were used to validate the proposed strategy. The performance indexes IAE, TV, and CV were computed and their results showed graphically for several operation points for a fair comparison. The presented SFSP-LPV controller demonstrated better results when its considered the criteria of IAE for most cases. The TV index showed an increase as the angle went up and the CV index showed intermediate values considering the comparison with others controllers. It should be also emphasized that the SFSP-LPV is internally stable and was able to control the unstable case for all scheduling range.

For practical implementation, the SFSP-LPV has as advantages simple design and tuning, while attaining good performance. Therefore, the proposed technique has great potential to control nonlinear dead-time plants modeled as LPV systems in industrial applications.

8.1 Further steps

In order to continue this research, the next steps to be carried out are:

1. Extend the cascade series predictor to high order systems.
2. Improve the cascade parallel controller to achieve ideal disturbance response.
3. Proposes an equivanlent SFSP to the proposed GPC controller.
4. Include the rules for the synthesis of the robustness filter $V(z,\theta)$ in the LMIs and consider that the Lyapunov matrix P depends on the scheduling parameter, thus making the controller less conservative.
5. Develop methods to avoid hidden couple terms problems in the LPV control system.

BIBLIOGRAPHY

ACKERMANN, J. E. On the synthesis of linear control systems with specified characteristics. *Automatica*, Elsevier, v. 13, n. 1, p. 89–94, 1977. Cited on page 36.

ALBERTOS, P.; GARCÍA, P. Decoupling mimo systems with multiple input/output time delays. In: IEEE. *2010 11th International Conference on Control Automation Robotics & Vision*. [S.l.], 2010. p. 1957–1962. Cited 2 times on pages 11 and 52.

ALEVISAKIS, G.; SEBORG, D. An extension of the smith predictor method to multivariable linear systems containing time delays. *International Journal of Control*, Taylor & Francis, v. 17, n. 3, p. 541–551, 1973. Cited 2 times on pages 11 and 50.

AMARAL, D. L. et al. A unified tuning rule of the simplified filtered smith predictor for siso and square mimo high-order dead-time processes. *Control Engineering Practice*, Elsevier, v. 141, p. 105697, 2023. Cited 3 times on pages 11, 55, and 56.

ANGELIS, G. Z. System analysis, modelling and control with polytopic linear models. 2003. Cited on page 63.

APKARIAN, P.; GAHINET, P.; BECKER, G. Self-scheduled H_∞ control of linear parameter-varying systems: a design example. *Automatica*, Elsevier, v. 31, n. 9, p. 1251–1261, 1995. Cited on page 73.

APKARIAN, P.; TUAN, H. D. Parameterized lmis in control theory. *SIAM journal on control and optimization*, SIAM, v. 38, n. 4, p. 1241–1264, 2000. Cited 2 times on pages 67 and 121.

ARTSTEIN, Z. Linear systems with delayed controls: A reduction. *IEEE Transactions on Automatic control*, IEEE, v. 27, n. 4, p. 869–879, 1982. Cited on page 18.

BAMIEH, B.; GIARRE, L. Identification of linear parameter varying models. *International Journal of Robust and Nonlinear Control: IFAC-Affiliated Journal*, Wiley Online Library, v. 12, n. 9, p. 841–853, 2002. Cited 2 times on pages 62 and 123.

BARROS, J. S. et al. Controle em cascata paralelo baseado no preditor de smith filtrado simplificado. 2017. Cited 3 times on pages 11, 48, and 49.

BELFORTE, G.; GAY, P. Optimal worst case estimation for lpv–fir models with bounded errors. *Systems & control letters*, Elsevier, v. 53, n. 3-4, p. 259–268, 2004. Cited on page 62.

BEZERRA-CORREIA, W.; CLAURE-TORRICO, B.; OLÍMPIO-PEREIRA, R. D. Optimal control of mimo dead-time linear systems with dead-time compensation structure. *Dyna*, 2006, Revista DYNA, v. 84, n. 200, p. 62–71, 2017. Cited 3 times on pages 11, 53, and 54.

BHASKARAN, A.; RAO, A. S. Predictive control of unstable time delay series cascade processes with measurement noise. *ISA transactions*, Elsevier, v. 99, p. 403–416, 2020. Cited 8 times on pages 10, 44, 45, 83, 84, 85, 86, and 139.

BLANCHINI, F. et al. Stable lpv realisation of the smith predictor. *International Journal of Systems Science*, Taylor & Francis, v. 47, n. 10, p. 2393–2401, 2016. Cited 3 times on pages 11, 74, and 75.

BLEKHERMAN, G.; PARRILO, P. A.; THOMAS, R. R. *Semidefinite optimization and convex algebraic geometry*. [S.l.]: SIAM, 2012. Cited on page 121.

BOLEA, Y. et al. An lpv fractional model for canal control. *IFAC Proceedings Volumes*, Elsevier, v. 42, n. 10, p. 1786–1791, 2009. Cited 5 times on pages 11, 62, 70, 71, and 73.

BOLEA, Y.; PUIG, V. Gain-scheduling multivariable lpv control of an irrigation canal system. *ISA transactions*, Elsevier, v. 63, p. 274–280, 2016. Cited 3 times on pages 11, 70, and 73.

BOLEA, Y.; PUIG, V.; BLESA, J. Gain-scheduled smith predictor pid-based lpv controller for open-flow canal control. *IEEE Transactions on Control Systems Technology*, IEEE, v. 22, n. 2, p. 468–477, 2013. Cited 7 times on pages 11, 70, 71, 73, 123, 125, and 135.

BOYD, S. et al. *Linear matrix inequalities in system and control theory*. [S.l.]: SIAM, 1994. Cited 2 times on pages 67 and 68.

BRIAT, C. Linear parameter-varying and time-delay systems. *Analysis, observation, filtering & control*, Springer, v. 3, p. 5–7, 2014. Cited 6 times on pages 59, 63, 64, 65, 67, and 69.

BRUZELIUS, F.; PETTERSSON, S.; BREITHOLTZ, C. Linear parameter-varying descriptions of nonlinear systems. In: IEEE. *Proceedings of the 2004 American Control Conference*. [S.l.], 2004. v. 2, p. 1374–1379. Cited on page 59.

BUTCHER, M.; KARIMI, A.; LONGCHAMP, R. On the consistency of certain identification methods for linear parameter varying systems. *IFAC Proceedings Volumes*, Elsevier, v. 41, n. 2, p. 4018–4023, 2008. Cited on page 62.

CAMACHO, E. F.; BORDONS, C. *Model Predictive Control*. London, U.K: Springer, 2002. Cited on page 50.

CAMPOS-RODRÍGUEZ, A. et al. Hybrid cascade control for a class of nonlinear dynamical systems. *J. Process Control*, Elsevier, v. 76, p. 141–154, 2019. Cited on page 39.

CERONE, V.; REGRUTO, D. Set-membership identification of lpv models with uncertain measurements of the time-varying parameter. In: IEEE. *2008 47th IEEE conference on decision and control*. [S.l.], 2008. p. 4491–4496. Cited on page 62.

CHEN, J.; HE, Z.-F.; QI, X. A new control method for mimo first order time delay non-square systems. *Journal of Process Control*, Elsevier, v. 21, n. 4, p. 538–546, 2011. Cited 2 times on pages 11 and 51.

CHILALI, M.; GAHINET, P.; APKARIAN, P. Robust pole placement in lmi regions. *IEEE transactions on Automatic Control*, IEEE, v. 44, n. 12, p. 2257–2270, 1999. Cited on page 73.

COX, P. B. *Towards efficient identification of linear parameter-varying state-space models*. Phd Thesis (PhD Thesis) — PhD dissertation, Eindhoven University of Technology, 2018. Cited on page 63.

ELAHI, A.; ALFI, A. Stochastic H∞ finite-time control of networked cascade control systems under limited channels, network delays and packet dropouts. *ISA Trans.*, Elsevier, v. 97, p. 352–364, 2020. Cited on page 39.

FLESCH, R. C.; SANTOS, T. L.; NORMEY-RICO, J. E. Unified approach for minimal output dead time compensation in mimo non-square processes. In: IEEE. *2012 IEEE 51st IEEE Conference on Decision and Control (CDC)*. [S.l.], 2012. p. 2376–2381. Cited on page 54.

FLESCH, R. C. et al. Unified approach for minimal output dead time compensation in mimo processes. *Journal of Process Control*, Elsevier, v. 21, n. 7, p. 1080–1091, 2011. Cited 5 times on pages 54, 110, 111, 113, and 114.

FRANKS, R.; WORLEY, C. Quantitative analysis of cascade control. *J. Ind. Eng. Chem.*, ACS Publications, v. 48, n. 6, p. 1074–1079, 1956. Cited on page 39.

FU, M. Pole placement via static output feedback is np-hard. *IEEE Transactions on Automatic Control*, IEEE, v. 49, n. 5, p. 855–857, 2004. Cited on page 69.

GARCÍA, P.; ALBERTOS, P. Dead-time-compensator for unstable mimo systems with multiple time delays. *Journal of Process Control*, Elsevier, v. 20, n. 7, p. 877–884, 2010. Cited 4 times on pages 11, 18, 50, and 53.

GARCIA, P. et al. Smith predictor-based control schemes for dead-time unstable cascade processes. *Ind. Eng. Chem. Res.*, ACS Publications, v. 49, n. 22, p. 11471–11481, 2010. Cited 3 times on pages 10, 42, and 43.

GARRIDO, J.; VÁZQUEZ, F.; MORILLA, F. Inverted decoupling internal model control for square stable multivariable time delay systems. *Journal of Process Control*, Elsevier, v. 24, n. 11, p. 1710–1719, 2014. Cited 3 times on pages 11, 51, and 52.

GARRIDO, J. et al. Practical advantages of inverted decoupling. *Proceedings of the Institution of Mechanical Engineers, Part I: Journal of Systems and Control Engineering*, SAGE Publications Sage UK: London, England, v. 225, n. 7, p. 977–992, 2011. Cited 3 times on pages 11, 51, and 52.

GÁSPÁR, P.; SZABÓ, Z.; BOKOR, J. Gray-box continuous-time parameter identification for lpv models with vehicle dynamics applications. In: IEEE. *Proceedings of the 2005 IEEE International Symposium on, Mediterrean Conference on Control and Automation Intelligent Control, 2005.* [S.l.], 2005. p. 393–398. Cited on page 63.

GIARRÉ, L. et al. Lpv model identification for gain scheduling control: An application to rotating stall and surge control problem. *Control Engineering Practice*, Elsevier, v. 14, n. 4, p. 351–361, 2006. Cited on page 62.

GILBERT, W. *Synthèse LPV polynomiale appliquée à la commande de turboréacteurs*. Phd Thesis (PhD Thesis) — Toulouse, INSA, 2008. Cited on page 124.

GILBERT, W. et al. Polynomial lpv synthesis applied to turbofan engines. *Control Engineering Practice*, Elsevier, v. 18, n. 9, p. 1077–1083, 2010. Cited 4 times on pages 119, 120, 121, and 122.

GIRALDO, S. A. C.; FLESCH, R. C.; NORMEY-RICO, J. E. Multivariable greenhouse control using the filtered smith predictor. *Journal of Control, Automation and Electrical Systems*, Springer, v. 27, n. 4, p. 349–358, 2016. Cited on page 19.

GIRALDO, S. A. C. et al. Decoupling filtered smith predictor design for multivariable systems with multiple time delays. In: IEEE. *2016 12th IEEE International Conference on Industry Applications (INDUSCON)*. [S.l.], 2016. p. 1–8. Cited on page 54.

GIRALDO, S. A. C. et al. A method for designing decoupled filtered smith predictor for square mimo systems with multiple time delays. *IEEE Transactions on Industry Applications*, IEEE, v. 54, n. 6, p. 6439–6449, 2018. Cited 2 times on pages 19 and 50.

HABIB, G. et al. Nonlinear model-based parameter estimation and stability analysis of an aero-pendulum subject to digital delayed control. *International Journal of Dynamics and Control*, Springer, v. 5, n. 3, p. 629–643, 2017. Cited 5 times on pages 123, 129, 130, 131, and 133.

HANG, C.; WANG, Q.-G.; YANG, X.-P. A modified smith predictor for a process with an integrator and long dead time. *Industrial & engineering chemistry research*, ACS Publications, v. 42, n. 3, p. 484–489, 2003. Cited on page 18.

HENRION, D. Positive polynomial matrices for lpv controller synthesis. In: *Robust Control and Linear Parameter Varying Approaches*. [S.l.]: Springer, 2013. p. 87–96. Cited on page 120.

HENRION, D.; LASSERRE, J.-B. Convergent relaxations of polynomial matrix inequalities and static output feedback. *IEEE Transactions on Automatic Control*, IEEE, v. 51, n. 2, p. 192–202, 2006. Cited on page 69.

HSU, K.; VINCENT, T. L.; POOLLA, K. Nonparametric methods for the identification of linear parameter varying systems. In: IEEE. *2008 IEEE International Conference on Computer-Aided Control Systems*. [S.l.], 2008. p. 846–851. Cited on page 63.

ISIDORI, A. Nonlinear control systems. *Communications and Control Engineering*, 1995. Cited on page 131.

JEROME, N.; RAY, W. H. High-performance multivariable control strategies for systems having time delays. *AIChE Journal*, Wiley Online Library, v. 32, n. 6, p. 914–931, 1986. Cited on page 50.

KAYA, I. Improving performance using cascade control and a smith predictor. *ISA Trans.*, Elsevier, v. 40, p. 223–234, 2001. Cited 3 times on pages 10, 39, and 40.

KAYA, İ.; NALBANTOĞLU, M. Simultaneous tuning of cascaded controller design using genetic algorithm. *Electr. Eng.*, Springer, v. 98, p. 299–305, 2016. Cited on page 39.

KHALIL, H. K. Nonlinear systems third edition. *Patience Hall*, v. 115, 2002. Cited on page 59.

KNOBLACH, A.; LOOYE, G. Efficient determination of worst-case gust loads using system norms. *Journal of Aircraft*, American Institute of Aeronautics and Astronautics, v. 54, n. 3, p. 1205–1210, 2017. Cited on page 120.

LACHHAB, N.; ABBAS, H.; WERNER, H. A neural-network based technique for modelling and lpv control of an arm-driven inverted pendulum. In: IEEE. *2008 47th IEEE Conference on Decision and Control*. [S.l.], 2008. p. 3860–3865. Cited on page 63.

LAURAIN, V. et al. Refined instrumental variable methods for identification of lpv box–jenkins models. *Automatica*, Elsevier, v. 46, n. 6, p. 959–967, 2010. Cited on page 62.

LAWRENCE, D. A.; RUGH, W. J. Gain scheduling dynamic linear controllers for a nonlinear plant. *Automatica*, Elsevier, v. 31, n. 3, p. 381–390, 1995. Cited on page 63.

LEE, L. H.; POOLLA, K. Identification of linear parameter-varying systems via lfts. In: IEEE. *Proceedings of 35th IEEE Conference on Decision and Control*. [S.l.], 1996. v. 2, p. 1545–1550. Cited on page 63.

LEITH, D. J.; LEITHEAD, W. Gain-scheduled and nonlinear systems: dynamic analysis by velocity-based linearization families. *International Journal of Control*, Taylor & Francis, v. 70, n. 2, p. 289–317, 1998. Cited on page 59.

LEITH, D. J.; LEITHEAD, W. E. Survey of gain-scheduling analysis and design. *International journal of control*, Taylor & Francis, v. 73, n. 11, p. 1001–1025, 2000. Cited 2 times on pages 59 and 68.

LIMA, D. M.; LIMA, B. M.; NORMEY-RICO, J. E. A predictor for square multivariable dead-time systems with multiple delays based on the kalman filter. *Journal of Process Control*, Elsevier, v. 124, p. 105–117, 2023. Cited on page 54.

LIMA, D. M.; SANTOS, T. L. M.; NORMEY-RICO, J. E. Robust nonlinear predictor for dead-time systems with input nonlinearities. *Journal of Process Control*, Elsevier, v. 27, p. 1–14, 2015. Cited on page 19.

LIU, T. et al. New modified smith predictor scheme for integrating and unstable processes with time delay. *IEE Proceedings-Control Theory and Applications*, IET, v. 152, n. 2, p. 238–246, 2005. Cited on page 18.

LJUNG, L. System identification. In: *Signal analysis and prediction*. [S.l.]: Springer, 1998. p. 163–173. Cited on page 61.

LOFBERG, J. Pre-and post-processing sum-of-squares programs in practice. *IEEE transactions on automatic control*, IEEE, v. 54, n. 5, p. 1007–1011, 2009. Cited on page 121.

LOVERA, M.; MERCERE, G. Identification for gain-scheduling: a balanced subspace approach. In: IEEE. *2007 American Control Conference*. [S.l.], 2007. p. 858–863. Cited on page 63.

LOVERA, M.; VERHAEGEN, M.; CHOU, C. State space identification of mimo linear parameter varying models. In: *Proceedings of the International Symposium on the Mathematical Theory of Networks and Systems*. [S.l.: s.n.], 1998. p. 839–842. Cited on page 63.

LUYBEN, W. L. Parallel Cascade Control. *Industrial and Engineering Chemistry Fundamentals*, v. 12, n. 4, p. 463–467, 1973. Cited on page 45.

MA, D.; LI, Z.; ZHAO, R. Output tracking with disturbance attenuation for cascade control systems subject to network constraint. *Asian J. Control*, Wiley Online Library, v. 22, n. 4, p. 1617–1627, 2020. Cited on page 39.

MATAUŠEK, M. R.; RIBIĆ, A. I. Control of stable, integrating and unstable processes by the modified smith predictor. *Journal of Process Control*, Elsevier, v. 22, n. 1, p. 338–343, 2012. Cited on page 18.

MAZZARO, M. C.; MOVSICHOFF, E.; PENA, R. S. Robust identification of linear parameter varying systems. In: IEEE. *Proceedings of the 1999 American Control Conference (Cat. No. 99CH36251)*. [S.l.], 1999. v. 4, p. 2282–2284. Cited on page 63.

MICHIELS, W.; NICULESCU, S.-I. On the delay sensitivity of smith predictors. *International journal of systems science*, Taylor & Francis, v. 34, n. 8-9, p. 543–551, 2003. Cited on page 18.

MOHAMMADPOUR, J.; SCHERER, C. W. *Control of linear parameter varying systems with applications*. [S.l.]: Springer Science & Business Media, 2012. Cited on page 57.

MORARI, M.; ZAFIRIOU, E. *Robust process control*. [S.l.]: Morari, 1989. Cited 2 times on pages 18 and 26.

MORATO, M. M.; NORMEY-RICO, J. E. A linear parameter varying approach for robust dead-time compensation. *IFAC-PapersOnLine*, Elsevier, v. 52, n. 1, p. 880–885, 2019. Cited 5 times on pages 11, 75, 76, 77, and 78.

MORATO, M. M.; NORMEY-RICO, J. E. A novel unified method for time-varying dead-time compensation. *ISA transactions*, Elsevier, v. 108, p. 78–95, 2021. Cited 5 times on pages 11, 75, 76, 77, and 78.

NANDONG, J.; ZANG, Z. Generalized multi-scale control scheme for cascade processes with time-delays. *J. Process Control*, Elsevier, v. 24, n. 7, p. 1057–1067, 2014. Cited on page 39.

NEMANI, M.; RAVIKANTH, R.; BAMIEH, B. A. Identification of linear parametrically varying systems. In: IEEE. *Proceedings Of 1995 34th Ieee Conference On Decision And Control*. [S.l.], 1995. v. 3, p. 2990–2995. Cited on page 63.

NICHOLS, R. A.; REICHERT, R. T.; RUGH, W. J. Gain scheduling for h-infinity controllers: A flight control example. *IEEE Transactions on Control systems technology*, IEEE, v. 1, n. 2, p. 69–79, 1993. Cited on page 63.

NOGUEIRA, F. G. et al. Development and field tests of a damping controller to mitigate electromechanical oscillations on large diesel generating units. *Electric power systems research*, Elsevier, v. 81, n. 2, p. 725–732, 2011. Cited on page 18.

NOGUEIRA, F. G. et al. Lpv-based power system stabilizer: Identification, control and field tests. *Control Engineering Practice*, Elsevier, v. 72, p. 53–67, 2018. Cited 3 times on pages 115, 121, and 124.

NORMEY-RICO, J. E.; BORDONS, C.; CAMACHO, E. F. Improving the robustness of dead-time compensating pi controllers. *Control Engineering Practice*, Elsevier, v. 5, n. 6, p. 801–810, 1997. Cited 2 times on pages 19 and 27.

NORMEY-RICO, J. E.; CAMACHO, E. F. *Control of dead-time processes*. [S.l.]: Springer, 2007. v. 462. Cited 6 times on pages 18, 21, 23, 24, 27, and 135.

NORMEY-RICO, J. E.; CAMACHO, E. F. Dead-time compensators: A survey. *Control engineering practice*, Elsevier, v. 16, n. 4, p. 407–428, 2008. Cited 3 times on pages 18, 25, and 50.

NORMEY-RICO, J. E.; CAMACHO, E. F. Unified approach for robust dead-time compensator design. *Journal of Process Control*, Elsevier, v. 19, n. 1, p. 38–47, 2009. Cited 2 times on pages 18 and 30.

NORMEY-RICO, J. E.; GARCIA, P.; GONZALEZ, A. Robust stability analysis of filtered smith predictor for time-varying delay processes. *Journal of Process Control*, Elsevier, v. 22, n. 10, p. 1975–1984, 2012. Cited on page 70.

NOWAK, P.; CZECZOT, J. Practical verification of active disturbance rejection controller for the pneumatic setup. In: IEEE. *2017 22nd international conference on methods and models in automation and robotics (MMAR)*. [S.l.], 2017. p. 19–24. Cited on page 18.

OGUNNAIKE, B.; RAY, W. Multivariable controller design for linear systems having multiple time delays. *AIChE journal*, Wiley Online Library, v. 25, n. 6, p. 1043–1057, 1979. Cited 2 times on pages 11 and 51.

OLIVEIRA, V. D.; KARIMI, A. Robust smith predictor design for time-delay systems with H_∞ performance. *IFAC Proceedings Volumes*, Elsevier, v. 46, n. 3, p. 102–107, 2013. Cited 5 times on pages 73, 123, 125, 127, and 135.

PADHAN, D.; MAJHI, S. Modified smith predictor based cascade control of unstable time delay processes. *ISA Trans.*, Elsevier, v. 51, p. 95–104, 2012. Cited 4 times on pages 10, 42, 43, and 44.

PADHAN, D. G.; MAJHI, S. An improved parallel cascade control structure for processes with time delay. *Journal of Process Control*, Elsevier, v. 22, n. 5, p. 884–898, 2012. Cited 4 times on pages 10, 45, 47, and 48.

PADHAN, D. G.; MAJHI, S. Enhanced cascade control for a class of integrating processes with time delay. *ISA Trans.*, Elsevier, v. 52, n. 1, p. 45–55, 2013. Cited 3 times on pages 10, 40, and 41.

PAIJMANS, B. et al. Interpolating affine lpv identification for mechatronic systems with one varying parameter. *Eur. J. Control*, v. 14, n. 1, 2008. Cited on page 63.

PASHAEI, S.; BAGHERI, P. Parallel cascade control of dead time processes via fractional order controllers based on smith predictor. *ISA transactions*, Elsevier, 2019. Cited 9 times on pages 11, 49, 92, 93, 94, 95, 97, 98, and 100.

PATARO, I. M.; COSTA, M. V. A. da; JOSEPH, B. Advanced simulation and analysis of mimo dead time compensator and predictive controller for ethanol distillation process. *IFAC-PapersOnLine*, Elsevier, v. 52, n. 1, p. 160–165, 2019. Cited on page 54.

PATARO, I. M.; COSTA, M. V. A. da; JOSEPH, B. Closed-loop dynamic real-time optimization (cl-drto) of a bioethanol distillation process using an advanced multilayer control architecture. *Computers & Chemical Engineering*, Elsevier, v. 143, p. 107075, 2020. Cited on page 54.

PEDRO, A.; PEDRO, G. State feedback control of mimo systems with multiple time delays. In: IEEE. *2016 35th Chinese Control Conference (CCC)*. [S.l.], 2016. p. 229–234. Cited 2 times on pages 11 and 53.

PIERRE, A.; PASCAL, G. A convex characterization of gain-scheduled H_∞ controllers. *IEEE Trans Autom Control*, v. 40, n. 5, p. 853–864, 1995. Cited 2 times on pages 69 and 73.

PREVIDI, F.; LOVERA, M. Identification of a class of non-linear parametrically varying models. *International Journal of Adaptive Control and Signal Processing*, Wiley Online Library, v. 17, n. 1, p. 33–50, 2003. Cited on page 63.

PREVIDI*, F.; LOVERA, M. Identification of non-linear parametrically varying models using separable least squares. *International Journal of Control*, Taylor & Francis, v. 77, n. 16, p. 1382–1392, 2004. Cited on page 63.

RAJA, G. L.; ALI, A. Modified parallel cascade control strategy for stable, unstable and integrating processes. *ISA transactions*, Elsevier, v. 65, p. 394–406, 2016. Cited 3 times on pages 10, 45, and 46.

RAJA, G. L.; ALI, A. Smith predictor based parallel cascade control strategy for unstable and integrating processes with large time delay. *Journal of Process Control*, Elsevier, v. 52, p. 57–65, 2017. Cited 3 times on pages 11, 45, and 48.

RAJA, G. L.; ALI, A. Enhanced tuning of smith predictor based series cascaded control structure for integrating processes. *ISA Trans.*, Elsevier, v. 114, p. 191–205, 2021. Cited 4 times on pages 10, 40, 41, and 42.

RAO, A. S. et al. Enhancing the performance of parallel cascade control using Smith predictor. *ISA Transactions*, ISA, v. 48, n. 2, p. 220–227, 2009. Cited 2 times on pages 10 and 47.

ROCA, L. et al. Filtered smith predictor with feedback linearization and constraints handling applied to a solar collector field. *Solar Energy*, Elsevier, v. 85, n. 5, p. 1056–1067, 2011. Cited on page 19.

RODRÍGUEZ, C. et al. On the filtered smith predictor with feedforward compensation. *journal of Process Control*, Elsevier, v. 41, p. 35–46, 2016. Cited 2 times on pages 18 and 19.

ROMERO-GARCÍA, J. et al. Filtered smith predictor to control ph during enzymatic hydrolysis of microalgae to produce l-aminoacids concentrates. *Chemical engineering science*, Elsevier, v. 82, p. 121–131, 2012. Cited on page 19.

RUGH, W. J.; SHAMMA, J. S. Research on gain scheduling. *Automatica*, Elsevier, v. 36, n. 10, p. 1401–1425, 2000. Cited 2 times on pages 59 and 63.

SANTOS, T. L.; BOTURA, P. E.; NORMEY-RICO, J. E. Dealing with noise in unstable dead-time process control. *Journal of Process Control*, Elsevier, v. 20, n. 7, p. 840–847, 2010. Cited on page 19.

SANTOS, T. L.; FLESCH, R. C.; NORMEY-RICO, J. E. On the filtered smith predictor for mimo processes with multiple time delays. *Journal of Process Control*, Elsevier, v. 24, n. 4, p. 383–400, 2014. Cited 3 times on pages 11, 54, and 55.

SANTOS, T. L.; FRANKLIN, T. S.; TORRICO, B. C. Anti-windup strategy for processes with multiple delays: A predictor-based approach. *Journal of the Franklin Institute*, Elsevier, v. 358, n. 3, p. 1812–1838, 2021. Cited on page 54.

SANTOS, T. L.; TORRICO, B. C.; NORMEY-RICO, J. E. Simplified filtered smith predictor for mimo processes with multiple time delays. *ISA transactions*, Elsevier, v. 65, p. 339–349, 2016. Cited 7 times on pages 11, 55, 110, 111, 112, 113, and 114.

SANTOSH, S.; CHIDAMBARAM, M. A simple method of tuning parallel cascade controllers for unstable foptd systems. *ISA transactions*, Elsevier, v. 65, p. 475–486, 2016. Cited 4 times on pages 10, 45, 46, and 47.

SANZ, R.; GARCÍA, P.; ALBERTOS, P. A generalized smith predictor for unstable time-delay siso systems. *ISA transactions*, Elsevier, v. 72, p. 197–204, 2018. Cited on page 83.

SCHERER, C. W. Lpv control and full block multipliers. *Automatica*, Elsevier, v. 37, n. 3, p. 361–375, 2001. Cited on page 69.

SCHERER, C. W. Lmi relaxations in robust control. *European Journal of Control*, Elsevier, v. 12, n. 1, p. 3–29, 2006. Cited 2 times on pages 68 and 121.

SCHERER, C. W.; HOL, C. W. Matrix sum-of-squares relaxations for robust semi-definite programs. *Mathematical programming*, Springer, v. 107, n. 1-2, p. 189–211, 2006. Cited on page 121.

SCHERER, C. W.; KOSE, I. E. Gain-scheduled control synthesis using dynamic d-scales. *IEEE Transactions on Automatic Control*, IEEE, v. 57, n. 9, p. 2219–2234, 2012. Cited on page 69.

SHAMMA, J. S.; ATHANS, M. Gain scheduling: Potential hazards and possible remedies. *IEEE Control Systems Magazine*, IEEE, v. 12, n. 3, p. 101–107, 1992. Cited on page 69.

SHIN, J.-Y. Analysis of linear parameter varying system models based on reachable sets. In: IEEE. *Proceedings of the 2002 American Control Conference (IEEE Cat. No. CH37301)*. [S.l.], 2002. v. 1, p. 35–40. Cited on page 59.

SHOGA, T. et al. Self-tuning regulator based cascade control for temperature of exothermic stirred tank reactor. *FME Trans.*, v. 47, n. 1, p. 202–211, 2019. Cited on page 39.

SMITH, O. J. M. Closer control of loops with dead time. *Chemical Engineering Progress*, v. 53, n. 5, p. 217–219, 1957. Cited By :36. Available at: <www.scopus.com>. Cited 3 times on pages 18, 23, and 24.

TAKAGI, T.; SUGENO, M. Fuzzy identification of systems and its applications to modeling and control. *IEEE transactions on systems, man, and cybernetics*, IEEE, n. 1, p. 116–132, 1985. Cited on page 68.

TORRICO, B. et al. New simple approach for enhanced rejection of unknown disturbances in lti systems with input delay. *ISA Trans.*, Elsevier, v. 94, p. 316–325, 2019. Cited 2 times on pages 33 and 35.

TORRICO, B. C. et al. Simple tuning rules for dead-time compensation of stable, integrative, and unstable first-order dead-time processes. *Industrial & Engineering Chemistry Research*, ACS Publications, v. 52, n. 33, p. 11646–11654, 2013. Cited 6 times on pages 18, 19, 34, 56, 78, and 122.

TORRICO, B. C. et al. Simple tuning rules for dead-time compensation of stable, integrative, and unstable first-order dead-time processes. *J. Ind. Eng. Chem.*, Elsevier, v. 52, p. 11646–11654, 2013. Cited 5 times on pages 31, 33, 35, 37, and 48.

TORRICO, B. C.; CORREIA, W. B.; NOGUEIRA, F. G. Simplified dead-time compensator for multiple delay siso systems. *ISA transactions*, Elsevier, v. 60, p. 254–261, 2016. Cited 7 times on pages 18, 19, 33, 34, 78, 115, and 118.

TORRICO, B. C. et al. Tuning of a dead-time compensator focusing on industrial processes. *ISA transactions*, Elsevier, v. 83, p. 189–198, 2018. Cited 6 times on pages 19, 33, 34, 35, 78, and 118.

TORRICO, B. C. et al. Simplified filtered smith predictor for high-order dead-time processes. *ISA transactions*, Elsevier, v. 109, p. 11–21, 2021. Cited 9 times on pages 19, 20, 31, 37, 38, 55, 87, 118, and 123.

TÓTH, R. *Modeling and identification of linear parameter-varying systems*. [S.l.]: Springer, 2010. v. 403. Cited 4 times on pages 61, 62, 63, and 133.

UMA, S. et al. Enhanced control of integrating cascade processes with time delays using modified smith predictor. *Chem. Eng. Sci.*, Elsevier, v. 65, n. 3, p. 1065–1075, 2010. Cited 2 times on pages 10 and 40.

VERDULT, V.; LJUNG, L.; VERHAEGEN, M. Identification of composite local linear state-space models using a projected gradient search. *International Journal of Control*, Taylor & Francis, v. 75, n. 16-17, p. 1385–1398, 2002. Cited on page 63.

WASSINK, M. G. et al. Lpv control for a wafer stage: beyond the theoretical solution. *Control Engineering Practice*, Elsevier, v. 13, n. 2, p. 231–245, 2005. Cited on page 63.

WATANABE, K.; ITO, M. A process-model control for linear systems with delay. *IEEE Transactions on Automatic control*, IEEE, v. 26, n. 6, p. 1261–1269, 1981. Cited on page 18.

WEI, X.; RE, L. D. On persistent excitation for parameter estimation of quasi-lpv systems and its application in modeling of diesel engine torque. *IFAC Proceedings Volumes*, Elsevier, v. 39, n. 1, p. 517–522, 2006. Cited on page 62.

WOLLNACK, S. et al. Fixed-structure lpv-io controllers: An implicit representation based approach. *Automatica*, Elsevier, v. 83, p. 282–289, 2017. Cited on page 63.

YIN, C.-q. et al. Improved cascade control system for a class of unstable processes with time delay. *Int. J. Control Autom. Syst.*, Springer, v. 17, n. 1, p. 126–135, 2019. Cited 3 times on pages 10, 42, and 44.

ZHENG, Q.; GAO, Z. Predictive active disturbance rejection control for processes with time delay. *ISA transactions*, Elsevier, v. 53, n. 4, p. 873–881, 2014. Cited on page 18.

ZHU, Y.; JI, G. Lpv model identification using blended linear models with given weightings. *IFAC Proceedings Volumes*, Elsevier, v. 42, n. 10, p. 1674–1679, 2009. Cited on page 62.

ZHU, Y.; XU, Z. A method of lpv model identification for control. *IFAC Proceedings Volumes*, Elsevier, v. 41, n. 2, p. 5018–5023, 2008. Cited on page 62.

APPENDIX

APPENDIX A – SIMULATION PARAMETERS AND EVALUATION

For all discussed examples the continuous model processes are discretized by the zero-order hold method. Sampling times are chosen based on the smallest time constants of each process studied, with values at least ten times smaller than these time constants.

Also, performances criteria, such as integrated absolute error (IAE), control signal total variation (TV), and control variance (CV), are calculated to better analyze and compare the performance of the proposed controllers. The indices are calculates such as:

$$IAE = \int_{t_0}^{t_1} |e(t)|dt, \tag{A.1}$$

$$TV = \sum_{i=t_2}^{t_3} |u_{i+1} - u_i|, \tag{A.2}$$

$$CV = \frac{1}{N-1} \sum_{i=t_3}^{N} |u_i - \mu|^2, \tag{A.3}$$

where N and μ are the number of samples and the mean of the control signal, respectively. The IAE index is calculated for two different situations: the first one is for tracking, that is, from initial time ($t_0 = 0$) until the instant where the disturb is applied ($t_1 = t_{disturb}$) and the second one is from disturbance rejection ($t_0 = t_{disturb}$) to the moment when the noise is applied; the TV index is computed considering the control signal from initial time ($t_2 = 0$), except for LPV examples where it is calculated only for disturbance rejection ($t_2 = t_{disturb}$), to the time where the noise is applied ($t_3 = t_{noise}$). Finally, the CV index is calculated from the time when the noise is applied ($t_3 = t_{noise}$) to end of simulation ($t = t_{end}$). A band-limited white noise with zero mean is used in the examples, considering the specified variance.